Université de Toulouse

THÈSE

En vue de l'obtention du

DOCTORAT DE L'UNIVERSITÉ DE TOULOUSE

Délivré par :
Institut National Polytechnique de Toulouse (INP Toulouse)

Discipline ou spécialité :

Génie des procédés et de l'Environnement

Présentée et soutenue par :
Jorge Raúl PEREZ GALLARDO

le : vendredi 25 octobre 2013

Titre :
Ecodesign of large-scale photovoltaic (PV) systems with multi-objective optimization and Life-Cycle Assessment (LCA)

Écoconception de systèmes photovoltaïques (PV) à grande échelle par optimisation multi-objectif et Analyse du Cycle de Vie (ACV)

Ecole doctorale :
Mécanique, Energétique, Génie civil et Procédés (MEGeP)

Unité de recherche :
Laboratoire de Génie Chimique - UMR 5503

Directeur(s) de Thèse :
Mme Catherine AZZARO-PANTEL (INP-Toulouse, France)
M. Stéphan ASTIER (INP-Toulouse, France)

Rapporteurs :

Mme Valérie LAFOREST (ENSM-Saint-Etienne, France)
M. Moises GRAELLS (UPC-Barcelone, Espagne)

Membre(s) du jury :

Mme Corinne ALONSO (LAAS CNRS-Toulouse, France)
M. Pascal ESCRIBE (EDF EN France Région Sud, France)
M. Serge DOMENECH (INP-Toulouse, France)
M. Xavier ROBOAM (INP-Toulouse, France)
M. Pascal MAUSSION (INP-Toulouse, France)

Abstract

.

Ecodesign of large-scale photovoltaic (PV) systems with multi-objective optimization and Life-Cycle Assessment (LCA)

Because of the increasing demand for the provision of energy worldwide and the numerous damages caused by a major use of fossil sources, the contribution of renewable energies has been increasing significantly in the global energy mix with the aim at moving towards a more sustainable development. In this context, this work aims at the development of a general methodology for designing PV systems based on ecodesign principles and taking into account simultaneously both techno-economic and environmental considerations. In order to evaluate the environmental performance of PV systems, an environmental assessment technique was used based on Life Cycle Assessment (LCA). The environmental model was successfully coupled with the design stage model of a PV grid-connected system (PVGCS). The PVGCS design model was then developed involving the estimation of solar radiation received in a specific geographic location, the calculation of the annual energy generated from the solar radiation received, the characteristics of the different components and the evaluation of the techno-economic criteria through Energy PayBack Time (EPBT) and PayBack Time (PBT). The performance model was then embedded in an outer multi-objective genetic algorithm optimization loop based on a variant of NSGA-II. A set of Pareto solutions was generated representing the optimal trade-off between the objectives considered in the analysis. A multi-variable statistical method (*i.e.*, Principal Componet Analysis, PCA) was then applied to detect and omit redundant objectives that could be left out of the analysis without disturbing the main features of the solution space. Finally, a decision-making tool based on M-TOPSIS was used to select the alternative that provided a better compromise among all the objective functions that have been investigated.

The results showed that while the PV modules based on c-Si have a better performance in energy generation, the environmental aspect is what makes them fall to the last positions. TF PV modules present the best trade-off in all scenarios under consideration.

A special attention was paid to recycling process of PV module even if there is not yet enough information currently available for all the technologies evaluated. The main cause of this lack of information is the lifetime of PV modules. The data relative to the recycling processes for m-Si and CdTe PV technologies were introduced in the optimization procedure for ecodesign. By considering energy production and EPBT as optimization criteria into a bi-objective optimization cases, the importance of the benefits of PV modules end-of-life management was confirmed. An economic study of the recycling strategy must be investigated in order to have a more comprehensive view for decision making.

Keywords: Ecodesign, Multi-objective Optimization, Life-Cycle Assessment (LCA), Photovoltaic (PV) system, Genetic Algorithm (GA), Principal Component Analysis (PCA), Multiple Criteria Decision Making (MCDM)

Résumé

Écoconception de systèmes photovoltaïques (PV) à grande échelle par optimisation multi-objectif et Analyse du Cycle de Vie (ACV)

En raison de la demande croissante d'énergie dans le monde et des nombreux dommages causés par l'utilisation des énergies fossiles, la contribution des énergies renouvelables a augmenté de manière significative dans le mix énergétique global dans le but de progresser vers un développement plus durable. Dans ce contexte, ce travail vise à l'élaboration d'une méthodologie générale pour la conception de systèmes photovoltaïques, basée sur les principes d'écoconception, en tenant compte simultanément des considérations technico-économiques et environnementales. Afin d'évaluer la performance environnementale des systèmes PV, une technique d'évaluation environnementale basée sur l'Analyse du Cycle de Vie (ACV) a été utilisée. Le modèle environnemental a été couplé d'une manière satisfaisante avec le modèle de conception d'un système PV connecté au réseau pour obtenir un modèle global, apte à un traitement par optimisation. Le modèle de conception du système PV résultant a été développé en faisant intervenir l'estimation du rayonnement solaire reçu dans une zone géographique concernée, le calcul de la quantité annuelle d'énergie produite à partir du rayonnement solaire reçu, les caractéristiques des différents composants et l'évaluation des critères technico-économiques à travers le temps de retour énergétique et le temps de retour sur investissement. Le modèle a ensuite été intégré dans une boucle d'optimisation multi-objectif externe basée sur une variante de l'algorithme génétique NSGA-II. Un ensemble de solutions du Pareto a été généré représentant le compromis optimal entre les différents objectifs considérés dans l'analyse. Une méthode basée sur une Analyse en Composantes Principales (ACP) est appliquée pour détecter et enlever les objectifs redondants de l'analyse sans perturber les caractéristiques principales de l'espace des solutions. Enfin, un outil d'aide à la décision basé sur M- TOPSIS a été utilisé pour sélectionner l'option qui offre un meilleur compromis entre toutes les fonctions objectifs considérées et étudiées.

Bien que les modules photovoltaïques à base de silicium cristallin (c-Si) ont une meilleure performance vis-à-vis de la production d'énergie, les résultats ont montré que leur impact environnement est le plus élevé des filières technologiques de production de panneaux. Les technologies en « couches minces » présentent quant à elles le meilleur compromis dans tous les scénarios étudiés.

Une attention particulière a été accordée aux processus de recyclage des modules PV, en dépit du peu d'informations disponibles pour toutes les technologies évaluées. La cause majeure de ce manque d'information est la durée de vie relativement élevée des modules photovoltaïques. Les données relatives aux procédés de recyclage pour les technologies basées sur CdTe et m-Si sont introduites dans la procédure d'optimisation par l'écoconception. En tenant compte de la production d'énergie et du temps de retour sur énergie comme critères d'optimisation, l'avantage de la gestion de fin de vie des modules PV a été confirmé. Une étude économique de la stratégie de recyclage doit être considérée et étudiée afin d'avoir une vision plus globale pour la prise de décision.

Mots-clés: Écoconception, Optimisation Multi-objectif, Systèmes Photovoltaïques (PV), Algorithme Génétique (AG), Analyse en Composantes Principaux (ACP), Méthode d'aide à la décision multi-critère (MADMC)

Resumen

Ecodiseño de sistemas fotovoltaicos (FV) a gran escala por optimización multi-objetivo y Análisis de Ciclo de Vida (ACV)

Debido a la creciente demanda de energía a nivel mundial y los numerosos daños causados por el uso de fuentes fósiles, la contribución de las energías renovables en el mix energético global se ha incrementado significativamente con el objetivo de avanzar hacia un desarrollo más sostenible. En ese contexto, el presente trabajo tiene como objetivo el desarrollo de una metodología general para el diseño de sistemas fotovoltaicos basados en los principios del ecodiseño considerando de manera simultánea los aspectos técnico-económicos y ambientales. Con el fin de evaluar el desempeño ambiental de los sistemas FV, una técnica de evaluación ambiental basada en el Análisis de Ciclo de Vida (ACV) fue utilizada. El modelo ambiental fue acoplado exitosamente con el modelo para el diseño de un sistema fotovoltaico conectado a la red eléctrica. El modelo para el diseño de un sistema fotovoltaico fue desarrollado a partir de la estimación de la radiación solar recibida en una ubicación geográfica específica, el cálculo de la energía anual generada a partir de la radiación solar recibida, las características de los diferentes componentes y la evaluación de los criterios tecno-económicos a través del tiempo de retorno energético (EPBT, en ingles) y el periodo de recuperacion de la inversion (PRI). En seguida, el modelo fue incrustado en un bucle externo destinado a la optimización multi-objetivo tomando como referencia una variante del algoritmo genético NSGA-II. Un conjunto de soluciones de Pareto fue generado, el cual representa el compromiso óptimo entre los objetivos considerados en el análisis. El método de Análsis de Componentes Principlaes (ACP) fue aplicado para detectar y eliminar los objetivos redundantes existentes sin alterar las principales características del espacio de soluciones. Finalmente, una herramienta de ayuda para toma de decisiones basado en M-TOPSIS fue utilizado para seleccionar la alternativa que ofrece un mejor compromiso entre todas las funciones objetivo consideradas y estudiadas.

Los resultados mostraron que los módulos fotovoltaicos basados en silicio cristalino (c-Si) tienen un mejor desempeño en la generación de energía, sin embargo el impacto ambiental que generan es el más elevado de entre todas las tecnologías de paneles solares consideradas. Los módulos fotovoltaicos fabricados a partir de TF presentan el mejor compromiso en todos los escenarios estudiados.

Una atención especial fue puesta a los procesos de reciclaje de módulos fotovoltaicos, a pesar de que actualmente no existe suficiente información disponible para todas las tecnologías evaluadas. La principal causa de esta falta de información es la vida útil de los módulos fotovoltaicos. Los datos relativos a los procesos de reciclado para las tecnologías de CdTe y m-Si fueron introducidos en el procedimiento de optimización basado en el ecodiseño. La importancia de los beneficios que tiene la gestión de los módulos fotovoltaicos al final de su vida útil fue puesta en evidencia al considerar la producción de energía y el tiempo de retorno energético como criterios de optimización. Un estudio económico de las estrategias de reciclage debe ser considerado e investigado con el fin de tener una visión más integral para la toma de decisiones futura.

Palabras claves: Ecodiseño, Optimización Multi-objetivo, Análisis de Ciclo de Vida (ACV), sistemas fotovoltaicos (FV), Algoritmos Genéticos (GA), Análisis de Componentes Principales (ACP), Métodos de Ayuda a la Toma de Decisiones Multi-critério

CONTENT

INTRODUCTION GÉNÉRALE

L'énergie du rayonnement solaire reçue sur la Terre constitue le seul véritable apport renouvelable extérieur au « système Terre ». Elle représente 8 000 fois la consommation de l'humanité pour une année et se décline en de nombreuses formes d'énergies renouvelables exploitables (rayonnement, vent, hydraulique, biomasse, …). Cet énorme potentiel est donc invoqué pour répondre aux défis posés à l'humanité en matière d'énergie et de développement durable. Notamment, la génération directe d'électricité à partir du rayonnement solaire apparaît des plus prometteuses. Elle s'opère par deux voies principales: les centrales thermosolaires à concentration et tous les systèmes à conversion photovoltaïque exploitables dans une très large gamme de puissances. Les installations photovoltaïques ont ainsi connu une croissance récente vertigineuse, la puissance installée dans le Monde passant de 1,4 à 102 GW crête en 10 ans, notamment de 13 à 25,5 GW crête au cours de la seule année 2012 en Europe, leader dans cette avancée vers un Monde de l'énergie renouvelé et différent. Mais apparaissent dans le même temps plusieurs inconvénients dénoncés, tels que par exemple les besoins en eau des centrales thermosolaires installées en milieux ensoleillés arides, les impacts nocifs de la fabrication des matériaux photovoltaïques ou encore l'emprise au sol et sur les paysages de toutes ces installations artificielles nouvelles. Emblématique d'un développement durablela filière solaire se doit donc de veiller particulièrement à limiter son impact écologique et de maîtriser son développement de façon exemplaire.

C'est dans ce contexte que les travaux de doctorat présentés dans ce mémoire ont été menés: ils concernent particulièrement la conception et l'implantation de grands systèmes de panneaux solaires installés au sol. La bourse de thèse associée a été octroyée par CONACYT (Consejo Nacional de Ciencia y Tecnología, Mexico). Les travaux effectués ont fait l'objet d'une collaboration entre, d'une part, l'équipe COOP du Département Procédés et Systèmes Industriels (PSI) au sein du Laboratoire de Génie Chimique, LGC UMR CNRS INPT UPS 5503 et d'autre part l'équipe Genesys du LAPLACE (Laboratoire Plasma et Conversion d'Energie), UMR CNRS INPT UPS 5213. Les deux équipes ont des compétences complémentaires:

- L'équipe **COOP (C**onception **O**ptimisation **et O**rdonnancement des **P**rocédés du département PSI**)** a pour thème général de recherche l'optimisation et la conception de procédés. La démarche s'inscrit de façon prépondérante dans le développement de stratégies d'optimisation en variables mixtes (variables continues liées aux conditions

d'exploitation, variables entières relatives à la structure du procédé ou à des choix décisionnels) via des méthodes stochastiques ou déterministes, avec une forte orientation vers les méthodes d'optimisation multicritère.

- Le Groupe **GENESYS** (**EN**ergie **E**lectrique et **SYS**témique) a pour objectifs de concevoir des dispositifs hétérogènes, en considérant le système dans sa globalité et sa finalité. Ses compétences se trouvent dans les méthodes de conception intégrée (synthèse, analyse, optimisation) notamment dans les nouvelles technologies de l'énergie.

L'étude présentée a bénéficié du support financier d'un BQR PRES Université de Toulouse baptisé **OSSOLEMIO O**ptimisation **S**ystèmes **SO**laires **L**arge **E**chelle **M**ult**I O**bjectifs (2010-2012) qui a plus largement été dédié à l'étude des deux grandes voies complémentaires de production d'électricité solaire citées ci-dessus et actuellement en d'une part les centrales thermosolaires à concentration par héliostats offrent la possibilité de stocker l'énergie solaire sous forme thermique avant conversion en électricité, ce qui permet de pallier l'intermittence de la production. On peut ainsi obtenir des températures élevées nécessaires à la production de chaleur, d'électricité ou d'hydrogène [cf thèse d'Alaric Montenon (Montenon, 2013)]. D'autre part les générateurs photovoltaïques implantés en toitures ou en en plein champ, fixes ou montés sur des suiveurs solaires, débitant au fil du soleil leur production dans le réseau électrique.

L'étude présentée ici ne s'intéresse qu'à l'implantation de panneaux fixes d'un parc photovoltaïque de production d'électricité connecté au réseau.

La conception de ces systèmes photovoltaïques à grande échelle est encore actuellement surtout basée sur une approche technico-économique qui a comme objectif de maximiser la production d'énergie. Mais certains éléments, tels que le niveau d'émissions globales, notamment en gaz à effet de serre doivent être pris en compte pour renforcer l'intérêt de la filière et lui assurer un caractère effectivement durable. En fonction des technologies et de l'implantation des modules, il s'agit ici de concevoir des champs de panneaux solaires de façon optimale en combinant des critères de production et d'impact environnemental, afin de développer une méthodologie d'écoconception. Il est donc important également de considérer le recyclage des panneaux afin de régénérer les matériaux qui les constituent. Une analyse du cycle de vie complet a donc constitué une étape préliminaire afin d'évaluer le coût écologique des panneaux et du câblage associé à intégrer dès la conception du système photovoltaïque. Compte tenu du nombre de paramètres et de critères à traiter, le cœur de l'étude vise à proposer une méthode de conception par optimisation qui sélectionne les solutions les plus durables parmi un très grand nombre de choix possibles.

Le mémoire de thèse est organisé en sept chapitres dont nous ne donnons ci-dessous que les titres, la présentation de leur contenu étant donnée à la fin du premier chapitre qui permet de poser les éléments motivant cette étude et d'introduire de façon plus détaillée les chapitres de ce document :

Chapitre 1 Motivation de l'étude et présentation de l'état de l'art

Chapitre 2 Analyse du Cycle de Vie pour les systèmes photovoltaïques

Chapitre 3 Cadre de modélisation et de simulation pour les centrales photovoltaïques à grande échelle

Chapitre 4 Méthodes et outils pour l'écoconception : combiner optimisation multi-objectif, analyse en composantes principales et aide à la décision multicritère

Chapitre 5 Ecoconception de centrales photovoltaïques à grande échelle

Chapitre 6 Recyclage de modules de panneaux solaires

Chapitre 7 Conclusions et perspectives

Chapter 1

MOTIVATION FOR THE STUDY AND STATE-OF-THE ART REVIEW

Ce chapitre d'introduction vise à définir le cadre de cette étude et justifie les objectifs généraux qui ont guidé ces travaux. La partie 1 présente brièvement le contexte énergétique général. Le cas de l'énergie solaire, sur laquelle est centrée l'étude est analysé en détail dans la partie 2. Les caractéristiques techniques des systèmes photovoltaïques sont présentées dans la partie 3 et le développement du marché photovoltaïque est positionné dans la partie 4. Les méthodes traditionnelles de conception et de dimensionnement du système photovoltaïque décrites dans la littérature spécialisée sont ensuite proposées, ce qui justifie l'intérêt de développer une méthode d'éco-conception combinant analyse de cycle de vie, optimisation multiobjectif et procédures multicritères d'aide à la décision pour les systèmes photovoltaïques à grande échelle, ce qui est la base de cette étude. L'organisation du manuscrit est présentée à la fin de ce chapitre.

Nomenclature

Acronyms

APAC	Asia-Pacific region
DC/AC	Direct Current / Alternative Current
CdTe	Cadmium telluride
CIS	Copper indium diselenide
CPV	Concentrating PV
DSSC	Dry-Sensitized Solar Cell
EPIA	European Photovoltaic Industry Association
GHG	Greenhouse Gas
LCA	Life-Cycle Assessment
LCI	Life-Cycle Inventory
LCIA	Life-Cycle Impact Assessment
MEA	Middle East and Africa
PV	Photovoltaic
PVGCS	Photovoltaic Grid-Connected System
ROW	Rest of the World
a-Si	Amorphous silicon
c-Si	Crystalline silicon
m-Si	Monocrystalline silicon
p-Si	Polycrystalline silicon
ribbon-Si	Silicon sheet-defined film growth
STE	Solar Thermal Energy
TF	Thin Film

1.1 Introduction

This introduction chapter aims at defining the context of this study and justifies the general objectives that have guided this work. It is divided into 7 sections. Section 1 presents briefly the general energy context. The case of solar energy, that constitutes the centre of this study is thoroughly analysed in section 2. The technical features of PV systems are presented in section 3 and the PV market development is positioned in section 4. The traditional PV System design and sizing methods reported in the dedicated literature are then proposed, which justifies the interest to develop an ecodesign method combining Life Cycle Assessment, Multi-Objective Optimization and Multiple Criteria Decision-Making procedures for large-scale PV systems which is the core of this study and which has received little attention till now to our knowledge. The organization of the manuscript ends this chapter.

1.2 General context

During the last decades, the new technological advances have drastically changed our lifestyle. These changes try to satisfy our primary needs as human beings but equally they intended to provide comfort by eliminating repetitive tasks and facilitating our daily life. To achieve these objectives, the generation and supply of energy has become a crucial element for the sustainability of modern society. The demand for the provision of energy is increasing rapidly worldwide and the trend is likely to continue in future. Increase in its production translates into better quality of life and creation of wealth. Electricity producing systems presently in use across the world can be classified into three main categories: fossil fuels, nuclear power and renewables (Prakash & Bhat, 2009). Fossil fuels in their crude form, i.e. wood, coal and oil is traditionally the most extensive energy resource used. Nuclear power has been only accessible within developed countries. Renewable energy resources are abundant in nature and easily accessible around the world. Renewable energy sector is now growing faster than the growth in overall energy market. Solar, wind, geothermal, modern biomass, as well as hydro are some of the sources used in this category.

In 2011, the worldwide electricity generation was 21,964 TWh which 67.9% was originated from fossil fuels, 11.7% from nuclear, and 20.2% from renewable sources (Observ'ER, 2012). The graphic in Figure 1-1 represents the allocation of each of the three systems in global electricity production by 2011. Likewise, the emphasis is on the distribution of power generation of the six main sources of renewable energy. Hydroelectricity is the main source for renewable energy with a share of 80.5%.

Nowadays it is clearer that fossil fuel-based energy sources are damaging the environment and human life. Environmental pollution (of air, water, etc.) is largely linked to the increasing use of energy. Climate change due to use of fossil fuel with emissions of sulphur dioxide (SO_2), nitrogen oxide (NO_X) and carbon dioxide (CO_2) is a worldwide problem that has a big impact in the future of all the species living in the Earth. The Kyoto Protocol (United Nations, 2013), an international environmental treaty, sets the obligations for industrialised countries to reduce overall emissions from six greenhouse

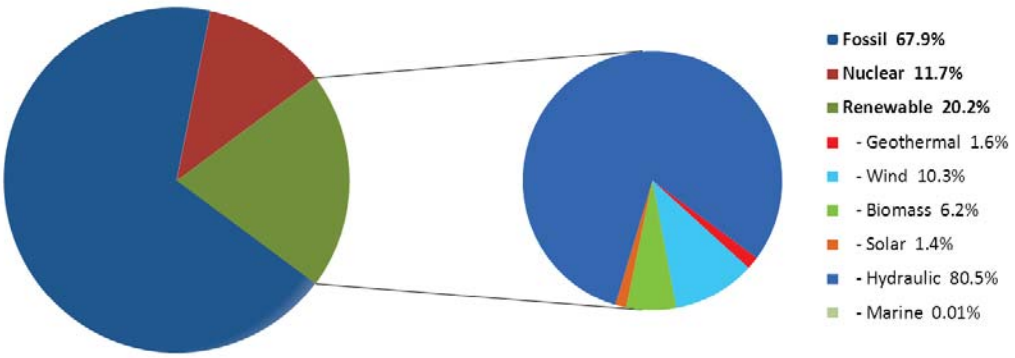

Figure 1-1 Structure of electricity production in 2011 (Observ'ER, 2012)

gases (GHG): carbon dioxide (CO_2), methane (CH_4), nitrous oxide (N_2O), sulphur hexafluoride (SF_6),hydrofluorocarbons (HFCs) and perfluorocarbons (PFCs). Because of this situation, the development of renewable energy systems is a current international priority for response to global warming. Some long-term scenarios postulate a rapidly increasing share of renewable technologies. Under these scenarios, in the second half of the 21st century, renewable source could satisfy between 20% to 50% of world's total energy demand with the right policies in place and new technology developments (Akella, Saini, & Sharma, 2009). Table 1-1 shows the evolution from 2001 to 2011 of world electricity production by source. From this information wind (28.3%) and solar (45.8%) sources have considerably increased their contribution among renewable sources.

Several problems and disadvantages of the use of renewable energy can be yet highlighted:

- A first apparent drawback, often cited is related to the low efficiency of the transformation of the initial energy provided by the source into electricity. But, it is important to underline that an usual 33% efficiency of conversion of traditional fossil or nuclear plants implies the dramatic waste of the two third of a precious natural reserve of energy, definitely lost for the future generations, while the typical 14% efficiency of a photovoltaic conversion simply means that only this proportion is extracted out of a permanently renewable source otherwise 100% available for the local environment for natural biosynthesis or local heating. Thence and moreover, such low conversion efficiency can augur a low local environmental impact. However and on another hand, as renewable sources are generally available with low space densities, a true difficulty is to harvest enough final energy required by supplied applications while not using a very large land space. This latter one is of course especially larger with lower efficiency conversion devices. Furthermore, improved devices with higher conversion efficiency are often much more expensive with these very new technologies still in early development. So, the main consequence of this situation is on one hand a larger spreading on land space which may modify the natural landscapes in a non-friendly way and on the other hand a high cost of the generated electricity (see following point). This may lead to search an optimum compromise between cost and occupied land space. So, in our opinion, a low conversion efficiency of a renewable energy should not be directly considered and cited as an obvious drawback by itself.

Table 1-1 World electricity production by source in TWh (2001-2011) (Observ'ER, 2012)

Source	2001	2008	2009	2010	2011	Variation 2001-2011
Renewable	*2,862.4*	*3,812.5*	*3,951.1*	*4,225.2*	*4,447.5*	*4.50 %*
- Geothermal	51.7	65.3	67.3	68.5	69.9	3.10 %
- Wind	37.9	219.6	276.4	351.5	459.9	28.30 %
- Biomass	134.1	232.0	250.8	270.1	276.0	7.50 %
- Solar	1.4	12.8	21.0	33.5	61.6	45.80 %
- Hydraulic	2,636.8	3,282.3	3,335.2	3,501.1	3,579.5	3.10 %
- Marine	0.575	0.546	0.527	0.558	0.555	-0.40 %
Fossil	*10,010.6*	*13,637.5*	*13,409.6*	*14,340.4*	*14,908.1*	*4.10 %*
Non-renewable waste	*39.3*	*38.7*	*40.0*	*43.1*	*40.3*	*0.30 %*
Nuclear	*2,637.7*	*2,730.8*	*2,696.4*	*2,755.1*	*2,568.2*	*-0.30 %*
Total Production	***15,55.,075***	***20,219.546***	***20,097.227***	***21,363.858***	***21,964.055***	

- The current cost of renewable energy technology is an impediment for its development. The establishment of government policies that subsidize the implementation of these facilities as well as investment in research of materials and mechanisms to increase processing efficiency and reduce manufacturing cost are necessary to achieve its growth and consolidate its position as the main source of replacing traditional methods of energy generation. Particularly, these technologies require expensive installation investments with long payback times.
- It must be also said that an enormous amount of fossil energy is required to manufacture, install and operate all forms of renewable energy systems. Without the input of fossil fuel the existing renewable energy projects probably could never have been built and could not be maintained in operation actually. The raw materials and components used require energy intensive extraction and fabrication techniques to be produced, and along with the finished products, also have to be transported across substantial distances. But, in most cases with the present improved technologies, the assessment on energy on the total life cycle is now positive which augurs of a sustainable development.
- A main drawback which becomes a very strong impediment for a large development of renewable sources of electricity is the dependency to geographic and meteorological conditions, making them sometimes very variable along different time scales (night and day, different seasons) and even sometimes and somewhere unpredictable and inconsistent. As the usual electric grid reliable work requires the very good knowledge of consumptions and productions and very good regulations often based on well controlled sources of electricity these properties set a new crucial problem to be solved by means of the so-called new "smart-grids" with new architectures and technologies, for example larger grid connected storage unities. Besides the necessary breakthroughs, this situation generates an increasing of the costs.

In that context, it is an imperative that the use of renewable energy must be efficiently integrated with the natural environment during its whole lifecycle following ecological design. **Ecodesign** is the use of the ecological design principles and strategies to design products, processes and systems that take

into account their impact on the environment at all stages of their life cycle, so that they integrate benignly and seamlessly with the natural environment that includes the biosphere, which contains all the forms of life that exist on earth. This goal must be the fundamental basis for the design of all our human-made environments. The PhD thesis focuses exclusively **on solar energy** with ecodesign guidelines in mind.

1.3 Solar energy

Solar energy is the renewable source that has the most important growth rate (see Table 1-1). Solar irradiation available is more than enough to satisfy the world's energy demands. The total solar energy that reaches the Earth's surface could meet global energy needs 10,000 times over (EPIA, 2011).

Where there is more Sun, more power can be generated that is why the sub-tropical areas of the world offer some of the best locations for solar power generation. Figure 1-2 compares the potential solar irradiation with existing energy sources. As it can be seen in this representation, maximizing the use of solar energy can meet the annual energy consumption across the planet.

The main advantages for solar energy are on the one hand:

- the power source, the Sun, is totally free.
- does not emit any GHG during the energy generation phase.
- can be used in any area on Earth, especially remote areas where it is too expensive to extend the electricity power grid. It can be on or off the grid.
- a very high reliability and a very low maintenance during their 20 - 30 years lifespan despite it is very new and sophisticated technologies.

On the other hand, the main disadvantages for solar energy are:

- the biggest disadvantage is the fact that it is not constant. Solar energy is harnessed when it is daytime. But also, beyond normal daily fluctuations, solar production largely varies with seasons outside the tropical latitudes and everywhere with meteorological conditions.
- large areas of land can be required to harness enough energy for aplications.
- solar systems, made with recent and sophisticated technologies are relatively expensive although prices are falling very rapidly and strongly with the market development.

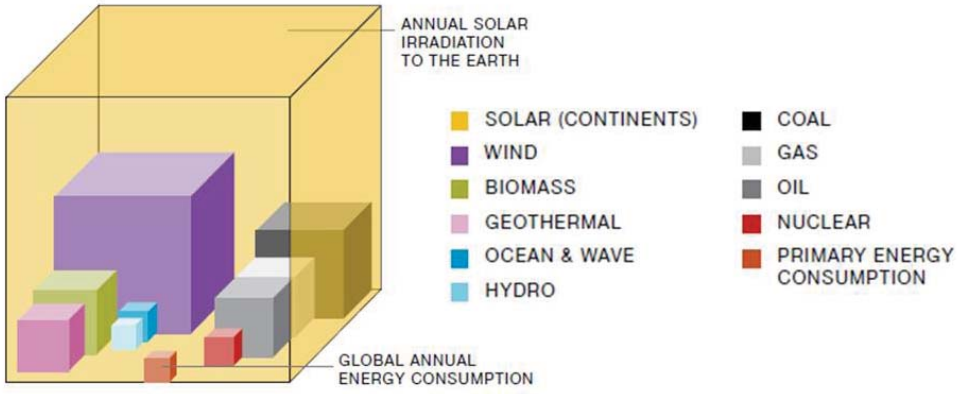

Figure 1-2 Solar irradiation versus global energy resources (EPIA, 2011)

- low conversion efficiency is often cited as a drawback but refer to 1.1 above.

Solar energy can be converted directly into other forms of energy, such as heat and electricity. Heat can be directly used for industrial or domestic use (hot washing water). Electricity can be generated by means of different ways as:

- **Solar thermal energy (STE)** is a technology for harnessing solar energy for thermal energy (heat). In STE, the light from the sun is concentrated to create heat, and that heat is used to run a heat engine, which turns a generator to make electricity. Water, oil, salts, air, nitrogen, helium are used as the fluid heated by the concentrated sunlight. Currently, there are three types of solar thermal power systems in use: the solar dish, solar power tower and parabolic trough (Solar Thermal, 2008).
- **Photovoltaic energy conversion (PV)** directly converts the light of Sun into electricity. Some materials that are sensitive to the solar radiation react in such a way that they can produce electricity. The conversion is generqlly accomplished through a thin plate of light sensitive material called solar cell or PV cell.

This work will address **PV energy conversion**.

1.4 PV System

PV technology has shown the potential to become a major source of power generation for the world. Proof of this is the fact that at the end of 2009 the PV cumulative installed capacity in the world was approaching 24 GW and in 2012, more than 100 GW are installed globally and they can produce at least 110 TWh of electricity every year (EPIA, 2013). This represents a growth of capacity of three times.

PV power generation employs PV modules composed of a number of solar cells containing a photovoltaic material that converts sunlight into electricity (see Figure 1-3 for a diagram of the photovoltaic effect). A typical PV system is basically made up of one or more photovoltaic PV modules, a mounting system that holds the PV modules and electrical interconnections, a DC/AC power converter (also known as inverter) which can deliver standard alternating voltage and current. A battery system for electricity storage may be included.

PV systems are classified in either off-grid systems or grid-connected systems (see Figure 1-4) (EPIA, 2011; Luque & Hegedus, 2003; Markvart & Castañer, 2003). Off-grid systems, also known as stand-alone systems, have no connection to an electricity grid. That is why a battery is required to deliver the electricity needed at anytime especially during night or after several days of low irradiation. Stand-alone systems fall into one of three main groups:

- Off-grid industrial applications. To power repeater station for mobile telephones, traffic signals, remote lighting, highways signs, marine navigation aids among others.
- Off-grid systems for electrification. To bring electricity to remote areas or developing countries

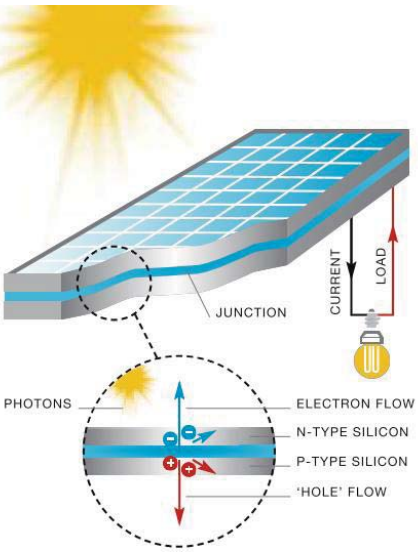

Figure 1-3 Photovoltaic effect (EPIA, 2011)

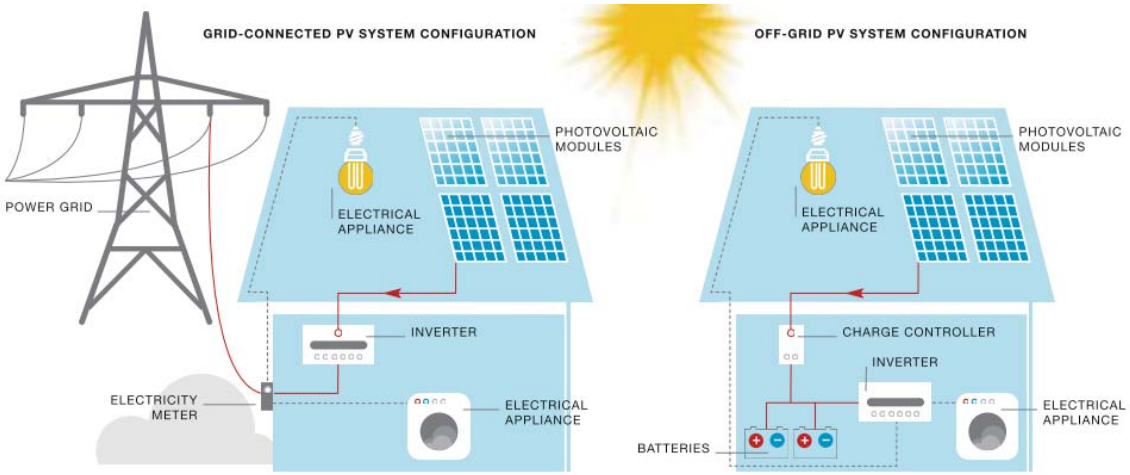

Figure 1-4 Different configurations of PV solar systems from (EPIA, 2011)

- Consumer goods. Like those found in several electrical applications such as calculators, toys, watches, etc.

Grid-connected systems (PVGCS) are the most popular type of solar PV system and will be the core of this study. Connection to the local electricity network allows any excess power produced to be sold. PVGCSs are classified in two main groups: residential and commercial systems and, industrial and utility-scale power plants. Residential and commercial systems are the most extensible used PVGCS because they can be installed on homes and businesses. By connecting to the local electricity network, owners can sell their excess power, but, when solar energy is not available, electricity can be drawn from the grid. This type of PVGCS generates up to 100 kWp (kilo Watt-peak). It must be said at this level of the presentation that kilo Watt-peak stands for peak power. This value specifies the output power delivered by a photovoltaic device (cell, module or system) working at its maximum power under set Standard Test Conditions i.e. a solar radiation of 1,000 watts per square meter, a cell temperature of 25°C and an Air Mass of 1.5.

Industrial and utility-scale power plants produce enormous quantities of electricity (>1 MWp). They need a large space to be installed. The solar panels are usually mounted on frames on the ground. However, they can also be installed on large industrial buildings such as warehouses, airport terminals or railway stations.

A PVGCS is integrated through the following key elements: PV modules, DC/AC inverter and mounting system.

1.4.1 *PV module*

PV modules are made of PV cells incorporated into a unit, usually by soldering them together under a sheet of glass. Module producers usually guarantee a power output of 80% of the nominal power even after 20-25 years. Modules can be connected to each other in series (known as an array) to increase the total voltage produced by the system. The arrays are connected in parallel to increase the system current.

PV modules are grouped as first, second or third generation according the technology uses for manufacturing the solar cell (Lund, Nilsen, Salomatova, Skåre, & Riisem, 2008; Petter Jelle, Breivik, & Drolsum Røkenes, 2012). The first generation includes modules made by silicon cells. Silicon cells have a quite high efficiency, but very pure silicon is needed so the manufacturing process requires a big amount of energy. Efficiencies of more than 20% have been obtained with silicon cells already produced in mass production (EPIA, 2011). Mono-crystalline (m-Si), poly-crystalline (p-Si) and silicon sheet-defined film growth (ribbon-Si) are considered in this generation. These technologies are named crystalline-Silicon technology (c-Si). Silicon-based modules dominate the current market (EPIA, 2013).

The so-called thin film (TF) PV modules are considered as second-generation PV technologies. It includes three main families: amorphous silicon (a-Si), Cadmium-Telluride (CdTe) and Copper-Indium-Selenide (CIS). TF solar cells are comprised of successive thin layers, just 1 to 4 μm thick (Luque & Hegedus, 2003). The combination of using less material and lower cost manufacturing processes allow the manufacturers to produce and sell PV modules at a much lower cost. In addition, TFs can be packaged into flexible and lightweight structures. The main disadvantage is the lower efficiency (7-12%) (EPIA, 2011).

Third-generation PV modules include technologies that are still under demonstration or have not yet been widely commercialised. There are four types of third-generation PV technologies: concentrating PV (CPV), dry-sensitized solar cells (DSSC), organic solar cells and, novel and emerging solar cell concepts. The goal of these technologies is to improve on the solar cells already commercially by growing the conversion efficiency, make them less expensive, and to develop more and different uses. In laboratory tests, they had reached an efficiency of 30% (EPIA, 2011).

According to EPIA (EPIA, 2013), c-Si technology has currently the highest market share (more than 80%) and is expected to maintain it in the future. TF technologies represented about 15% of the

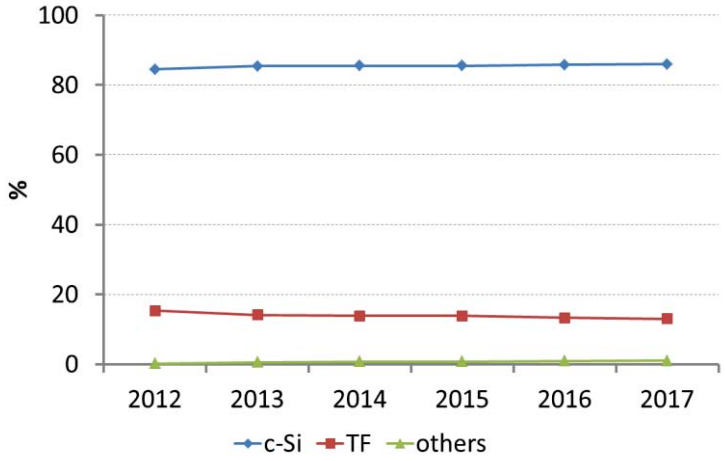

Figure 1-5 PV module technology market share, based on (EPIA, 2013)

market share in 2012, while third-generation technology represented less than 1% of market share but it is attended to get 1% of market for 2017. Figure 1-5 shows the PV technology market share in 2012 and the projection of PV market until 2017.

1.4.2 *DC /AC Inverter*

The DC/AC inverter is the second most important component. PV modules produce direct current (DC). However, most appliances run on alternating current (AC). Consequently, an inverter must be used to convert the DC into AC. Inverters are widely used for many industrial applications. The PV inverter has another very important role in PV systems achieving a Maximum Power Point Function (MPPT). This MPPT function consists in varying the electrical operating point of the PV array in order to maintain its output power at the maximum value possible which mainly depends on the environmental conditions: solar irradiation and temperature, that is, the variable bias point at which the PV array produces highest power extraction. Changes of temperature and insolation change the voltage where maximum power extraction occurs. Today, intelligent inverter control includes very effective maximum power point tracking systems (MPPT).

Inverters have often been the source of poor reliability in early systems. Feedback to manufacturers and more robust components has greatly reduced these problems, taking benefit of the tremendous development of power electronics and of the PV systems market.

Today most inverter models are additionally equipped with data loggers and measurement computers, which allow the power, voltage, current and other operating parameters to be recorded continuously and often available by an internet link.

1.4.3 *Mounting system*

The structures of mounting system are typically pre-engineered systems of aluminium or steel racks. Mounting structures vary depending on where the PV systems are sited, with different solutions of ground-mounted systems. PV modules must be mounted such that they face the best angle. Because of their low value and substantial weight, mounting and racking structures are generally assembled locally.

Simple fixed platforms are commonly the most used, due their very high reliability. It is possible to install tracking platforms that can tilt the PV sensors surface along one or two axis by means of electric motors and a control device that determines the actual position of the sun. Not surprisingly, tracking can provide a significant energy boost so long that it is reliable. However, this comes at a cost and reduced reliability, as the tracking mechanics are more complicated and expensive.

1.5 Historical PV market development

Figure 1-6 exhibits the evolution of PV cumulative installed capacity in the world from 2000 to 2012. Figure 1-6 also displays the cumulative capacity by region. Europe leads with more than 70 GW installed about 70% of total, particularly thanks to a very strong policy of Germany, the far leader. Next in the ranking are Asia-Pacific region (APAC) with 12.4 GW installed, America with almost 8.7 GW and not far away China with 8.3 GW. Middle East and Africa (MEA) and the Rest of the World (ROW) represent about 3 GW of world's total PV capacity in 2012.

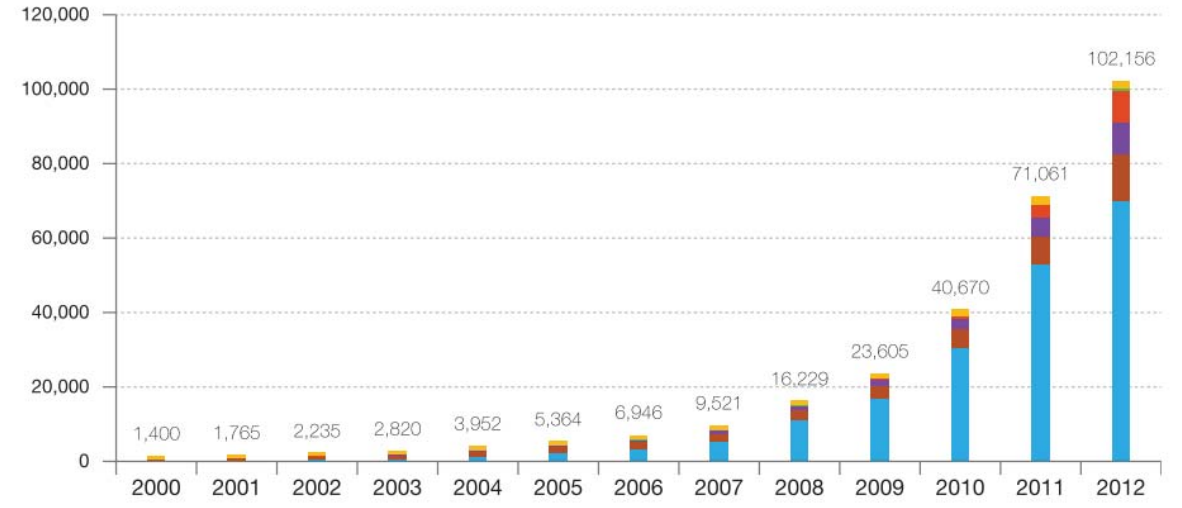

	2000	2001	2002	2003	2004	2005	2006	2007	2008	2009	2010	2011	2012
ROW	751	807	887	964	993	1,003	1,108	1,150	1,226	1,306	1,590	2,098	2,098
MEA	n/a	n/a	n/a	n/a	1	1	1	2	3	25	71	192	601
China	19	24	42	52	62	70	80	100	140	300	800	3,300	8,300
Americas	146	178	225	290	394	501	650	863	1,209	1,752	2,780	4,959	8,717
APAC	355	495	686	916	1,198	1,500	1,825	2,096	2,631	3,373	4,956	7,628	12,397
Europe	129	262	396	598	1,305	2,289	3,281	5,310	11,020	16,850	30,472	52,884	70,043
Total	1,400	1,765	2,235	2,820	3,952	5,364	6,946	9,521	16,229	23,605	40,670	71,061	102,156

Figure 1-6 Evolution of global cumulative installed capacity 2000-2012 (MW) (EPIA, 2013)

Table 1-2 Top 10 countries with the highest PV cumulative installed capacity in 2012 (EPIA, 2013)

	Country	Cumulative in GW		Country	Cumulative in GW
1	Germany	32.4	6	Spain	5.2
2	Italy	16.3	7	France	4.0
3	China	8.3	8	Belgium	2.7
4	United States	7.8	9	Australia	2.4
5	Japan	6.9	10	Czech Republic	2.1

Table 1-2 shows the top 10 countries with the highest PV cumulative installed capacity in 2012. Not surprisingly, Germany continues to be, and with a large difference, the world leader (32.4 GW).

According to the predictions made by the European Photovoltaic Industry Association (EPIA) (EPIA, 2013), a fastest PV growth is expected to continue in China and India, followed by Southeast Asia, Latin America and the MEA countries. The projections for the growth of PV cumulative installed capacity in the world until the year 2017 by region are presented in Figure 1-7 with two possible scenarios. The first called *Business-as-Usual scenario* assumes a pessimistic market with no major reinforcement or replacement of existing support mechanisms. This scenario also assumes that if the country is close to energy transition, markets are significantly slowing down because the policy mechanisms designed to accelerate investment in renewable energy technologies are phased out. The second scenario called *Policy-Driven scenario* assumes the continuation, adjustment or introduction of adequate support mechanisms with strong policies to allow considering PV as a major power source in the coming years.

1.5.1 *European Market*

During 2012 in Europe around 17 GW of new PV installations were mounted. That is why PV became the number-one electricity source among the countries of European Union (EU) in terms of added installed capacity. Figure 1-8 shows the number of new power generation capacities by source added in 2012. It can be seen that for traditional sources (fossil fuel and nuclear) the installed capacity balance turned negative last year. A significant number of facilities were dismantled.

Germany contributed to 44.31% of new PV installations that allow the European market to keep a reasonable level in relation to the other regions. Figure 1-9 indicates the percentage of new grid-connected PV capacities by country in Europe during 2012.

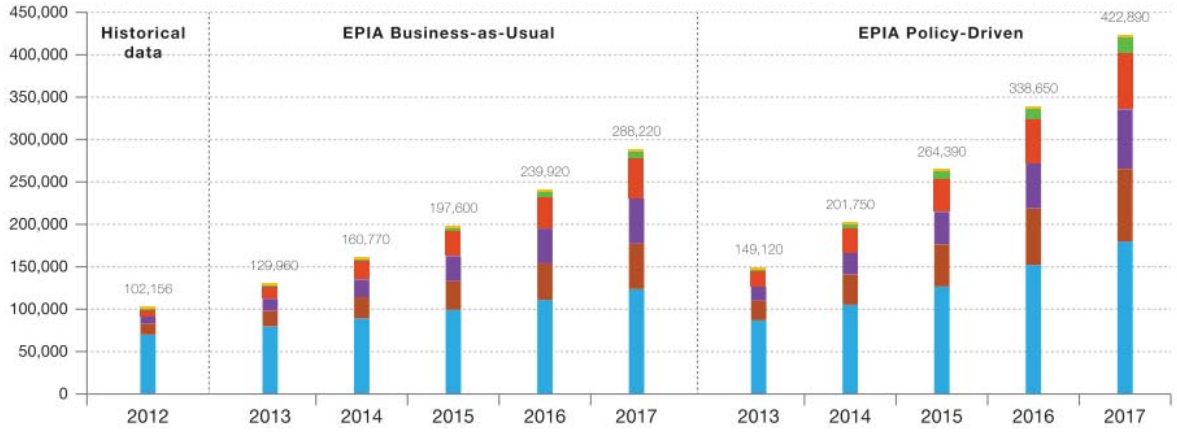

	2012	2013	2014	2015	2016	2017	2013	2014	2015	2016	2017
ROW*	2,098	2,098	2,098	2,098	2,098	2,098	2,098	2,098	2,098	2,098	2,098
MEA	601	1,260	2,180	3,480	5,380	7,780	2,100	4,800	8,200	12,700	18,750
China	8,300	14,300	21,300	29,300	37,300	47,300	18,300	28,300	39,300	51,300	66,300
Americas	8,717	14,430	21,090	29,880	41,090	53,820	16,810	25,900	38,400	53,790	70,380
APAC	12,397	18,130	25,060	33,720	43,230	53,590	22,990	35,470	49,760	66,760	85,810
Europe	70,043	79,750	89,040	99,120	110,830	123,640	86,820	105,180	126,630	152,010	179,560
Total	102,156	129,960	160,770	197,600	239,920	288,220	149,120	201,750	264,390	338,650	422,890

Figure 1-7 Evolution of global PV cumulative installed capacity per region until 2017 in MW (EPIA, 2013)

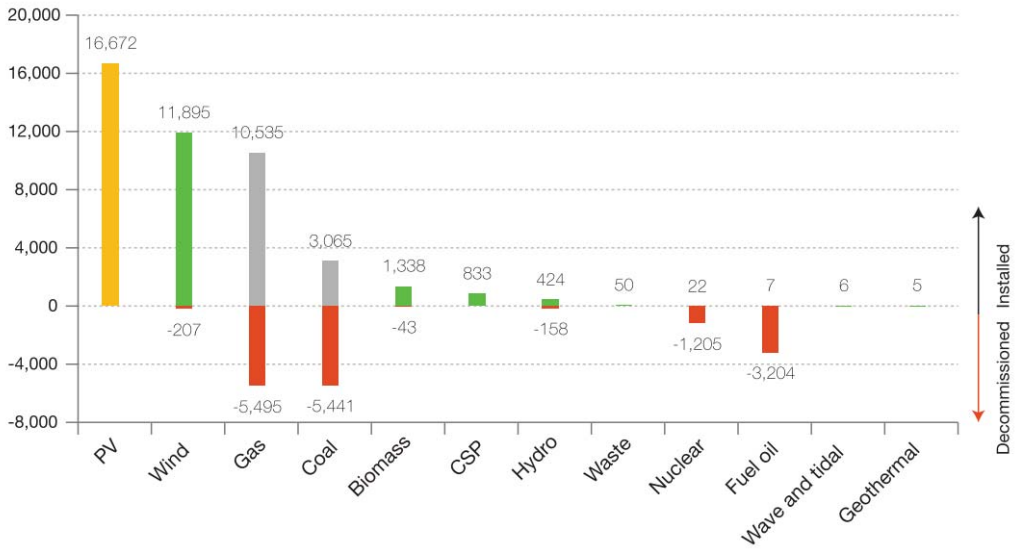

Figure 1-8 Power generation capacities added in the EU 27 in 2012 (MW) (EPIA, 2013)

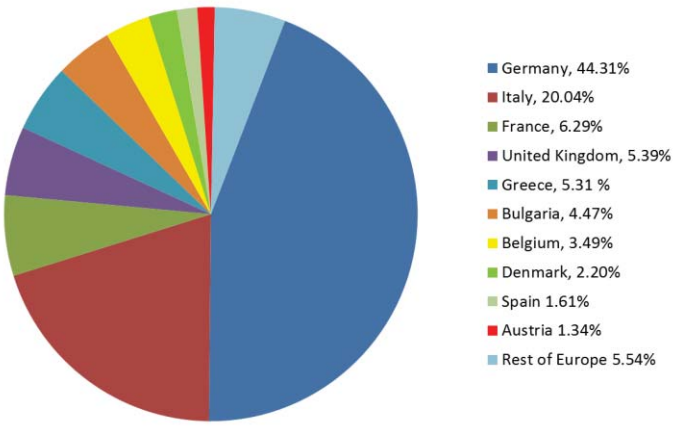

Figure 1-9 European new grid-connected PV capacities in 2012 (EPIA, 2013)

1.5.2 *Production market of PV modules*

The regional share of actual production of different PV module technologies in 2012 is presented in Figure 1-10. PV industry remained strong in Asia with China playing a leading role. China leads the production market of crystalline modules (c-Si) while the APAC region, with Japan and Malaysia as top producers, leads the TF production market with more than 60% of production share.

EPIA 2012 (EPIA, 2013) report indicates that no major changes should be expected in the main PV technologies, crystalline silicon (c-Si) and TF in the next five years. A slightly higher growth rate is expected for c-Si (6.34%) mainly due to the uncertainty of amorphous silicon (a-Si) technologies, for which the growth rate might be reduced by around 3% until 2017. The reason is the lower module efficiency of a-Si in comparison with the rapid evolution of CdTe and Copper Indium Gallium Selenide (CIGS) with efficiencies below 10% on module level. It is expected that by 2017 CdTe has a 5.95% growth while for CIGS growth will be 8.70%.

Moreover, the permanent decreasing of PV crystalline silicon (c-Si) due to a fast growing of production unities and market, particularly in China, slows down the diffusion of theoretically less

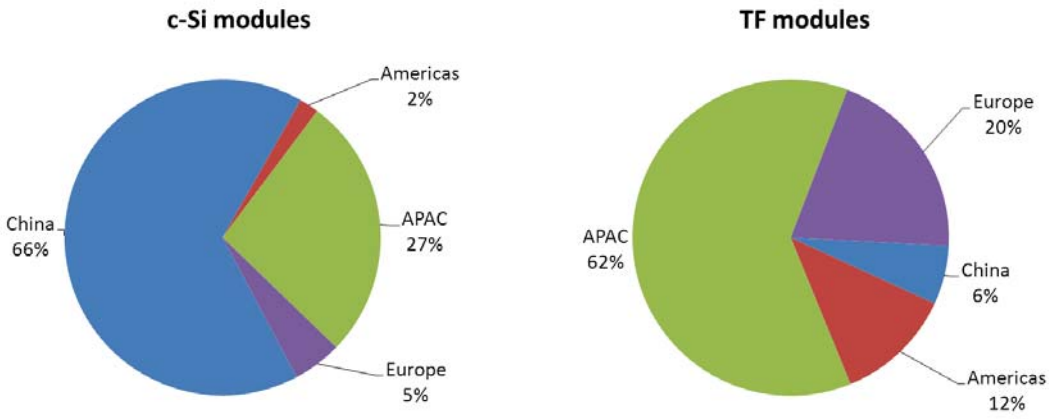

Figure 1-10 Global PV production in 2012 by region (EPIA, 2013)

expensive other technologies.

1.5.3 *PVGCS situation*

In 2012 utility-scale applications reached more than 9 GW. EPIA expects utility-scale plants to grow much faster than rooftop applications. In the Policy-Driven scenario, utility-scale market could quadruple from 9 to 37 GW. This can be explained by the nature of the investors in the most promising markets and the reduced opposition to ground-mounted PV systems (Figure 1-11).

At the regional level, the utility-scale segment is expected to at best stagnate in Europe even as it booms in the Americas and Asia including China. In both scenarios, the APAC region including China should see the largest share of new utility-scale applications, ahead of the Americas.

The design and sizing of large-scale PV plants with more efficient energy production are then needed.

1.6 PV System design

Several works have been devoted to the optimized design of PV systems, mainly from a techno-economic viewpoint. The majority of the reported works in the dedicated literature is related either to the minimization of an economic criterion or to the maximization of annual energy produced.

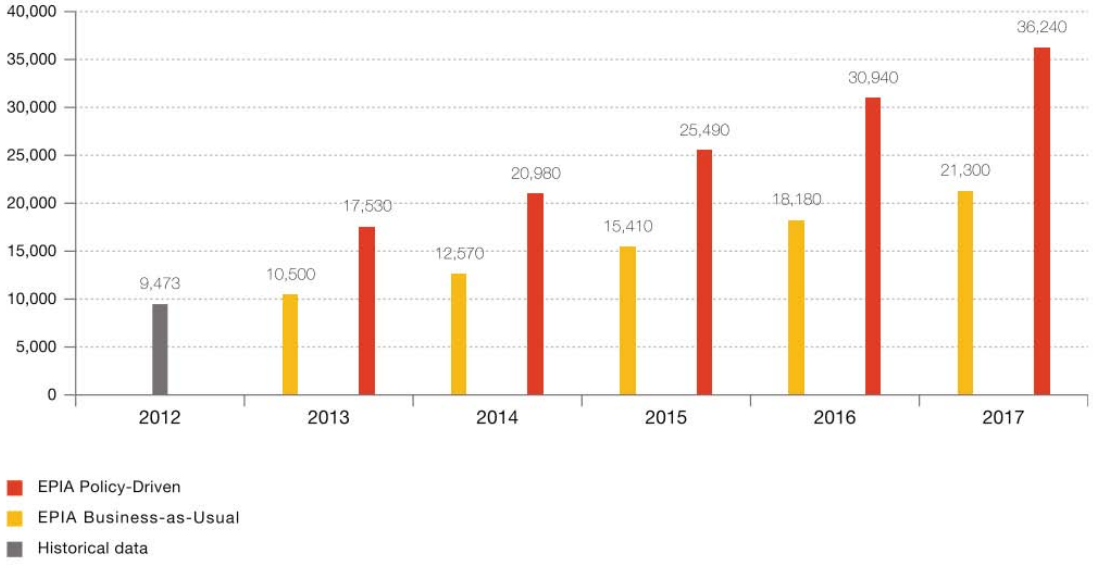

Figure 1-11 Global utility-scale PV development scenarios until 2017 (MW) (EPIA, 2013)

However, these studies have adopted mainly simulation approaches to evaluate the system performance and are exclusively devoted to the electrical performance. An optimal unit sizing method has not been established to rationally determine device capacities in consideration of device operational strategies for seasonal and hourly variations of solar insolation and electricity demand.

Generally, two approaches have been adopted. The former one is a deterministic approach where the system performance is evaluated on the basis of original data on solar isolation and electricity demand obtained through measurement. The latter is a probabilistic approach which is based on probability distributions of solar insolation and electricity demand assumed from their original data.

The performance of the PV system depends upon several factors, especially the meteorological conditions such as solar radiation, ambient temperature and wind speed. Normally, the information provided about the PV module and other components from the manufacturers is used for sizing the PV system by a rough estimation of the system output based on average values of daily meteorological data inputs. The parameters that are most used for sizing a PVGCS are field surface, tilt angle and array size. A summary of some works in this field is proposed in Table 1-3.

From the abovementioned works, it is possible to establish a general scheme for the configuration of a PVGCS, as shown in Figure 1-12.

It must be yet emphasized that even if power generation from PV systems is free from fossil fue1 use and greenhouse gas (GHG) emissions, a considerable amount of energy is consumed in the manufacturing and transport of the elements of the system. Besides, the amount of energy and emissions from a decommissioning phase of the system must not be neglected. Moreover, any artificial installation implies an ecological impact on the local or even the global environment. For any energy source versus the aim of sustainable development, if to be “renewable” is an obvious “necessary condition”, it is not a “sufficient condition”! Indeed, many other impact factors than energy resource exhaustion can be considered to be taken into account.

Ecodesign methods are thus necessary to check whether renewable energy systems as PV systems are truly environment-friendly (green). Generally the environmental assessment is performed as a post-design stage of the PV systems. The objective of this work is to integrate the environmental assessment from the design stage. Table 1-4 displays some of the works that have evaluated environmental impacts generated by PV systems.

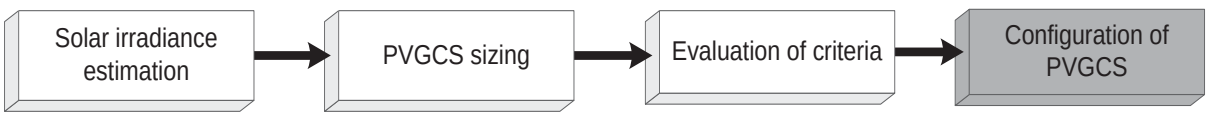

Figure 1-12 General scheme for the configuration of a PVGCS

Table 1-3 Summary of literature works for sizing PV systems

Authors	Year	Subject
(Pehnt, 2006)	2006	Dynamic life cycle assessment (LCA) of renewable energy technologies
(Prakash & Bhat, 2009)	2009	Energy, economics and environmental impacts of renewable energy systems
(Ménard et al., 2011)	2011	Environmental impact assessment of electricity production by photovoltaic system using GEOSS recommendations on interoperability
(Beylot et al., 2012)	2012	Environmental impacts of large-scale grid-connected ground-mounted PV installations
(Alsema & Wild-scholten, 2006)	2006	Environmental Impacts of Crystalline Silicon Photovoltaic Module Production System boundary LCA study New LCI data set
(Raugei, Bargigli, & Ulgiati, 2007)	2007	Life cycle assessment and energy pay-back time of advanced photovoltaic modules: CdTe and CIS compared to poly-Si
(Nishimura et al., 2010)	2010	Life cycle assessment and evaluation of energy payback time on high-concentration photovoltaic power generation system
(Desideri, Proietti, Zepparelli, Sdringola, & Bini, 2012)	2012	Life Cycle Assessment of a ground-mounted 1778kWp photovoltaic plant and comparison with traditional energy production systems
(Sherwani & Usmani, 2010)	2010	Life cycle assessment of solar PV based electricity generation systems: A review
(Kannan, Leong, Osman, Ho, & Tso, 2006)	2006	Life cycle assessment study of solar PV systems: An example of a 2.7kWp distributed solar PV system in Singapore
(Hondo, 2005)	2005	Life cycle GHG emission analysis of power generation systems: Japanese case
(Raugei & Frankl, 2009)	2009	Life cycle impacts and costs of photovoltaic systems: Current state of the art and future outlooks
(Sumper, Robledo-García, Villafáfila-Robles, Bergas-Jané, & Andrés-Peiró, 2011)	2011	Life-cycle assessment of a photovoltaic system in Catalonia (Spain)
(Dones & Frischknecht, 1998)	2000	Life-cycle Assessment of Photovoltaic Systems: Results of Swiss Studies on Energy Chains
(Ito, Komoto, & Kurokawa, 2010)	2010	Life-cycle analyses of very-large scale PV systems using six types of PV modules
(Fthenakis & Kim, 2011)	2011	Photovoltaics: Life-cycle analyses
(Akella, Saini, & Sharma, 2009)	2009	Social, economic and environmental impacts of renewable energy systems

Table 1-4 Summary of literature works for environmental assessment of PV systems

Authors	Year	Subject
(Mirhosseini, Agelidis, & Ravishankar, 2012)	2012	Modeling of large-scale grid-connected photovoltaic systems: Static grid support by reactive power control
(Li et al., 2010)	2010	Modeling and simulation of large-scale grid-connected photovoltaic system
(Kornelakis & Koutroulis, 2009)	2010	Contribution for optimal sizing of grid-connected PV-systems using PSO
(Notton, Lazarov, & Stoyanov, 2010)	2010	Optimal sizing of a grid-connected PV system for various PV module technologies and inclinations, inverter efficiency characteristics and locations
(Wissem, Gueorgui, & Hédi, 2012)	2012	Modeling and techno–economic optimization of an autonomous photovoltaic system
(Mondol, Yohanis, & Norton, 2009)	2009	Optimizing the economic viability of grid-connected photovoltaic systems
(Gautam & Kaushika, 2002)	2002	Development of an efficient algorithm to the electrical performance simulation of solar photovoltaic arrays
(Weinstock & Appelbaum, 2004)	2004	Optimal Solar Field Design of Stationary Collectors
(Weinstock & Appelbaum, 2009)	2009	Optimization of Solar Photovoltaic Fields
(Weinstock & Appelbaum, 2007)	2007	Optimization of Economic Solar Field Design of Stationary Thermal Collectors
(Fernández-Infantes, Contreras, & Bernal-Agustín, 2006)	2006	Design of grid connected PV systems considering electrical, economical and environmental aspects: A practical case
(Gong & Kulkarni, 2005)	2005	Design optimization of a large scale rooftop photovoltaic system
(Mellit, Kalogirou, Hontoria, & Shaari, 2009)	2009	Artificial intelligence techniques for sizing photovoltaic systems: A review
(Smiley, Jones, & Stamenic, 2000)	2000	Optimizing photovoltaic array size in a hybrid power system
(Kumar Sharma, Colangeki, & Spagna, 1995)	1995	Photovoltaic technology: basic concepts, sizing of a standalone photovoltaic system for domestic applications and preliminary economic analysis
(Posadillo & López Luque, 2008)	2008	Approaches for developing a sizing method for stand-alone PV systems with variable demand

1.7 Organization of the manuscript

This PhD work aims at determining a general methodology for designing PVGCS, taking into account simultaneously both techno-economic and environmental considerations.

The manuscript consists of six chapters that are organized as follows:

Chapter 1 is focused on the presentation of the general context of PV systems as well as on the literature review for designing and sizing PV systems and justifies the scientific objectives of this work.

In **Chapter 2**, the methodology chosen for the assessment of environmental impacts asscoiated with PVGCS based on Life Cycle Assessment methodoloy is presented.

Chapter 3 is dedicated to the presentation of the model that has been developed for sizing a large-scale PV system.

Chapter 4 discusses the methods and tools that are the support of the methodological study for ecodesign. They combine multi-objective optimization, principal component analysis and multiple criteria decision-making

The integration of the environmental and sizing PVGCS models in the multi-objective optimization framework is presented in **Chapter 5**. Different examples serve as an illutrsation of the performances of the proposed methodology for sizing a PV system taking into account simultaneously techno-economic and environmental criteria. Particular emphasis is devoted to the reduction of the objectives in the multi-objective approach to make the analysis more consistent and facilitate result interpretation.

Chapter 6 presents a review of current recycling processes of PV modules. In addition, two examples of integration of the recycling process in the environmental assessment model developed in Chapter 2 will show the importance of recycling in the ecodesign procedures. Finally, the manuscript ends with conclusions and perspectives in **Chapter 7**. A vision of the report structure is presented in Figure 1-13:

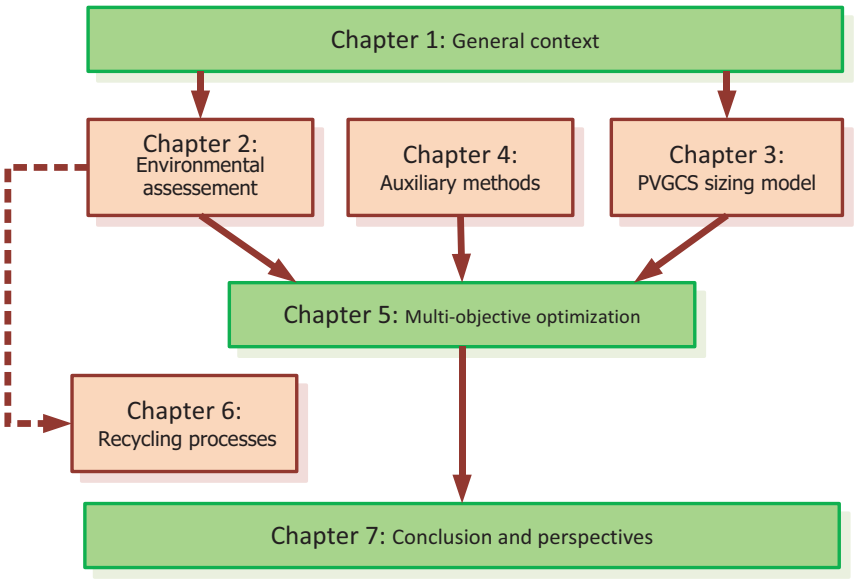

Figure 1-13 Organization of manuscript

Chapter 2

LIFE-CYCLE ASSESSMENT (LCA) FOR PV SYSTEMS

L'objectif de ce chapitre est de présenter le modèle environnemental retenu dans le cadre de cette étude. L'approche par Analyse du Cycle de Vie (ACV) largement appliquée dans plusieurs domaines, notamment pour la production d'énergie, est utilisée pour mesurer la performance environnementale des systèmes photovoltaïques.

Ce chapitre présente tout d'abord les procédés de fabrication utilisés pour cinq technologies de modules PV (m-Si, p-Si, a-Si, CdTe et CIS). La connaissance du procédé est perçue comme un point fondamental pour comprendre les limitations liées à une technologie d'un point de vue environnemental. Une analyse de la littérature dédiée des approches d'évaluation environnementale est ensuite menée. Les principes fondamentaux de l'ACV finalement retenue sont ainsi décrits. Trois exemples d'études de l'ACV sont proposées. Le premier exemple traite le cas du module PV basé sur la technologie m-Si, de la production du silicium de qualité solaire à l'assemblage du module PV. L'influence du « mix » énergétique est pris en compte. La deuxième illustration est consacrée à la comparaison des impacts environnementaux de 3 technologies (m-Si, p-Si, Si en ruban). En final, l'évaluation et la comparaison de 5 configurations de systèmes photovoltaïques connectés au réseau sont présentées. Le modèle environnemental proposé ici sert de brique de base pour l'intégration de l'analyse environnementale dans le cadre d'une optimisation multiobjectif pour le dimensionnement de champs de panneaux solaires. Le cas du recyclage des panneaux fera l'objet d'un chapitre dédié en fin de manuscrit. Le manque de données lors du démarrage de ces travaux et qui perdure pour certaines technologiques n'a pas permis une vision holistique sur laquelle reposer certes une démarche ACV.

Nomenclature

Acronyms

AA	Aquatic Acidification midpoint category
AE	Aquatic Ecotoxicity midpoint category
AEU	Aquatic Eutrophication midpoint category
C	Carcinogen midpoint category
CBA	Cost-Benefit Analysis
CBD	Chemical Bath Deposition
CdTe	Cadmium Telluride
CIS	Copper indium diselenide
CSS	Closed Space Sublimation
CSVT	Closed Space Vapour Transport
CVD	Chemical Vapor Deposition
CZ	Czochralski process
DC/AC	Direct Current / Alternative Current
EIA	Environmental Impact Assessment
ERA	Environmental Risk Assessment
EVA	Ethylene Vinyl Acetate
FU	Functional Unit
GW	Global Warming midpoint category
IO	Ionizing Radiation midpoint category
LCA	Life-Cycle Assessment
LCI	Life-Cycle Inventory
LCIA	Life-Cycle Impact Assessment
LO	Land Occupation midpoint category
ME	Mineral Extraction midpoint category
MFA	Material Flow Analysis
MILP	Material Intensity Per unit Service
NC	Non-Carcinogen midpoint category
NR	Non-Renewable energy midpoint category
OLD	Ozone Layer Depletion midpoint category
PV	Photovoltaic
PVGCS	Photovoltaic Grid-Connected System
RE-PECVD	Radio Frequency Plasma Enhanced Chemical Vapor Deposition
RI	Respiratory Inorganic midpoint category
RO	Respiratory Organic midpoint category
m-Si	Monocrystalline silicon
p-Si	Polycrystalline silicon
a-Si	Amorphous silicon
TAN	Terrestrial Acidification/Nitrification midpoint category
TCO	Transparent Conducting Oxide
TE	Terrestrial Ecotoxicity midpoint category
TF	Thin Film PV technology

Symbols

η	PV module efficiency, %
EI	Overall environmental impact indicator
$FD_{i,d}$	Damage characterization factor for the impact category i in the damage category d
$FI_{s,i}$	Characterization factor for the substance s in the impact category i
M_s	Mass of substance s
N_k	Normalised score of the impact or damage categories k
PF_k	Weighting factor for impact category k
SD_d	Damage score for the damage category d
SI_i	Characterization score for the impact category i
VR_k	Reference value for the impact or damage categories k

2.1 Introduction

During the last years, climate change and other environmental threats have come more into focus by government and enterprises. Nowadays, environmental considerations are integrated as an important element in the evaluation of projects and other decision made by business, individuals, and public administrations. For this purpose, the development and use of environmental assessment and management techniques to better understand the environmental impacts are thus required. These techniques aim at identifying opportunities for reducing the environmental impacts and risks of projects, processes, products, and services.

Among the environmental assessment techniques, the methodological development in Life Cycle Assessment (LCA) technique has been strong, and LCA is now broadly applied in practice in several fields such as energy production.

LCA provides a well-established and comprehensive framework to compare renewable energy technologies with fossil-based and nuclear energy technologies (Akella et al., 2009; Bhat & Prakash, 2009; World Energy Council, 2004). The improvement among renewable energy technologies can also be compared by LCA (Akella et al., 2009; Bhat & Prakash, 2009). Even if renewable energy technologies are free of fossil fuel use and greenhouse gas (GHG) emissions during the energy generation phase, a considerable amount of energy and resources are generally consumed for the manufacturing of the different elements required to achieve the energy generation but also in the disposal of these elements at their end-of-life.

This chapter first discusses the environmental assessment of manufacturing processes used for PV modules by use of the LCA technique that will be further used to perform the environmental assessment of a PVGCS. Then, the manufacturing processes of the currently five most sold PV technologies (m-Si, p-Si, a-Si, CdTe and CIS) are described. Process knowledge is indeed considered as a cornerstone to properly apply the LCA methodology, since silicon production is highly energy intensive. To streamline the presentation of some processes which be exhaustive, some explanations

are as an additional focus. It is necessary to understand the bottlenecks of the manufacturing processes that are involved in the various technologies.

Subsequently, a literature review of some of the most common techniques for environmental assessment will be presented in order to better position the LCA technique. The fundamentals and principles of LCA will be thus described.

This chapter concludes with three examples of LCA studies. The first example assesses the manufacturing process of m-Si PV module from solar grade silicon production to the PV module assembly. In this example, the influence of the energy mix will be analyzed. A comparison of environmental impacts between the three crystalline silicon-based technologies (m-Si, p-Si and ribbon-Si) is proposed as a second example of application. Finally, the evaluation and comparison of five configurations of PVGCS are presented. The environmental model resulting will be then considered as the basis for the integration of environmental analysis in multi-objective optimization for sizing a large-scale PV system.

2.2 Manufacturing processes for PV technologies

The manufacturing process of the product or system under study is a key element of the environmental study in order to determine to the system boundaries and to identify the material and energy requirements and the associated emissions. In this section, the manufacturing processes of the main commercial PV modules technologies are described.

As mentioned in Chapter 1, PV technologies are classified according to first, second or third generation. Only, the first and second PV module generation will be taken into consideration because they correspond to more than 80% of the current PV global market. It must be highlighted that there is a lack of information on the manufacturing process of the third generation of PV modules for a reliable study. Several of the modules of the latest generation are still in development phase.

2.2.1 *Crystalline silicon technology*

Crystalline silicon (c-Si) PV modules are made from thin slice cells, called wafers, cut from a single crystal or a block of silicon. There are three main types of crystalline cells mono-crystalline (m-Si), polycrystalline or multi-crystalline (p-Si) and ribbon and sheet-defined film growth (ribbon-Si). The main difference between them is how the wafers are made.

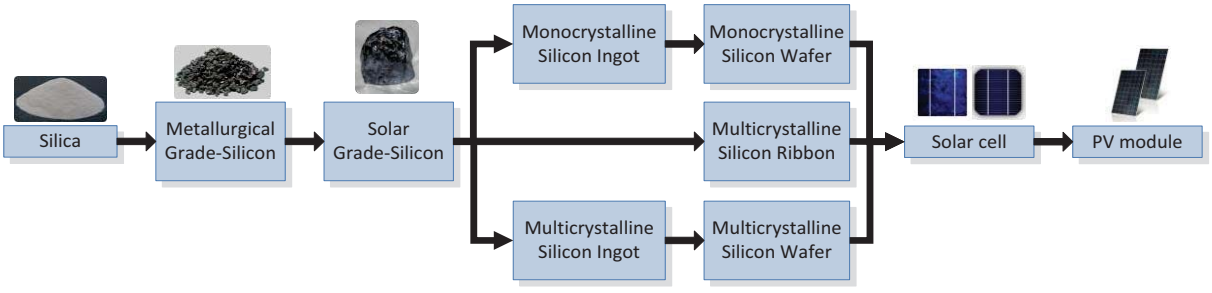

Figure 2-1 Production flow of crystalline silicon PV modules based on (de Wild-Scholten & Alsema, 2005)

Figure 2-1 contains the main stages of the manufacturing process for the three types of crystalline modules. The three technologies share the same process both at the beginning and end. The difference, as mentioned above, corresponds to wafer manufacturing process. Each step is described in detail (Luque & Hegedus, 2003; Singh Solanki, 2011):

Mining and refining of silica

Silicon is the second most abundant element in the Earth's crust. Quartz and sand are the raw materials for the production of silica (SiO_2). The mining of quartz or sand is a widely established technology. In this study, the process characteristics for this step are assumed identical for all three cases. After mining, the sand is transported, classified, scrubbed, conditioned, floated and deslimed.

Reduction of silica to Metallurgical Grade silicon

Silica is reduced to silicon with carbon by a thermal reaction according to:

$$SiO_2 + 2C \rightarrow Si + 2CO \quad (2.1)$$

The carbon used in the reduction is supplied by cokes, low ash coal and wood scrap. The reaction is made in an arc furnace at temperature of more than 1,600°C. The resulting silicon is primarily used in the metallurgical industry and is thus called metallurgical grade silicon (MG-Si). The MG-Si is 98% pure.

Production of Solar Grade silicon

MG-Si still contains too many impurities to be used in solar cell manufacturing. The polysilicon required for solar cells can be up to 99.999999% pure. This polysilicon is named Solar Grade silicon (SoG-Si). SoG-Si is usually produced by ether the Siemens process or fluidized-bed process. It important to highlight that less than 5% of worldwide MG-Si produced is used in making SoG-Si. Figure 2-2 summarizes the SoG-Si operations.

Production of wafers

The arrangement of Si atoms in SoG-Si and the size are yet not adequate. An atomic arrangement is needed to give a defined shape (circular or square) but also the final characteristics of PV module. The manufacturing process for each of the three crystalline silicon-based PV technologies is presented in Figure 2-3.

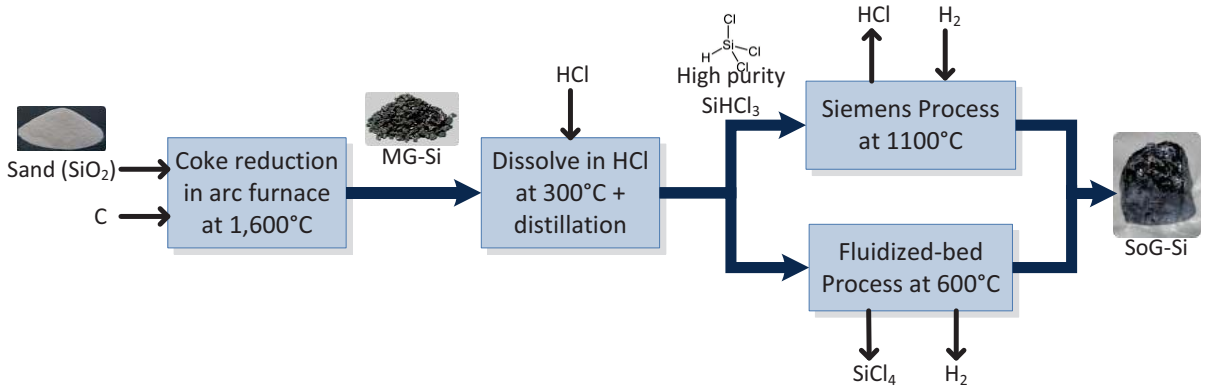

Figure 2-2 Main manufacturing processes of SoG-Si

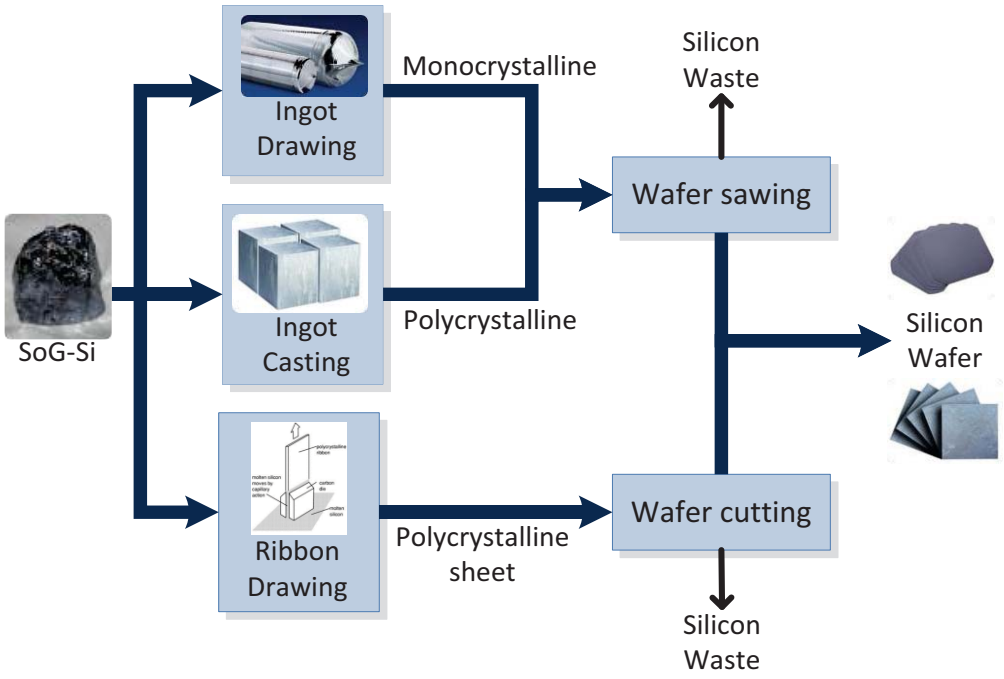

Figure 2-3 Manufacturing processes of silicon wafer

Focus on SoG-Si solidification processes

First, a High Purity Si Containing Gases is needed for both processes. MG-Si is pulverized in fine power and reacted with anhydrous hydrogen chloride in a fluidized-bed reactor at 300°C in the presence of catalyst. During the process, trichlorosilane ($SiHCl_3$) and several other unwanted chlorides are formed, following an exothermic reaction:

$$Si + 3HCl \rightarrow SiHCl_3 + H_2 + Heat \quad (2.2)$$

In the next step, using a fractional distillation, $SiHCl_3$ is easily separated from the other impurities.

a/ Siemens process

The high purity trichlorosilane is converted in solid SoG-Si by chemical vapor deposition (CVD) process. Solidification of Si is done using a Siemens type reactor. In a Siemens reactor, a thin Si rod is heated at more than 1,100°C. A mixture of $SiHCl_3$ and H_2 is introduced in the chamber and the $SiHCl_3$ is reduced following the equation:

$$2SiHCl_3 + 2H_2 \rightarrow 2Si + 6HCl \quad (2.3)$$

As the process continues, the Si rod becomes thicker and thicker. The rod rises to 30 cm in diameter and 2 m in length. The deposited Si is of polycrystalline type.

b/ Fluidized-bed process

In fluidized-bed process, the $SiHCl_3$ is decomposed in silane according to:

$$4SiHCl_3 \rightarrow SiH_4 + 3SiCl_4 \quad (2.4)$$

Using a CVD in a fluidized-bed reactor silane is converted into solid SoG-Si. In this process, silane is solidified using Si seed particles. At 600°C, the gas phase

decomposition of silane takes place by reaction (see Equation (2.5)) and the Si atoms get deposited on the floating seed particles.

$$SiH_4 \rightarrow Si + 2H_2 \quad (2.5)$$

The particles grow up to 2 mm in size. When the weight of the Si particles is high enough, they fall on the bottom of the reactor, where they are collected for further use.

Focus on CZ/FZ processes

In CZ process, the SoG-Si is placed in a quartz crucible. Si is melted by induction heating and then cooled to form a long solid block called an ingot. A seed crystal gives the arrangement of Si atoms. Melts attain a temperature or more than 1,400°C. The ingot's diameter can reach be up to 300 mm. The length of ingot is 1 or 2 m. CZ process is the most commonly used process for ingot pulling.

In FZ process, the contact of melt with any crucible is avoided. The melt zone is a float zone. A seed crystal is melted with polysilicon rod using induction heating. As the process proceeds, the heated zone is moved upwards. The left behind melted zone solidifies in the form of m-Si ingot.

The m-Si wafers have a regular, perfectly-ordered crystal structure. To achieve this configuration, two processes are generally used: Czochralski process (CZ process) and float zone process (FZ process).

The p-Si wafers have square shape. This allows higher packing density of cells in the module. In p-Si ingots manufacturing process, SoG-Si is melted and poured into a square-shaped SiO-SiN-coated graphite crucible. The controlled directional solidification of the crucible results in p-Si block consisting of several smaller crystallites of varying sizes and orientation.

The m-Si and p-Si ingots need to be diced in order to obtain Si wafer. A wire saw is used to slice the wafer from the ingot. The saw is about the same thickness as the wafer. This method of slicing produces significant wastage up to 40% of the silicon (known as kerf loss).

Ribbon/sheet-Si produce wafer equivalent sheets directly from high purity polysilicon (without growing ingots and then sawing). The main problems found in this process are as follows: the required purity level could not be achieved and many defects are created in the crystal during the crystallization process.

The *edge defined film-fed growth (EFG)* technique is the most advanced for producing thin sheets of Si. Here a thin sheet is pulled from molten Si. The sheet is formed by the capillarity action of molten Si, and capillarity is defined by a graphite die. The material quality obtained is similar to p-Si. The Si sheet thickness is about 250 μm. The Si wafers are cut using laser scribing. The use of a laser cutter reduces kerf loss.

Focus on Transforming the wafer into a solar cell

The solar cell is the unit that produces electricity. It is created using four main steps:

a. Surface treatment: The wafer's top layer is removed to make it perfectly flat.

b. Creation of the potential difference (p-n) junction.

c. Deposition of an anti-reflective coating.

d. Add metal grid (metallization)

Focus on Module manufacturing

The solar cells are placed between layers of coating material to protect them from the environment and breakage. Transparent glass is used for the front, while a weatherproof backing (typically a thin polymer) is applied to the back of the module. The cover is attached using thin sheets of ethylene vinyl acetate (EVA). Frames can be placed around the modules to increase their strength.

2.2.2 *Amorphous silicon thin-film*

The amorphous silicon or a-Si material has become an interesting material when it was discovered that its conductivity can be changed. The term "amorphous" is given to non-crystalline materials prepared by deposition from gases. The a-Si alloyed with hydrogen (a-Si:H) shows a very high absorption coefficient in the visible range and requires only about a micron thick layer. The manufacturing process of a-Si-based PV modules has a similar beginning to PV modules based crystalline silicon (Section 2.2.1). Figure 2-4 represents the manufacturing process flow for a-Si:H-based PV.

Mining and refining of silica and MG-Si process are the same as used for obtaining PV modules of c-Si. Silane (SiH_4) is produced in a fluidized-bed process according to the reaction (2.4). The remaining steps are detailed in the boxes (Luque & Hegedus, 2003; Markvart & Castañer, 2003; Singh Solanki, 2011).

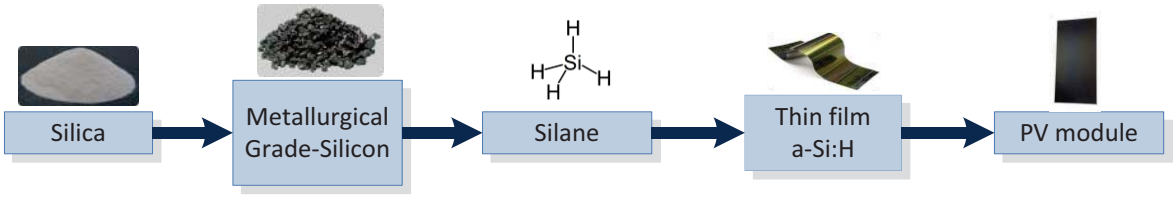

Figure 2-4 Production flow of a-Si PV modules

Focus on thin film single junction a-Si:H

The key component is deposition of a-Si:H layer with desired composition and thickness. Radio frequency plasma enhanced chemical vapor deposition (RE-PECVD) technique is the most commonly used to deposit the a-Si:H film. Figure 2-5 shows a typical RE-PECVD chamber. In this process, a mixture of SiH_4 and H_2 flows into a vacuum chamber that is evacuated by a pump. Two electrode plates are installed inside, and a radio frequency power is applied between them in which plasma will occur. The plasma excites and decomposes the gas and generates radicals and ions in the chamber. Various substrates may be mounted on one or both of the electrodes, and thin hydrogenated silicon films grow on the substrates as these radicals diffuse into them. The substrates are heated to achieve optimum film quality.

The typical parameters for obtaining high quality a-Si:H using RE-PECVD are the following one: silane flow of 20 sccm to 50 sccm (standard cubic centimeters per minute), chamber pressure of 0.5 to 1 Torr, substrate temperature of 150 – 350°C, RF power should be 20 – 50 $\mu W/cm^2$, electrode to substrate distance between 1-3 cm. A typical deposition rate is 0.1-0.2 nm per second. About 300 nm thickness of absorbed layer is required.

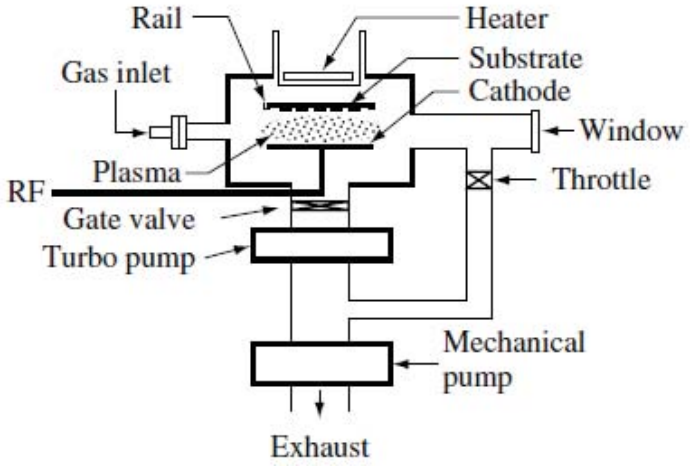

Figure 2-5 Principle of a RF-PECVD deposition tool (Luque & Hegedus, 2003)

Focus on module manufacturing

The process consists of four steps: substrate washing, sputter deposition of the back reflector, a-Si semiconductor deposition, and the transparent conducting oxide (TCO) deposition. At the end of TCO deposition process, the a-Si solar cell is cut by a slab cutter. It is then covered with EVA and Tefzel (a modified ethylene-tetrafluoroethylene fluoroplastic), and vulcanized in a furnace for lamination. This is then followed by selected module framing. The typical structure of a.Si:H solar cell is given in Figure 2-6.

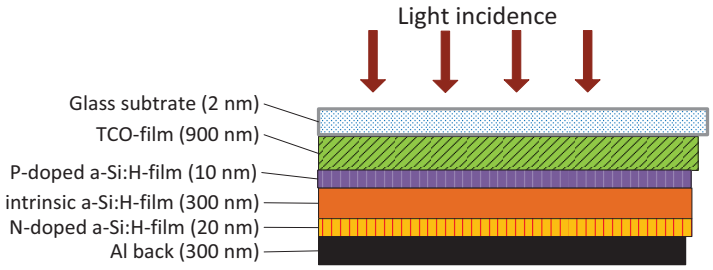

Figure 2-6 Structure of a-Si:H-based solar cell (Singh Solanki, 2011)

2.2.3 *Cadmium Telluride thin-film*

The CdTe (cadmium telluride) is a binary compound semiconductor of Cd (cadmium) and Te (tellurium). It is typically deposited in polycrystalline form. Due to a high absorption coefficient, a maximum thickness of about 1μm of material is required. CdTe layers are chemically and thermally stable and are less prone to efficiency degradation.

CdTe is manufactured from pure Cd and Te, both of which are by-products of smelting prime metals (e.g. Cu, Zn, Pb, and Au). Figure 2-7 shows a flow diagram from raw material acquisition to manufacturing stage of CdTe-based PV module. First cadmium production process will be described from Zn production. The different steps are detailed below (V. M. Fthenakis, 2004; V. Fthenakis, Wang, & Kim, 2009; Luque & Hegedus, 2003; Markvart & Castañer, 2003; Singh Solanki, 2011).

Mining zinc ores

Cadmium minerals are not found alone. They are mainly generated as a by-product of smelting zinc ores. Zinc is found in the earth's crust as zinc sulfide (ZnS). Zinc ore contains, beside Zn, Cd, Cu, Pb, Ag and Fe. The ore is excavated by drilling machines, processed through a primary crusher, and then conveyed to surface where is screening and milling to reduce the ore to powder. The particles are separated from the gangue and concentrated in a liquid medium by gravitation and/or selective flotation, followed by cleaning, thickening, and filtering.

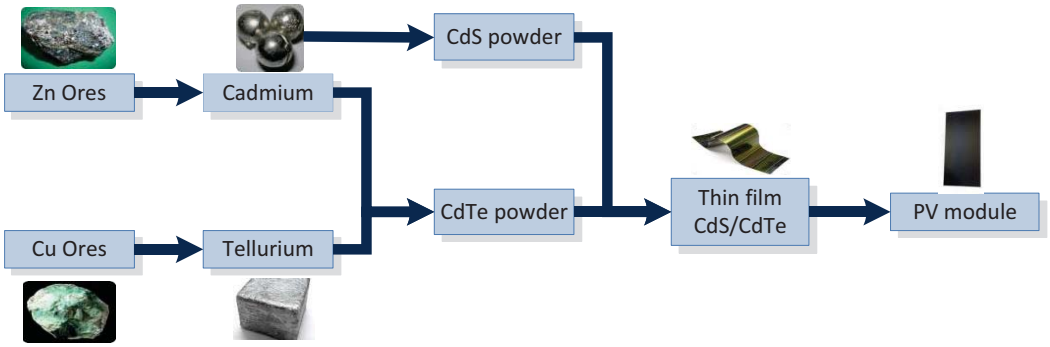

Figure 2-7 Production flow of CdTe PV modules (V. Fthenakis et al., 2009)

Cadmium production

Zinc concentrate is transferred to smelters/refiners to produce the primary metals. Sulfuric acid and other metals, e.g. Cd, are frequent by-products from most smelters. Zn can be refined by either pyrometallurgical or hydrometallurgical treatment. The process consists of five steps but only the first three are important for Cd production (see Figure 2-8).

Tellurium minerals, as Cd, are not found alone. It is a rare metal than can be extracted as by-product of processing copper ores. The production process for Cu is described to explain Te production.

Mining copper ores

Primary Cu is obtained mainly from sulfide ores. Cu ores contain, beside Cu, Fe, Te, Se, Mo, Ag and other metals. The ore is mined then it is crushed, ground and concentrated. In concentrated process, ground ore is slurred with water. The process continues as described in Figure 2-9.

Purification of Cd and Te

Metallurgical grade Cd and Te (i.e. 99.99% pure) metal is used in current applications except for semiconductor materials that require higher purity. To elaborate semiconductor CdTe, a high purity (i.e. 99.9999%) of Cd and Te powders are needed. Purification can be made by electrolysis and subsequent melting and atomization or by vacuum-distillation followed by zone refining.

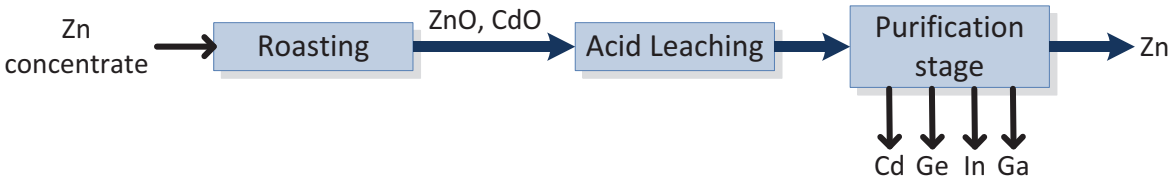

Figure 2-8 Flows in Zn refining (V. Fthenakis et al., 2009)

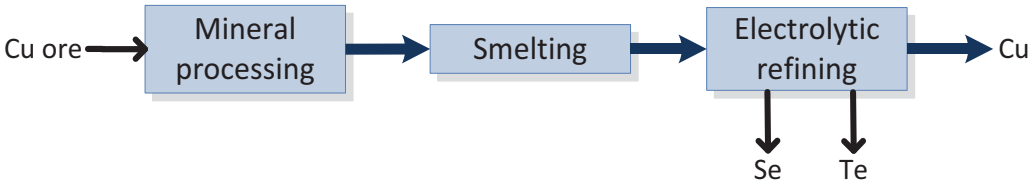

Figure 2-9 Extractive metallurgy of Cu (V. Fthenakis et al., 2009)

Focus on cadmium production steps

a/ Roasting. Oxidizing roast at high temperature removes sulfur and converts the zinc, iron, cadmium, and other metals to oxides. The concentrates are fed to fluidized-bed furnaces where they are burnt with air and direct oxygen. Zinc calcine, mainly composed by Zn oxide with small amount of Fe, Cd, and others metal is cooled, passed through a mill and collected in cyclones and electrostatic precipitators.

b/ Leaching. Leaching of the metals from the calcine is accomplished by sulfuric acid. This process dissolves the zinc to make a solution of zinc sulfate and other acid-soluble

metals. The leachate, that contains Cd, is sent to the purification section.

c/ Purification. Cd, Ge, In and Ga are removed. The Cd extracted at this step is formed into briquettes that then are melted. This refining Cd has metallurgical grade (99.95% pure) and is cast and cut into sticks.

Focus on tellurium production

After separation, Cu is transferred to smelters where it is processed in furnaces. Impurities in Cu typically include Se and Te. Cu production follows with either pyrometallurgical or hydrometallurgical refined process. The pyrometallurgy of Cu is a multistage process, beginning with the mining and concentrating of low-grade ores, and followed by smelting and electrolytic refining to produce a pure copper cathode (see Figure 2-9). In electrolytic refining, the impurities are separated by electrolysis in a solution containing copper sulfate and sulfuric acid. The metallic impurities precipitate forming sludge. The sludge contains Cu, Te, Se and other metals. Oxidative pressure-leaching with dilute sulfuric acid at 80–160°C is used to remove Cu and 50-80% of Te. Tellurium is recovered from solution by cementation with copper. Copper telluride is leached with caustic soda and air to produce a sodium telluride solution. The latter is used as the feed for producing commercial grade Te metal or TeO_2.

Focus on thin-film CdTe/CdS

CdTe is commonly deposed using Closed Space Sublimation (CSS) process, also known as Closed Space Vapour Transport (CSVT). A schematic CSS process is shown in Figure 2-10. It contains a CdTe plate (source plate) which is transported to the substrate in vapour form. The driving force for transfer is the temperature difference between the source (650-750°C) and the substrate (600°C). The pressure is about 10 Torr. The space between both plates lies between 1-15 µm and the growth rate is 1-5 µm/min. An inert gas such as N_2, Ar, or He is used for CCS. CdS film can be deposited by the same process as CdTe.

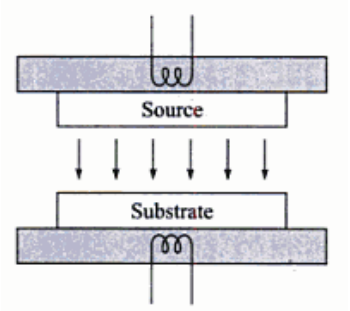

Figure 2-10 Schematic CSS deposition tool (Singh Solanki, 2011)

Focus on module manufacturing

The cells are deposited in superstrate arrangement (see Figure 2-11). The process starts with transparent conducting oxide (TCO) coated glass layer, such as SnO_2 at around 250°C. After cleaning the TCO layer, the area of the cell is defined by laser scribing. Then, an n-CdS film is deposited, followed by the p-conducting CdTe film at about 500°C. The absorbed layer is laser scribed according to cell area defined by first laser cut. The junction is activated with a $CdCl_2$ treatment. The treatment consists of doping of solution of $CdCl_2$ in methanol onto CdTe coated substrate, letting the methanol solvent evaporate and heat treating the substrate at 450°C for 15 min. Then, back metal layer is deposited. Another laser cut is made in which the series connection of solar cell get completed. The last step is encapsulation with EVA and finally covering of the module with top glass cover.

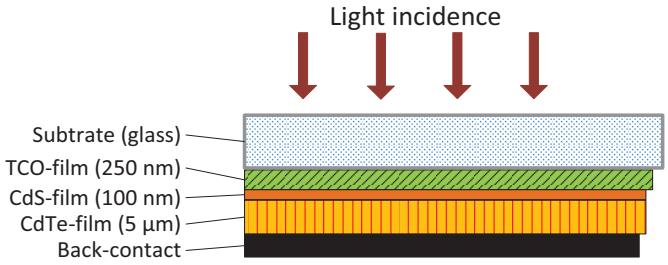

Figure 2-11 Structure of CdTe-based solar cell (Singh Solanki, 2011)

2.2.4 *Copper Indium Selenide (CIS) thin-film*

$CuInSe_2$-based solar cells is a promising solar cell technologies due to its low-cost, high-rate semiconductor deposition over large areas using layers only a few microns thick and for fabrication of monolithically interconnected modules. Perhaps more importantly, very high efficiencies have been demonstrated with CIS at both the cell and the module levels in laboratory. The performance is increased by adding gallium (Ga) to the compound, thus making it $Cu(In,Ga)Se_2$ or CIGS.

The CIS manufacturing process is summarized in Figure 2-12. Indium (In) and Ga can be acquired as by-products of the production of Zn. About 5% of the global production of gallium is obtained from residues in zinc processing but 95% of the global supply is obtained as a by-product of alumina production from bauxite. Selenium (Se) is obtained as by-product from Cu ores. Processes for Zn and Cu were described in the previous section. In Figure 2-8, In and Ga production starts during the purification process of Zn. As indicated in Figure 2-9, Se is obtained during the electrolytic refining process for Cu. The next steps for the manufacture of CIS-based PV module are described in respective boxes (V. M. Fthenakis, 2004; V. Fthenakis et al., 2009; Luque & Hegedus, 2003; Markvart & Castañer, 2003; Singh Solanki, 2011). The copper production process was described in the previous section and the process flow is given in Figure 2-9.

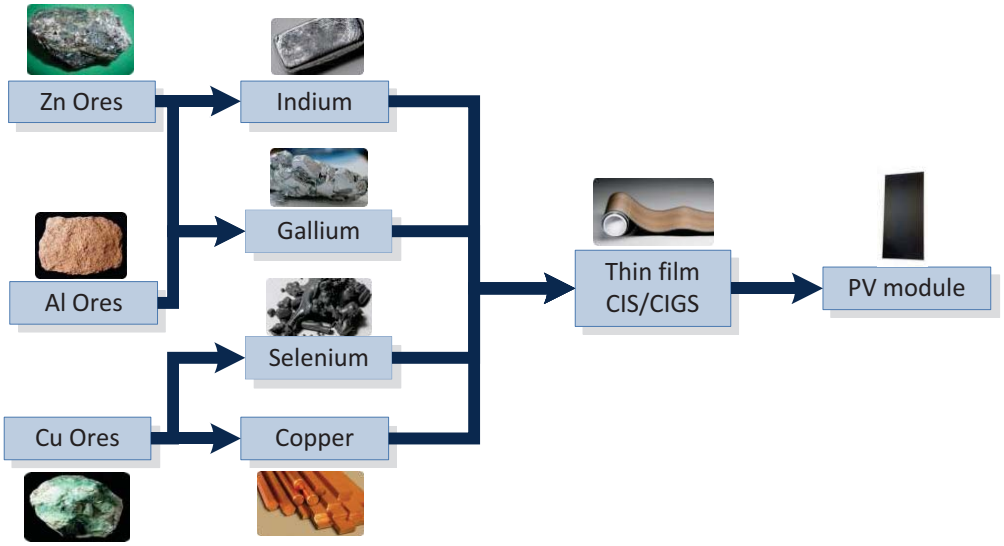

Figure 2-12 Production flow of CIS PV module

Focus on indium production

Soda is added to the residue resulted in the purification process of Zn that contains particles of In in order to precipitate it. About 10% of In remains in the residue, which is leached with sodium hydroxide to create crude indium hydroxide. The crude indium hydroxide is leached with dilute hydrochloric acid. The solution is purified by cementation of copper and arsenic with iron, followed by cementation of tin and lead with indium. Finally, In is removed by adding aluminium to create indium cement. Further purification is done by electrolysis to produce high purity grade (99.9999%). Figure 2-13 represents the production process of In.

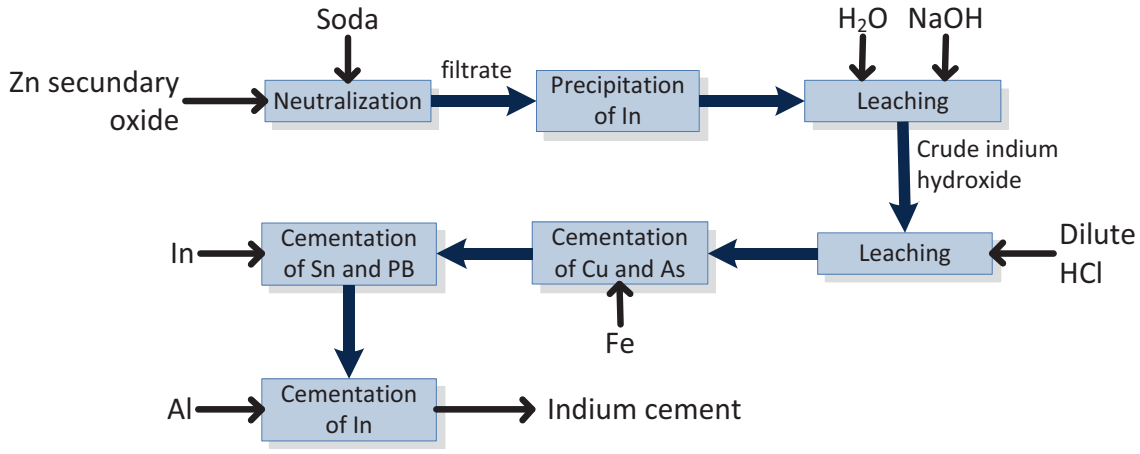

Figure 2-13 Process flows for In production (V. Fthenakis et al., 2009)

Focus on gallium production

Most gallium is extracted from the crude aluminum hydroxide solution of the Bayer

process for producing alumina (see Figure 2-14). In the Bayer process, bauxite is digested by washing with a hot solution of sodium hydroxide (NaOH) at 175°C under pressure. This converts the aluminium oxide in the ore to soluble sodium aluminate. The solution is clarified by filtering off the solid impurities, commonly with a rotary sand trap, and a flocculent such as starch, to get rid of the fine particles. The alkaline solution is cooled and treated by bubbling carbon dioxide into it, through which aluminium hydroxide precipitates. Gallium is separated by selective precipitation. Hydrochloric acid is used to dissolve gallium from the metal hydroxides. Then the gallium is separated by solvent extraction with ether. Finally, the crude gallium is recovered by electrolysis. The metal produced can be purified by melting in temperature controlled vessels.

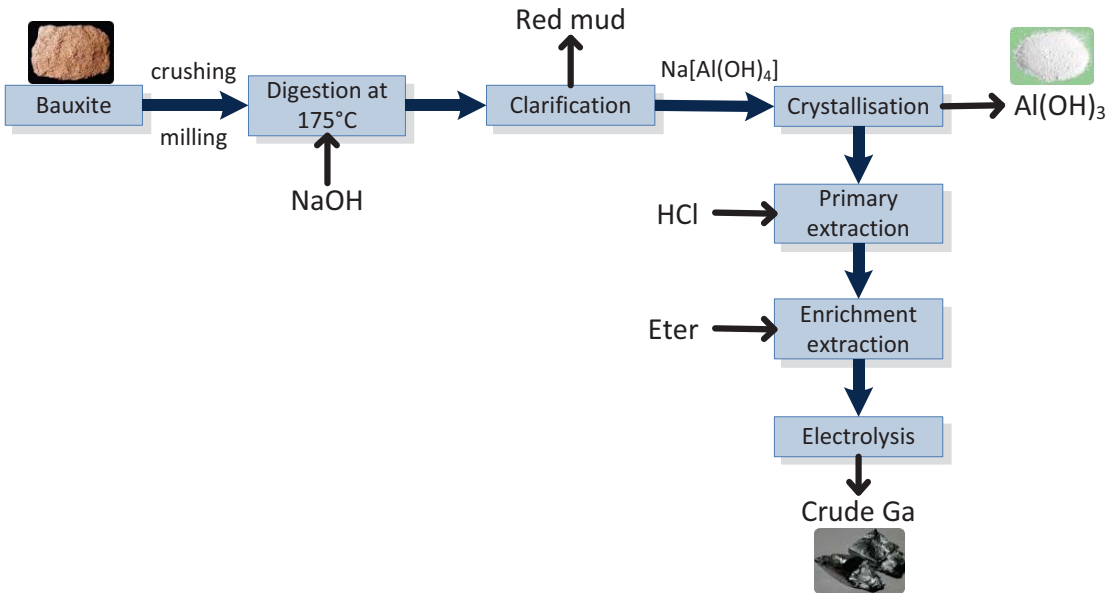

Figure 2-14 Process flows for Ga production (V. Fthenakis et al., 2009)

Focus on selenium production

It is recovered as a by-product, mostly from the anode slimes in the electrolytic refining of copper. Two major processes of extracting selenium from copper refinery slime include roasting with soda ash and roasting with sulphuric acid. Soda ash roasting is a traditional method to recover selenium. This method is described in Figure 2-15.

Electrolytic copper refinery slimes are intensely mixed with soda ash binder and water to form a paste which is roasted at 530-650°C. Then the paste is leached in water to dissolve sodium selenate. Residues are separated from the selenate with filtration. Sulphuric acid is used to remove the impurities in hydrolysis. Hydrochloric acid or ferrous iron salt is used for the reduction of hexavalent selenium. Iron chloride is discarded, which contain small amounts of selenium but is also extremely corrosive and creates problems for disposal. The remaining solution is precipitated with sulphur

dioxide and then filtrated. The final steps are melting and shooting to produce selenium metal.

After Se is extracted from copper refinery slimes, the average purity is approximately 99%. For photovoltaic, the simplest and the most common method of achieving 99.99% pure selenium is vacuum distillation.

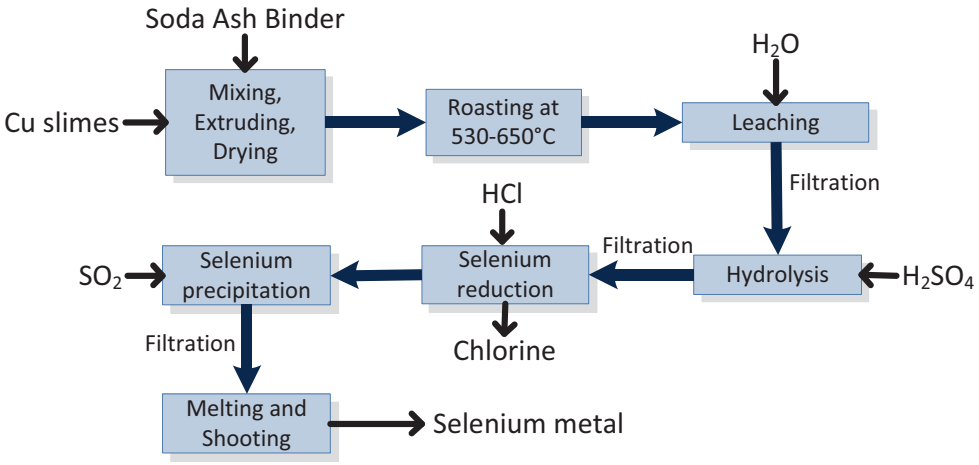

Figure 2-15 Process flows for Se production (V. Fthenakis et al., 2009)

Focus on thin-film CIS/CIGS

The CIGS absorbed layer is commonly deposited with co-evaporation techniques (see Figure 2-16). The substrate in the co-evaporation process reaches a temperature range between 400 and 600°C. In this process, all the elements are evaporated together on the substrate. The deposition of the material and formation of the compound happens together. This is achieved by thermal evaporation from elemental sources at temperatures greater than 1,000°C for Cu, In and Ga. A mass controller is used. The CIGS absorbed layer thickness is about 2 μm.

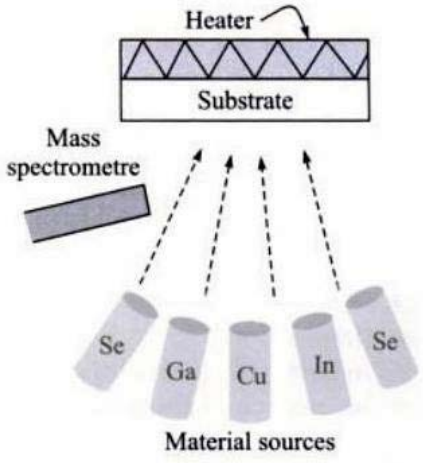

Figure 2-16 Deposition of CIGS layer using co-evaporation (Singh Solanki, 2011)

Focus on module manufacturing

The process starts with the deposition of the absorber layer on the molybdenum coated glass substrate. A soda-lime substrate composed of about 70% silica, 15% sodium oxide, 9% calcium oxide, and 6% of others compounds is chosen due to the importance of Na. The CIGS layer is deposited. After the absorbed layer, the buffer layer of CdS is deposited using chemical bath deposition (CBD) method. On the top of CdS buffer layer, a TCO layer is added. The ZnO is typically used as TCO.

Finally, the electrical wire and buss bars are attached. These are metal stripes that can be soldered, welded, or glued to contact areas near the edges of the substrate plates. Lamination with a front cover glass, which is usually EVA is next. Edge sealing and framing finished the product. The arrangement of CIS-based solar cell is found in Figure 2-17.

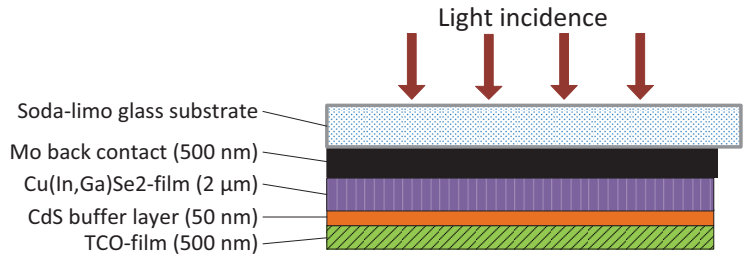

Figure 2-17 Structure of CIS-based solar cell (Singh Solanki, 2011)

2.2.5 *Discussion*

A valid question raised in scrutinizing technologies regarded as environmentally friendly is whether they are truly "sustainable" or not. For alternative energy systems in particular, this query translates in one key sense to whether they represent a net gain – do they generate more energy than was used to create them in the first place and if so to what extent?

From the description of the manufacturing processes for the top five PV modules technologies describe above is possible to note the large amount of energy that is required for both the production and purification of the raw material to obtain the degree of purity that allows them an efficient conversion energy, and the high temperatures required for each one of the processes for the manufacture of the module.

When comparing the embodied primary energy of the five production processes from the information above, it is emphasized that technologies based on c-Si (m-Si and p-Si mainly) are those that require the highest amount of material and energy on the one hand by the dimensions and thickness of the module and on the other hand by the purification process and growth of Si to form the ingot that subsequently will be transformed into the wafer.

The main advantage presented by the TF PV modules is related, because of their thickness, to the smaller amount of material and energy needed for manufacturing them. As mentioned in the previous

chapter, the combination of less materials and energy needed to manufacture a PV module results in a much lower cost on manufacturing and therefore a lower price compared to c-Si PV modules.

Some works try to answer if indeed the energy produced by a PV module during its lifetime is enough to offset the amount of energy they consume during the manufacturing process (Ayompe, Duffy, McCormack, & Conlon, 2010; Dale, 2012; Knapp & Jester, 2000; Lloyd & Forest, 2010; Nawaz & Tiwari, 2006). They conclude that not all financial cost reductions lead to reductions in embodied energy, an economic analysis should be supplemented with energy analysis. Also PV systems with lower energy costs provide more net energy.

The net gain concept must be extended as well to pollutants (e.g. SOx, NOx, particulates) or global greenhouse gas emissions (e.g. CO_2). A truly sustainable technology should represent a net gain to the humanity that wish to continue its standard of living, historically correlated with energy use. The presentation of environmental assessment techniques is then proposed in what follows to identify the method that will be selected.

2.3 Environmental assessment techniques

According to Sadler (Sadler & Verheem, 1996), environmental assessment is defined as "a systematic process for evaluating and documenting information on the potentials, capacities and functions of natural systems and resources in order to facilitate sustainable development planning and decision making in general, and to anticipate and manage the adverse effects and consequences of proposed undertakings in particular". There are many different procedures and methods to assess the environmental issues or impacts of plans, projects and programmes. Table 2-1 summarizes some of these techniques.

Among the techniques mentioned in Table 2-1, LCA is the most well-known and powerful tool (Finnveden et al., 2009; Heijungs, Huppes, Zamagni, & Masoni, 2011; Manuilova, Suebsiri, & Wilson, 2009). Studies have shown that LCA can complement and add value to the other techniques (Finnveden et al., 2009; Manuilova et al., 2009). There is no single tool or approach to address all the problems of environmental management. The Society of Environmental Toxicology and Chemistry (SETAC) conducted a discussion within a working group in order to define the relationship of LCA with the others techniques (Heijungs et al., 2011).

In addition to the advantages described, LCA employs many of the principles of the other techniques, e.g. LCA always requires to establish the inventory of flow of materials and substances as MFA, some of the LCA methods to assess the human health impacts use ERA principles, LCA shares with the EIA and MILP the use of characterization indices and impact factors.

Furthermore, LCA allows the comparison between different environmental impacts through design of alternative scenarios or making the comparison of different product's processes that perform the same function. These reasons explain why LCA has been selected as an environmental assessment technique in this work. A more detailed description of the LCA technique will be discussed in the following section of this chapter.

Table 2-1 Environmental assessment techniques

Method	Description and key points	Strengths	Weaknesses
Cost-benefit analysis (CBA) (Burgess & Brennan, 2001; Hanley & Spash, 1993; Pearce, Giles, & Mourato, 2006)	Constitutes an "environmental economics" approach. This approach tries to estimate the economic value of any loss (cost) or gain (benefit) of environmental quality to use these values in the traditional costs and benefits evaluation of a project. Determines whether and how much a project can contribute to national economic welfare, which of several options should be selected for action, and when the investment is to be executed. The essential steps are: defining the project, identifying economically relevant impacts, physically quantifying impacts, calculation monetary valuation, discounting, weighting, and sensitivity analysis.	- The effect of time is considered. - Decision makers are already familiar with monetary units.	- Many environmental cost and benefits cannot easily be quantified. - Some of the traditional elements of the CBA are questionable as for environmental analysis ,e.g. discount rate - Some valuation techniques are unlikely to be practicable in the framework of most current engineering design decisions.
Environmental Impact Assessment (EIA) (Burgess & Brennan, 2001; Kessler, 200AD; Manuilova, Suebsiri, & Wilson, 2009)	Analyses and evaluates the positive and negative impacts that human activities can have on the environment. Considers all possible environmental and socio-economic issues associated with the proposed project in a qualitative and quantitative way. Provide decision makers with the resulting information. Uses environmental indices. EIA has three major phases: screening and scoping of the project, environmental impact assessment, and decision-making and review.	- Environmental damage of the project can then be minimised and any environmental benefits identified. - Considers local impacts. - EIA is a systematic process.	- A specific site and time must be defined to estimate environmental impacts. - Only direct impacts that fall within the boundaries of the system under study are analysed. - Rigorous and quantitative analysis of the data is often required to make sense of the large amounts of uncollected data. - It is more a legal procedure than a detailed environmental assessment tool.
Exergy analysis (Brunner & Rechberger, 2011; Szargut, 2005)	Measures the maximum amount of work that can be obtained by bringing a resource into equilibrium with its surroundings through a reversible process	- Provides information to identify the location, resources and causes of problems form deviations of the ideal system in balance.	- Only focuses a thermodynamic viewpoint. - Complexity in defining the reference state (ideal system in balance).

Table 2-1 Continuation…

Method	Description and key points	Strengths	Weaknesses
Life Cycle Asseessment (LCA) (Ayres & Ayres, 2002; Finnveden et al., 2009; Manuilova et al., 2009)	Identifies and quantifies the process flows and systems which are major contributors to environmental degradation. Encompasses extraction and processing of raw materials, manufacturing and assembly processes, product distribution, use, re-use, maintenance, recycling and final disposal Regulated and guided by the ISO norm. Four main steps are comprised: goal and scope definition, inventory analysis, impact assessment, and interpretation.	- Considers a range of environmental impact categories. - Total economic and environmental burdens of a process can be quantified by performing an LCA in conjunction with a techno-economic feasibility study. - A non-site-specific approach to environmental impacts is required - Long term strategic planning - Identifies the areas for improvement which will have the greatest influence on total life cycle impacts	- Lack of data can restrict the conclusions that can be drawn from a specific study. - The intrinsic risks of the processes are not addressed. - LCI data must be used cautiously since production processes differ from country from country.
Material Flow Analysis (MFA) (Ayres & Ayres, 2002; Brunner & Rechberger, 2011)	Delivers a complete and consistent set of information about all flows and stocks of a particular material within a system. Is based on two fundamental principles: system approach and mass balance. This permit to create a list of the amounts of the different flows. Usually comprises four steps: goal and systems definition, process chain analysis, accounting and balancing, modelling and evaluation.	- The analysis can be applied at industrial, national or worldwide scale. - Requires the history of pollution and consumption of resources in an area or region. - Mass balance are required to evaluate the stock of material ignored or underestimated.	- Focus on a single material. - To determine the environmental impacts a LCA or exergy analysis is needed.
Material Intensity Per unit Service (MILP) (Brunner & Rechberger, 2011; Ritthof, Liedtke, & Merten, 2002; Schmidt-Bleek, 1993)	Measures the total mass flow of material caused by production, consumption and waste disposal of defined service unit (fabrication of a kitchen, washing cycle of a dishwasher,…) or product. Only uses the input flows (consider input flows equal to output flows). The material input is calculated in five categories: abiotic raw materials, biotic raw materials, water, erosion, and air. All material consumption during manufacture, use and recycling or disposal is calculated back to resource consumption by using simple calculation factors expressed in kg or ton. The aim is to reduce the total amount of the addition of all the material and energy flows expressed in kg or tons.	- Allow comparisons of resource consumption of different solutions to produce the same service. - Reveals the magnitude of resource use along the life-cycle and help to focus efforts on the most significant phases to reduce environmental burden of the product. - Measures material and energy in the same unit constitutes an excellent communication tool to identify the main problems.	- Does not take into account ecotoxicity of materials or biodiversity.

2.4 LCA Methodology

As abovementioned, Life cycle assessment (LCA) evaluates the environmental impacts of products, processes and services. The results of LCA can identify major emissions, thereby enabling consideration of measures for their reduction.

LCA evaluates the material and energy flows involved in the whole life cycle of the product as it is represented in Figure 2-18. It is possible to classify them in:

- Elementary flows: consist of flows that each process exchanged with the ecosphere: *primary resources* as water, fuels, minerals..., and *waste emissions* as solid waste, effluents and gaseous emissions.
- Intermediate flows: material or energy flows between the different stages of the life cycle.

For an adequate interpretation of the results that will be generated by an LCA, the goal must be appropriately defined and will guide the LCA operator to manage and focus the efforts to collect the information that best suit the purpose and interpret the outcomes appropriately.

For Jolliet et al. (Jolliet, Saadé, & Crettaz, 2010), LCA evaluates the environmental impact of a product, service or system related to a particular function, considering all stages of its life cycle. It identifies all the points on which a product can be improved and it contributes to the development of new products.

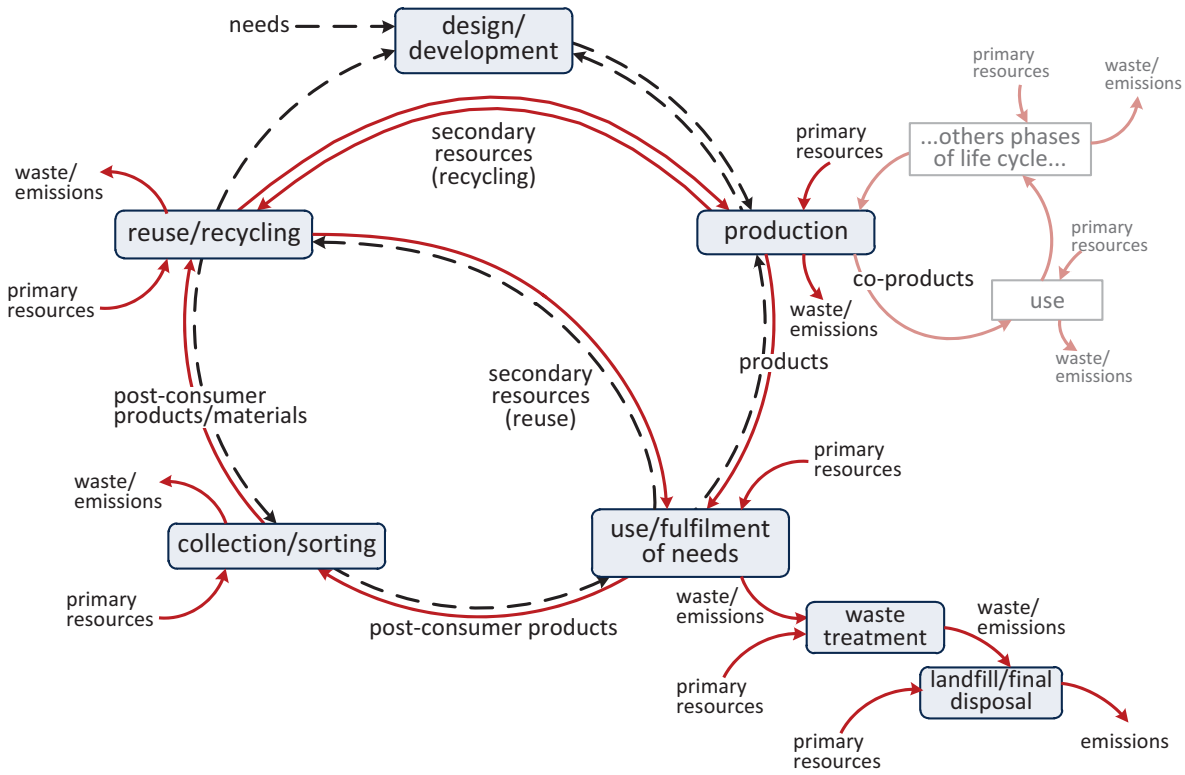

Figure 2-18 Schematic representation of the life cycle of a generic product (based on (Rebitzer et al., 2004))
(the full arrows represent material and energy flows, while the dashed arrows represent information flows, the presence of a secondary life cycle (in watermark) shows that several life cycles can be nested into each other).

From the LCA investigations that were already implemented and mentioned in numerous studies, (Jolliet et al., 2010) for instance, several strengths of the LCA methodology can be highlighted.

- In eco-design, LCA can help to take into account environmental criteria during the design phase of a new product or product improvement already created. This is typically one of the first motivations of this work.
- In the evaluation and improvement of product, LCA can identify critical areas on which it is possible to focus to optimize the environmental performance and to compare different manufacturing processes.
- LCA can also be useful to obtain elements of decision support for the implementation of industrial policy (choice of design, product improvement, selection of procedures, etc..) or public policies (choice of recovery processes, eco-labelling criteria, etc..).

The objective of this study is to develop an environmental module for PV modules based on LCA that reflects the different options in PV manufacturing, based on existing data.

Two main advantages can be found by using LCA for PV systems:

1. When using LCA, the system can be optimized from an environmental viewpoint taking into account CO_2 emissions, human health impacts and effects on the local fauna and flora ….
2. The second advantage is comparability. When comparing energy generation technologies (e.g., when searching for the installation of a PV system as a supply of alternative energy as opposed to other generation systems, or when installing energy supply systems based on multiple generation technologies), LCA can provide quantitative results, thereby enabling comparison of each technology on an equal footing.

The application of LCA requires a protocol defined by the International Organization for Standardization (ISO) that has developed and formalized a series of standards for the Environmental Management. These standards include the ISO-14040 (International Standard Organization, 1997), which describes the principles and framework for LCA and ISO-14044 (International Standard Organization, 2000), which explains the requirements and guidelines of LCA. The research and analysis scheme for LCA consists in four stages as shown in Figure 1-8. Only the key points are briefly recalled in what follows.

2.4.1 *Goal and scope definition*

Defining the objectives and scope of the study is the first and essential step to guarantee the quality of the study. The definition of the problem establishes a rigorous framework for the study. It involves an accurate description of the study to be performed and the identification of the purpose, to whom it may concern and the possible applications.

The scope determines which product system or process will be analysed, the unit processes evaluated, functional unit, system boundaries, impact categories, data requirements, and limitations. Some important concepts in the LCA are:

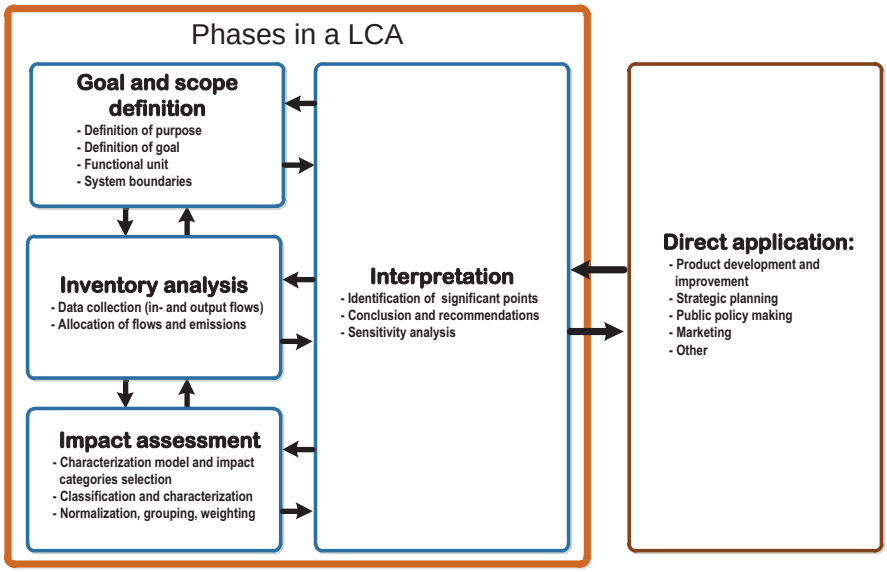

Figure 2-19 LCA framework (ISO 14040:1997)

A *unit process* describes a stage within the life cycle of a product and serves as the basic element of analysis in the LCA. The identification of unit processes facilitates the quantification of the inputs and outputs flows at each phase of the life cycle. The set of unit processes gives the *product system.* It involves the production, use, and disposal of a product or service throughout its life cycle.

System boundaries specify the unit processes, defined at the scope of the analysis, to be included in the LCA. The accurate description of the system and of its boundaries has strong implications for the results of the assessment.

It necessary to define a reference unit to quantify the inputs and outputs flows. This unit is called the *functional unit* (FU). The FU must be fully specified and measurable. It also serves as the basis for comparison when considering the environmental impacts of multiple product systems.

2.4.2 *Inventory analysis*

Life-cycle inventory (LCI) analysis involves data collection and calculation procedures to quantify relevant input and output flows of the product system(s). The LCI phase requires the highest efforts and resources of an LCA. Data collection consists in the identification and quantification of relevant inputs and outputs for each unit process of a specific product system taking into account the FU. Data for each unit process within the system boundary include energy and raw material flows, products and co–products, waste and emissions to air, water, and soil (Figure 1-10).

Data for each unit process are either provided directly from industry or using an LCI database, such as Ecoinvent, European Life Cycle Database (ELCD) or US life cycle inventory database. Databases provide industrial data on energy supply, resource extraction, material supply, chemicals, metals, agriculture, waste management services, and transport services for a variety of generic unit processes that allow for the development of more complex product systems (Ecoinvent Center, 2010).

The LCI must be done from the process tree in which the reference flows were defined and related to

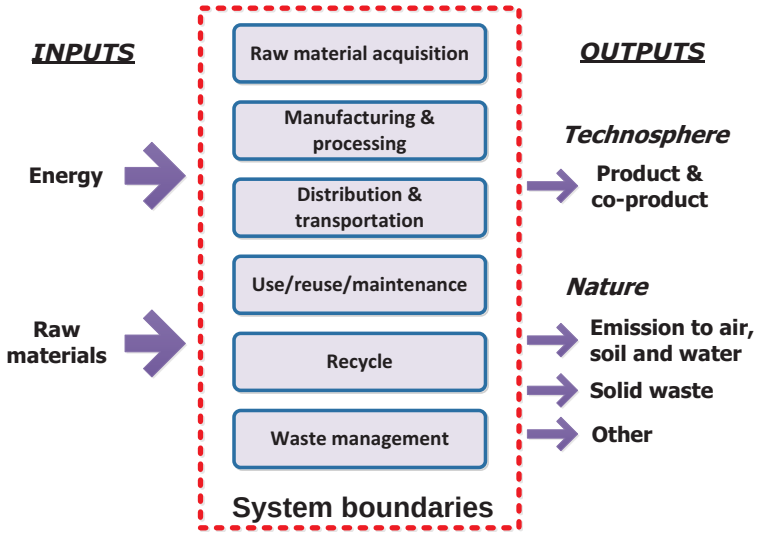

Figure 2-20 LCI schema

the FU. The process tree represents the set of unit processes that constitute the system under analysis. For each unit process, its inputs (intermediate flows of the system) and direct emissions (elementary flows) are determined. The next step is to search for the values of the indirect emissions and extractions related to each of the inputs flows. Indirect emissions and extractions are calculated by multiplying the quantity of input flows per FU and the emission factors per unit of input flow. Total emissions and extraction will be the sum of the direct elementary flows and the indirect emissions and extractions related to the inputs.

2.4.3 *Impact assessment*

The Life-cycle impact assessment (LCIA) stage uses the LCI results to evaluate the significance of potential environmental impacts. The impacts are the effects of the flows measured in LCI, such as the health effects caused by the inhalation of given emissions. The structure of this phase distinguishes between mandatory and optional elements (Figure 2-21).

2.4.3.1 Selection of impact categories and characterization models

The selection of impact categories must be comprehensive in the sense that they cover all relevant environmental issues related to the analysed system. Two main schools of methods have been developed depending on the level of analysis along the cause-effect chain (Finnveden et al., 2009; Jolliet et al., 2003). The primary effects represent the direct result of activities studied e.g. the greenhouse gas emissions. They can be distinguished from side effects, which are the consequences of primary effects. For example, the ozone layer depletion generates the growth of UV radiation that reaches the ground, this situation increasing the human health problems.

Problem-oriented methods will model the relatively early stages in the cause-effect chain to limit uncertainties. These methods are known as *midpoint* method. Damage-oriented methods, the so-called *endpoint* methods, try to consolidate the impact on the final results, as far as possible in the cause-effect chain. They provide more concrete information, but they remain more uncertain.

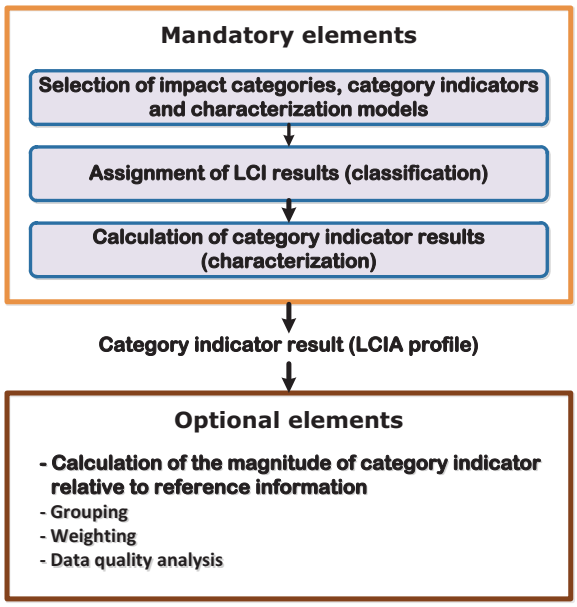

Figure 2-21 Elements of LCIA (ISO 14042:2000)

The methods for analysis of the impacts have been widely described in the literature. These methods are the result of several years of work and each has their specificities. In 2010, the European Commission (European Commission, Joint Research Centre, & Institute for Environment and Sustainability, 2010) published a guide with the description of some of these methods. In this publication, an analysis of the strengths, particularities, methodology used and impact categories pre-selected of each method was made. Table 2-2 presents some of the most used LCIA methodologies described by the European Commission.

In this work, the IMPACT 2002+ approach was selected as LCIA method. IMPACT 2002+ (IMPact Assessment of Chemical Toxics) proposes a feasible implementation of a combined midpoint/damage approach, linking all types of life cycle inventory results via 14 midpoint categories to four damage categories (Jolliet et al., 2003). IMPACT 2002 + combines the advantages that different existing LCIA methods have as well as internal developments in various impacts categories. In IMPACT 2002 +, the characterization factors for Human Toxicity and Aquatic & Terrestrial Ecotoxicity from the methodology IMPACT 2002, the other characterization factors are adapted from existing

Table 2-2 Methods for LCIA (European Commission et al., 2010)

		Impact modelling depth			
Methodology	**Developed by**	Midpoint	Endpoint	Normalisation	**Source**
CML 2002	CML (Netherlands)	X		X	(Guinée et al., 2002)
Eco-indicator 99	PRé (Netherlands)		X	X	(M. Goedkoop & Spriensma, 2001)
IMPACT 2002+	Ecole Polytechnique Fédérale de Lausanne (Switzerland)	X	X	X	(Jolliet et al., 2003)
ReCiPe	Radboud University Nijmegen + PRé + CML + RIVM (Netherlands)	X	X	X	(Mark Goedkoop et al., 2009)

characterizing methods, i.e. Eco-indicator 99, CML 2001, IPCC and the Cumulative Energy Demand. New concepts and methods were developed, especially for the comparative assessment of human toxicity and ecotoxicity (Frischknecht et al., 2007).

2.4.3.2 Impacts and damages classification

In classification phase, emissions and extractions flows obtained in the LCI are assigned to the impact categories selected, some emissions or extractions can contribute to several categories. According to the characterization method selected, the classification of impacts is different because of the impact categories pre-selected. Impact categories include climate change, stratospheric ozone depletion, photooxidant formation (smog), eutrophication, acidification, water use, noise, etc. (Pennington et al., 2004)

It is possible to elaborate a damage classification (endpoint). Three major groups, commonly referred to as areas of protection (European Commission et al., 2010; Pennington et al., 2004), are considered for the classification of damages: resource use, human health consequences and ecological consequences.

2.4.3.3 Characterization of impacts and damages

This step consists of modelling, by using factors, the classified LCI flow data for each of the impact categories. To all classified flows a quantitative characterization factor shall be assigned for each category to which the flow relevantly contributes. This factor expresses how much that flow contributes to the impact category indicator (at midpoint level) or damage category indicator (at endpoint level).

For midpoint level indicators, this relative factor typically relates to a reference flow, e.g. *kg CO_2-equivalents* per kg elementary flow in case of Global Warming Potential. For endpoint level indicators, it typically relates to a specific damage that relates to the broader area of protection, e.g. for species loss measured the *potentially displaced fraction of species for an affected area and duration* (PDF*m²*a) is used (European Commission et al., 2010).

The characterization of each impact categories is the sum of the product of the mass of the substances listed at the LCI classified by impact category and their own characterization factor. (Equation (2.6))

$$\mathrm{SI_i} = \sum_{S} FI_{s,i} \times M_S \qquad (2.6)$$

where SI_i represents the characterization score for the impact category i, $FI_{s,i}$ is the characterization factor for the substance S in the impact category i, and M_s is the mass of substance s from the LCI.

The impact categories can be grouped into the damage categories. Each impact category has a higher or lower contribution for the selected damage category. Therefore, a damage characterization factor is needed.

To pass from the impact characterization through the damage evaluation and calculate the damage score, the characterization score should be multiplied by its damage characterization factor. (Equation (2.7))

$$SD_d = \sum_i FD_{i,d} \times SI_i \quad (2.7)$$

SD_d represents the damage score for the damage category *d*, $FD_{i,d}$ is the damage characterization factor for the impact category *i* in the damage category *d*.

The characterization factors differ from one characterization method to another. They are available in the literature, in the form of databases, as well as in LCA support software tools. Table 2-3 and Figure 2-22 contain the midpoint and damage categories which IMPACT 2002+ works and the reference flow for each category.

Where:

- Kg_{eq} *Substance x* (kg equivalent of a reference substance x) expresses the amount of a reference flow x that equals the impact of the considered pollutant.
- *DALY* (Disability Adjusted Life Years) characterizes the disease severity, accounting for both mortality and morbidity.

Table 2-3 Characterisation reference substances and reference flow used in IMPACT 2002+ (Based on (Margni, Jolliet, & Humbert, 2005))

Midpoint category	Midpoint reference flow (Kg_{eq} Substance x)	Damage category	Reference flow
Human Toxicity (carcinogens + non-carcinogens)	Kg_{eq} chloroethylene into air	Human health	DALY
Respiratory effects (inorganic)	Kg_{eq} PM2.5 into air		
Ionizing radiation	Bq_{eq} carbon-14 into air		
Ozone layer depletion	Kg_{eq} CFC-11 into air		
Photochemical oxidation (Respiratory organics)	Kg_{eq} ethylene into air		
Aquatic ecotoxicity	Kg_{eq} triethylene glycol into water	Ecosystem quality	PDF*m²*a
Terrestrial ecotoxicity	Kg_{eq} triethylene glycol into soil		
Terrestrial acid/nutri	Kg_{eq} SO_2 into air		
Land occupation	M^2_{eq} organic arable land-year		
Aquatic acidification	Kg_{eq} SO_2 into air		*Under development*
Aquatic eutrophication	Kg_{eq} PO_4^3 into water		*Under development*
Global warming	Kg_{eq} CO_2 into air	Climate change	Kg_{eq} CO_2 into air
Non-renewable energy	MJ Total primary non-renewable or kg_{eq} crude oil (860kg/m^3)	Resources	MJ
Mineral extraction	MJ additional energy or kg_{eq} iron		

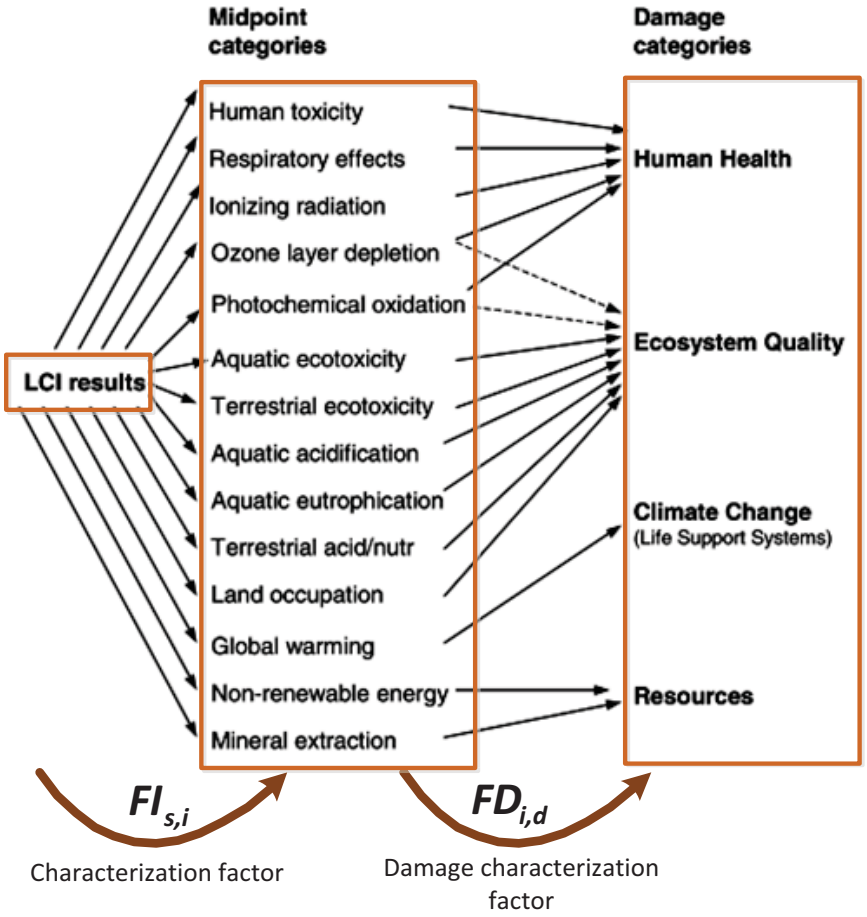

Figure 2-22 General approach of LCIA of emissions on the major categories of environmental damage

- *PDF*m²*yr* (Potentially Disappeared Fraction of species per m^2 per year) is the unit to "measure" the impacts on ecosystems. PDF*m^2*yr represents the fraction of species disappeared on 1 m^2 of earth surface during one year.

2.4.3.4 Optional elements: Normalisation, Grouping and Weighting

The purpose of the *normalisation* is to facilitate interpretation of the LCIA results by analyzing the importance of the respective contribution to the overall environmental impact. As impact or damage categories have different units, normalisation is used to make these categories dimensionless.

Normalized LCIA results are obtained by dividing the LCIA results by the reference value, separately for each impact category (Equation (2.8)). Each characterization method proposes its own reference value. There are numerous methods of selecting a reference value, including the total emissions or resource use for a given area that may be global, regional or local in a given period of time, or the total emissions or resource use for a given area in a per capita basis in a given period of time. Normalisation results can provide input to grouping or weighting.

$$N_k = \frac{S_k}{VR_k} \tag{2.8}$$

N_k represents the normalised score of the impact or damage categories k, S_k is the characterization or damage score of the impact or damage categories k, and VR_k is the reference value for the impact or damage categories k.

Grouping is a qualitative or semi-qualitative process that involves sorting and / or ranking among normalised scores. Grouping may result in a broad ranking, or hierarchy, of impact categories with respect to their importance. Such a ranking can provide structure to help draw conclusions on the relative importance of different impact or damage categories (Pennington et al., 2004). For example, categories could be grouped in terms of high importance, moderate importance and low priority issues. *Weighting* involves assigning distinct quantitative weights to all impact categories expressing their relative importance. A weighting of the normalised indicator results may be performed. This can include aggregation to a single indicator. It is often applied in the form of linear weighting factors:

$$EI = \sum_k PF_k S_k \quad or \quad EI = \sum_k PF_k N_k \tag{2.9}$$

where *EI* is the overall environmental impact indicator, PF_k is the weighting factor for impact category k.

Methods for weighting can be based on (Pennington et al., 2004):

- A distinction between impact indicators defined early (midpoints) or late (endpoints) in the impact chain.
- The expressed preference. People are asked the relative importance of damages or impact categories.
- Distance to target, where characterization results are related to target levels.
- Monetization. These monetized weighting factors are derived from reactions to different situations, such as insurance payouts, health care expenditures, fines, costs incurred.

2.4.4 *Interpretation of results*

The interpretation of LCIA results is the last phase. It analyzes the results provides in the phase above based on the objectives and scope of the study previously defined. Conclusions are thus made, and areas for improvement can be detected in order to start looking for possible alternatives of solutions to finally take a decision.

The interpretation proceeds through three main activities:

- Identify the significant issues. An analysis and organization of the results must be done to identify the main contributors to the LCIA results (processes and elementary flows) and the most relevant impact categories. Significant choices as assumptions, foreground and background data used for deriving the process inventories, LCIA methods used, as well as the normalisation and weighting factors must also be identified because of the potential influence in the precision of the final results of the LCA.
- Determine the influence of significant issues on the overall results of the LCA. The evaluation is performed in close interaction with the identification of significant issues in order to determine the reliability and robustness of the results. The evaluation involves completeness

check, sensitivity check in combination with scenario analysis and potentially uncertainty analysis and consistency check.

- Formulate the conclusions and recommendations of the LCA study. Recommendations based on the final conclusions of the LCA study must be logical and be reasonable and plausible founded in the conclusions and strictly relate to the intended applications as defined in the goal of the study.

2.4.5 *Limitations of LCA*

LCA studies present various limitations like:

- A LCA study, because of its "holistic" nature, requires a lot of time and economical resources. The more detailed a LCA is the more time-consuming and expensive it will be. High costs are partly caused by the need for professional consultation and expert knowledge in the stages of impact and improvement analyses.
- LCA is a tool based on linear modelling so it regards all processes as linear. Some progress is being made in reducing this limitation.
- There is not a unique LCA methodology even if the main steps are regulated and guided by the ISO norm. Each impact assessment method has its own impact and/or damage categories, characterization factors and references values for the normalisation. This situation makes difficult the comparison of LCA studies between products or processes if they were not made under the same impact assessment method.
- The assumptions made in such studies (for example the boundary determination, the source of data and the impact assessment choice) might be subjective.
- The accuracy of a LCA study depends on the quality and the availability of the relevant data, and if these data are not accurate enough, the accuracy of the study is limited. These facts affect the precision of the final results.
- Because LCA studies are focused on national and regional level, they might not be suitable for local applications.
- The availability, customization and updating of the database is another problem. Even if the databases are being developed for several countries, considering its particularities, and the format for databases is being standardised, data are frequently obsolete, incomparable, or of unknown quality. Some of the data are available in aggregated format.
- LCA approach cannot replace the decision making process. It only provides information for decision support.

2.4.6 *LCA software tools*

Nowadays, many LCA software tools have been developed based on the methodology of LCA. Most of them include a certain number of databases and impact assessment methods.

These tools facilitate the estimation of total emissions and extraction for the LCI as well as the calculation of characterization, damage and normalised score. Some of them generate a report with the

Table 2-4 Main LCA software tools

Software name	Supplier	Website
TEAM	ECOBILAN-PricewaterhouseCoopers	http://ecobilan.pwc.fr/fr/boite-a-outils/team.jhtml
GaBi Software	PE INTERNATIONAL	http://www.gabi-software.com/france/software/
Umberto	ifu Hamburg GmbH	http://www.umberto.de/en/
SimaPro	PRé Consultants	http://www.pre-sustainability.com/simapro-lca-software
openLCA	GreenDelta GmbH	http://www.openlca.org/openlca

results obtained through graphs. Evaluation of scenarios and sensitivity analysis are other optional features of these software tools. Table 2-4 shows some of the LCA software tools currently available on the market.

To perform the LCA study for PVGCS, the SimaPro software tool with the EcoInvent database was selected. It is widely mentioned in the dedicated literature for this kind of study.

The environmental impact results are available through graphs or tables that can be exported. Several processes or scenarios can be compared.

2.5 LCA study for m-Si based PV module

The LCA methodology is first applied to a simple case, the production of a PV module, in order to fully understand each of the abovementioned steps. In this first example, a description of each step of the LCA applied to the manufacturing process of the m-Si based PV module is made. The data were collected from the literature, particularly from the work developed by Alsema et al (Alsema & Wild-scholten, 2006; de Wild-Scholten & Alsema, 2005).

2.5.1 *Goal and scope definition*

As shown in Figure 2-19, the first step in the methodology is to define the objective and scope of the study.

The objective of this study is to identify and evaluate the overall environmental impacts associated of a PV module made by m-Si solar cells. The assessment was mainly focused on energy and material flows during the production of the PV modules.

System boundaries are set as shown in Figure 2-23. The evaluation begins with the purification of Si to obtain SoG-Si using the Siemens process to the final assembly of PV module. The description of each of the processes taken into account is given in Section 2.2.1.

The functional unit for this LCA is a finished piece of m-Si based PV module. The characteristics of the PV module are the same as Alsema et al. consider in their work (de Wild-Scholten & Alsema, 2005). The PV module is composed by 72 m-Si solar cells of 125 mm x 125 mm (1.25 m^2 module area), with glass/EVA/Tedlar lamination. Glass thickness was set at 3.6 mm and the aluminium frame is 3.8 kg. The m-Si wafers are made following CZ process.

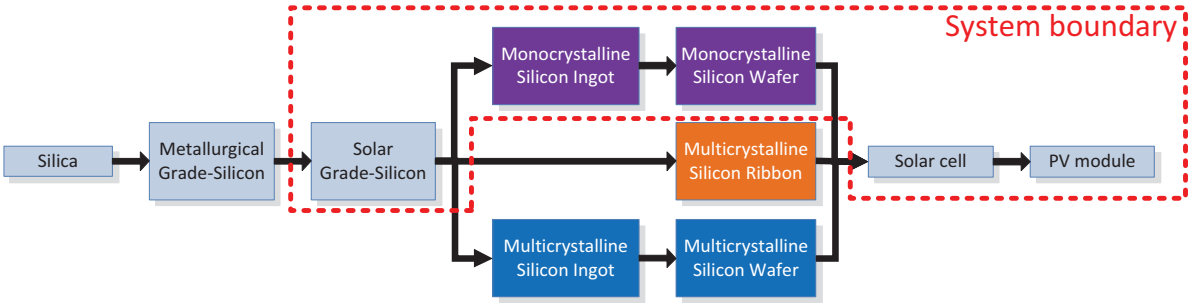

Figure 2-23 System boundaries for m-Si PV module LCA

The PV module is assumed to be manufactured in Germany. The energy mix of Germany is then used in the computations.

2.5.2 *Inventory analysis*

From the data given by Alsema et al. for each unit process involved in the system boundary considering the interconnexion of the units constituting the whole manufacturing process, the material requirements and the emissions per PV module of m-Si (LCI) are calculated. Table 2-5 shows input and output flows for each unit process.

As it can be seen, each unit process has its own reference flow (per kg feedstock, m² of wafer or per solar cell). Yet it must be kept in mind that finally all material must be estimated per functional unit (per piece of PV module). Table 2-6 shows the amount of total inputs (intermediate flows) and direct emission for each process unit considering the FU.

The next step is to calculate the total emissions and extraction flows. SimaPro and more precisely Ecoinvent database are particularly useful. The different unit processes considered within the boundaries of the system is created in SimaPro. Inputs and outputs as indicated in Figure 2-23 are introduced by using the processes that are then included into the Ecoinvent database. The program calculates both direct and indirect emissions and displays the total emissions. For the manufacture of the PV module, the program identifies 890 different types of substances that are released either into water, land and air. Table 2-7 shows only some of the 890 emissions that are produced during the manufacture of m-Si based PV module.

2.5.3 *Impact assessment*

The third step in the LCA methodology involves the assessment of environmental allocation caused by the emissions that were listed in the previous step. One of the characterization methods listed in Table 2-2 is required. As mentioned in Section 2.4.3.1, IMPACT 2002+ was chosen because it allows the classification and characterization of environmental impacts (midpoint) and damage consequences (endpoint).

The selected LCIA method is found within Ecoinvent database, taking into account the classification and characterization of each of the 890 substances into the categories considered by IMPACT 2002+ (see Table 2-3). For the sake of illustration, Table 2-8 and Table 2-9 indicate the total characterization score for two midpoint categories, i.e. Global Warming and Respiratory Inorganic respectively.

Table 2-5 LCI data for manufacturing process of m-Si PV module from (de Wild-Scholten & Alsema, 2005)

1 kg of polycrystalline SoG-Si by Siemens process	Amount	Unit
Materials		
MG-silicon	1.13	kg
Chemicals inorganic	2.00	kg
Heat, natural gas	185.00	MJ
Electricity/heat		
Natural gas	45.00	kWh
Electricity, hydropower	65.00	kWh

1 m² of m-Si wafer by CZ process	Amount	Unit
Materials		
Polycrystalline SoG-Si	1.5800	kg
Sand	0.3600	kg
Flat glass, uncoated	0.0100	kg
Steel	1.4900	kg
Silicon carbide	2.6100	kg
Argon	6.2000	kg
Dipropylene glycol	0.3000	kg
Adhesive for metals	0.0020	kg
Surfactant	0.2400	kg
Sodium hydroxide, 50% in H_2O	0.0150	kg
Hydrochloric acid, 30% in H_2O	0.0027	kg
Acetic acid, 98% in H_2O	0.0390	kg
Tap water	0.0060	kg
Water, deionised	65.0000	kg
Electricity/heat		
Electricity, medium voltage	45.000	kWh
Natural gas	65.000	kWh
Final waste flows		
Silicon waste	0.400	kg
Waste to treatment		
Waste, silicon wafer production	6.000	kg

1 piece of m-Si solar cell	Amount	Unit
Resource		
Water, cooling	1.56×10^{-2}	m^3
Materials		
m-Si wafer	1.060	p
Phosphorus	2.27×10^{-5}	kg
Metallization paste	1.17×10^{-3}	kg
Polystyrene, expandable	6.36×10^{-6}	kg
Nitrogen	2.89×10^{-2}	kg
Oxygen	1.59×10^{-3}	kg
Argon	4.01×10^{-4}	kg
Ammonia	1.05×10^{-4}	kg
Silicon tetrahydride	1.89×10^{-5}	kg
Sodium hydroxide, 50% in H2O	2.45×10^{-3}	kg
Acetic acid, 98% in H2O	4.42×10^{-5}	kg
Hydrochloric acid, 30% in H2O	7.12×10^{-4}	kg
Hydrogen fluoride	5.89×10^{-4}	kg
Nitric acid, 50% in H2O	4.17×10^{-4}	kg
Phosphoryl chloride	3.39×10^{-6}	kg
Phosphoric acid, industrial grade, 85% in H2O	1.19×10^{-4}	kg
Sodium sulphate	1.17×10^{-3}	kg
Calcium chloride	3.37×10^{-4}	kg
Isopropanol	1.23×10^{-3}	kg
Ethanol	9.98×10^{-6}	kg
Solvents, organic	2.24×10^{-5}	kg
Water, deionised	2.15	kg
Electricity/heat		
Electricity, medium voltage	5.90×10^{-1}	kWh
Natural gas	7.42×10^{-2}	MJ
Fuel oil	5.11×10^{-4}	kg
Emissions to air		
Aluminium	1.21×10^{-5}	kg
Hydrogen chloride	4.16×10^{-6}	kg
Hydrogen fluoride	7.56×10^{-8}	kg
Lead	1.21×10^{-5}	kg
Particulates, unspecified	4.15×10^{-5}	kg
Silicon	1.13×10^{-6}	kg
Silver	1.21×10^{-5}	kg
Sodium hydroxide	7.56×10^{-7}	kg
Tin	1.21×10^{-5}	kg
VOC, volatile organic compounds	3.02×10^{-3}	kg
Final waste flows		
Photovoltaic cell waste	4.13×10^{-3}	kg

1 piece of m-Si PV module	Amount	Unit
Materials		
m-Si cell	73.4000	p
Aluminium	3.8000	kg
Solar glass	11.4000	kg
Ethylene vinyl acetate copolymer	1.3000	kg
Polyvinylfluoride	0.1600	kg
Polyethylene terephthalate (PET)	0.1600	kg
Copper	0.1400	kg
Tin	0.0070	kg
Lead	0.0040	kg
Nickel	0.0002	kg
Flux, wave soldering	0.0100	kg
Methanol	0.0162	kg
Silicone product	0.0029	kg
Cardboard carbon storage	1.3700	kg
Tap water	27.0000	kg
Electricity/heat		
Electricity, medium voltage	8.3300	kWh
Final waste flows		
Photovoltaic cell waste	0.0150	kg
Waste to treatment		
Recycling glass	0.1100	kg
Ethylvinylacetate treatment	0.0100	kg
Recycling PET	0.0100	kg

Table 2-6 LCI of total flows for production of 1 piece of m-Si PV module

SoG-Si	Amount	Unit
Materials		
MG-silicon	131.05	kg
Chemicals inorganic	231.94	kg
Heat, natural gas	21,454.82	MJ
Electricity/heat		
Natural gas	5,218.74	kWh
Electricity, hydropower	7,538.18	kWh

Wafer	Amount	Unit
Materials		
Polycrystalline SoG-Si	115.97	kg
Sand	26.42	kg
Flat glass, uncoated	0.73	kg
Steel	109.37	kg
Silicon carbide	191.57	kg
Argon	455.08	kg
Dipropylene glycol	22.02	kg
Adhesive for metals	0.147	kg
Surfactant	17.62	kg
Sodium hydroxide, 50% in H_2O	1.10	kg
Hydrochloric acid, 30% in H_2O	0.20	kg
Acetic acid, 98% in H_2O	2.86	kg
Tap water	0.44	kg
Water, deionised	4,771.00	kg
Electricity/heat		
Electricity, medium voltage	10,643.00	kWh
Natural gas	5,651.80	kWh
Final waste flows		
Silicon waste	29.36	kg
Waste to treatment		
Waste, silicon wafer production	440.40	kg

Solar cell	Amount	Unit
Resource		
Water, cooling	1.150	m^3
Materials		
m-Si wafer	77.804	p
Phosphorus	0.002	kg
Metallization paste	0.086	kg
Polystyrene, expandable	0.0005	kg
Nitrogen	2.121	kg
Oxygen	0.117	kg
Argon	0.029	kg
Ammonia	0.008	kg
Silicon tetrahydride	0.001	kg
Sodium hydroxide, 50% in H2O	0.180	kg
Acetic acid, 98% in H2O	0.003	kg
Hydrochloric acid, 30% in H2O	0.052	kg
Hydrogen fluoride	0.043	kg
Nitric acid, 50% in H2O	0.031	kg
Phosphoryl chloride	0.0002	kg
Phosphoric acid, industrial grade, 85% in H2O	0.009	kg
Sodium sulphate	0.086	kg
Calcium chloride	0.025	kg
Isopropanol	0.090	kg
Ethanol	0.0007	kg
Solvents, organic	0.002	kg
Water, deionised	157.810	kg
Electricity/heat		
Electricity, medium voltage	43.306	kWh
Natural gas	5.446	MJ
Fuel oil	0.038	kg
Emissions to air		
Aluminium	0.0009	kg
Hydrogen chloride	0.0003	kg
Hydrogen fluoride	5.549×10^{-6}	kg
Lead	0.0009	kg
Particulates, unspecified	0.003	kg
Silicon	8.29×10^{-5}	kg
Silver	0.0009	kg
Sodium hydroxide	5.55×10^{-5}	kg
Tin	0.0009	kg
VOC, volatile organic compounds	0.223	kg
Final waste flows		
Photovoltaic cell waste	0.303	kg

m-Si PV module	Amount	Unit
Materials		
m-Si cell	73.4000	p
Aluminium	3.8000	kg
Solar glass	11.4000	kg
Ethylene vinyl acetate copolymer	1.3000	kg
Polyvinylfluoride	0.1600	kg
Polyethylene terephthalate (PET)	0.1600	kg
Copper	0.1400	kg
Tin	0.0070	kg
Lead	0.0040	kg
Nickel	0.0002	kg
Flux, wave soldering	0.0100	kg
Methanol	0.0162	kg
Silicone product	0.0029	kg
Cardboard carbon storage	1.3700	kg
Tap water	27.0000	kg
Electricity/heat		
Electricity, medium voltage	8.3300	kWh
Final waste flows		
Photovoltaic cell waste	0.0150	kg
Waste to treatment		
Recycling glass	0.1100	kg
Ethylvinylacetate treatment	0.0100	kg
Recycling PET	0.0100	kg

Table 2-7 LCI of total emission for manufacturing a m-Si based PV module (extracted from SimaPro)

Substance	Emission to	Amount	Unit
1-Butanol	Air	5.47×10^{-10}	kg
1-Butanol	Eau	2.57×10^{-06}	kg
1-Pentanol	Air	3.31×10^{-10}	kg
1-Pentanol	Eau	7.94×10^{-10}	kg
1-Pentene	Air	2.50×10^{-10}	kg
1-Pentene	Eau	6.00×10^{-10}	kg
1-Propanol	Air	4.54×10^{-08}	kg
1-Propanol	Eau	1.94×10^{-09}	kg
1,4-Butanediol	Air	1.14×10^{-08}	kg
1,4-Butanediol	Eau	4.56×10^{-09}	kg
2-Aminopropanol	Air	7.65×10^{-11}	kg
2-Aminopropanol	Eau	1.92×10^{-10}	kg
2-Butene, 2-methyl-	Air	5.55×10^{-14}	kg
2-Methyl-1-propanol	Air	1.01×10^{-09}	kg
2-Methyl-1-propanol	Eau	2.44×10^{-09}	kg
2-Methyl-2-butene	Eau	1.33×10^{-13}	kg
2-Nitrobenzoic acid	Air	1.36×10^{-10}	kg
2-Propanol	Air	1.52×10^{-4}	kg
2-Propanol	Eau	7.83×10^{-10}	kg
Carbon dioxide	Air	0.019	kg
Carbon dioxide, biogenic	Air	439.29	kg
Carbon dioxide, fossil	Air	8196.96	kg
Carbon dioxide, land transformation	Air	0.965	kg
Carbon disulphide	Air	0.009	kg
Carbon disulphide	Eau	3.35×10^{-08}	kg
Carbon monoxide	Air	3.25×10^{-05}	kg
Carbon	Sol	0.086	kg

Substance	Emission to	Amount	Unit
Heat, waste	Air	1.93×10^{5}	MJ
Heat, waste	Eau	3,426.05	MJ
Heat, waste	Sol	297.17	MJ
Helium	Air	0.001	kg
Heptane	Air	0.007	kg
Hexane	Air	0.062	kg
Hydrocarbons, aliphatic, alkanes, cyclic	Air	9.41×10^{-06}	kg
Hydrocarbons, alkanes, unspecified	Air	0.041	kg
Hydrocarbons, alkanes, unspecified	Eau	0.004	kg
Hydrocarbons, alkenes, unspecified	Air	4.38×10^{-09}	kg
Hydrocarbons, alkenes, unspecified	Eau	2.47×10^{-08}	kg
Hydrocarbons, aliphatic, unsaturated	Air	0.007	kg
Hydrocarbons, aliphatic, unsaturated	Eau	0.0004	kg
Hydrocarbons, aromatic	Air	0.014	kg
Hydrocarbons, aromatic	Eau	0.018	kg
Hydrocarbons, chlorinated	Air	3.27×10^{-05}	kg
Hydrocarbons, unspecified	Eau	0.015	kg
Methane, bromo-, Halon 1001	Air	5.42×10^{-14}	kg
Methane, bromochlorodifluoro-, Halon 1211	Air	0.0001	kg
Methane, bromotrifluoro-, Halon 1301	Air	1.76×10^{-05}	kg
Methane, chlorodifluoro-, HCFC-22	Air	0.0004	kg
Methane, chlorotrifluoro-, CFC-13	Air	5.20×10^{-10}	kg
Methane, dichloro-, HCC-30	Air	4.92×10^{-07}	kg
Methane, dichloro-, HCC-30	Eau	0.0007	kg
Methane, dichlorodifluoro-, CFC-12	Air	5.81×10^{-07}	kg
Methane, dichlorofluoro-, HCFC-21	Air	7.82×10^{-09}	kg
Methane, fossil	Air	17.66	kg

Table 2-8 Characterization of LCI emission into GW impact category

	Emission to	Amount	Unit	$FI_{s,i}$	Score kg CO_2 eq
TOTAL					15,789.18
Carbon dioxide	Air	1.89×10^{-2}	kg	1.00	1.89×10^{-2}
Carbon dioxide. fossil	Air	1.52×10^{4}	kg	1.00	1.52×10^{4}
Carbon dioxide. land transformation	Air	1.80	kg	1.00	1.80
Carbon monoxide	Air	3.25×10^{-5}	kg	1.57	5.11×10^{-5}
Carbon monoxide. fossil	Air	7.77	kg	1.57	1.22×10^{1}
Chloroform	Air	1.44×10^{-5}	kg	9.00	1.30×10^{-4}
Dinitrogen monoxide	Air	7.21×10^{1}	kg	156.00	1.13×10^{2}
Ethane. 1.1.1.2-tetrafluoro-. HFC-134a	Air	6.42×10^{-4}	kg	400.00	2.57×10^{-1}
Ethane. 1.1.1-trichloro-. HCFC-140	Air	4.55×10^{-8}	kg	42.00	1.91×10^{-6}
Ethane. 1.1.2-trichloro-1.2.2-trifluoro-. CFC-113	Air	1.00×10^{-5}	kg	2,700.00	2.71×10^{-2}
Ethane. 1.1-difluoro-. HFC-152a	Air	1.38×10^{-6}	kg	37.00	5.09×10^{-5}
Ethane. 1.2-dichloro-1.1.2.2-tetrafluoro-. CFC-114	Air	1.94×10^{-4}	kg	8,700.00	1.68
Ethane. hexafluoro-. HFC-116	Air	4.95×10^{-5}	kg	18,000.00	8.90×10^{-1}
Methane	Air	3.41×10^{-3}	kg	7.60	2.59×10^{-2}
Methane. biogenic	Air	1.86	kg	7.60	1.42×10^{1}
Methane. bromo-. Halon 1001	Air	5.61×10^{-14}	kg	1.00	5.61×10^{-14}
Methane. bromochlorodifluoro-. Halon 1211	Air	1.72×10^{-4}	kg	390.00	6.69×10^{-2}
Methane. bromotrifluoro-. Halon 1301	Air	1.92×10^{-5}	kg	2,700.00	5.18×10^{-2}
Methane. chlorodifluoro-. HCFC-22	Air	6.69×10^{-4}	kg	540.00	3.61×10^{-1}
Methane. chlorotrifluoro-. CFC-13	Air	5.20×10^{-10}	kg	16,300.00	8.48×10^{-6}
Methane. dichloro-. HCC-30	Air	1.10×10^{-6}	kg	3.00	3.30×10^{-6}
Methane. dichlorodifluoro-. CFC-12	Air	8.01×10^{-7}	kg	5,200.00	4.16×10^{-3}
Methane. dichlorofluoro-. HCFC-21	Air	8.07×10^{-9}	kg	65.00	5.24×10^{-7}
Methane. fossil	Air	3.43×10^{1}	kg	10.35	3.55×10^{2}
Methane. monochloro-. R-40	Air	1.29×10^{-6}	kg	5.00	6.44×10^{-6}
Methane. tetrachloro-. CFC-10	Air	1.10×10^{-4}	kg	580.00	6.38×10^{-2}
Methane. tetrafluoro-. CFC-14	Air	4.30×10^{-4}	kg	8,900.00	3.83
Methane. trichlorofluoro-. CFC-11	Air	4.46×10^{-9}	kg	1,600.00	7.14×10^{-6}
Methane. trifluoro-. HFC-23	Air	1.20×10^{-7}	kg	10,000.00	1.20×10^{-3}
Sulfur hexafluoride	Air	1.19×10^{-3}	kg	32,400.00	3.86×10^{1}

Table 2-9 Characterization of LCI emission into RI impact category

	Emission to	Amount	Unit	$FI_{s,i}$	Score kg PM2.5 eq
TOTAL					5.1569
Ammonia	Air	3.38×10^{-1}	kg	0.121	4.10×10^{-2}
Carbon monoxide	Air	3.25×10^{-5}	kg	0.001	3.40×10^{-8}
Nitrogen oxides	Air	1.70×10^{1}	kg	0.127	2.16
Particulates. < 10 um	Air	3.12×10^{-4}	kg	0.536	1.67×10^{-4}
Particulates. < 10 um (mobile)	Air	1.82×10^{-6}	kg	0.536	9.77×10^{-7}
Particulates. < 10 um (stationary)	Air	7.58×10^{-6}	kg	0.536	4.06×10^{-6}
Particulates. < 2.5 um	Air	1.40	kg	1	1.40
Sulfur dioxide	Air	1.99×10^{1}	kg	0.078	1.55
Sulfur oxides	Air	1.03×10^{-4}	kg	0.078	8.07×10^{-6}
Sulfur trioxide	Air	1.31×10^{-7}	kg	0.062	8.20×10^{-9}

Table 2-10 Characterization score of impact categories

Impact category	Amount	Unit
Carcinogens	77.43	kg C_2H_3Cl eq
Non-carcinogens	53.03	kg C_2H_3Cl eq
Respiratory inorganics	5.16	kg PM2.5 eq
Ionizing radiation	448,213.72	Bq C-14 eq
Ozone layer depletion	0.0016	kg CFC-11 eq
Respiratory organics	2.73	kg C_2H_4 eq
Aquatic ecotoxicity	499,953.26	kg TEG water
Terrestrial ecotoxicity	103,003.74	kg TEG soil
Terrestrial acid/nutri	118.31	kg SO_2 eq
Land occupation	50.49	m^2org.arable
Aquatic acidification	33.29	kg SO_2 eq
Aquatic eutrophication	4.16	kg PO_4 P-lim
Global warming	15,789.18	kg CO_2 eq
Non-renewable energy	289,745.99	MJ primary
Mineral extraction	60.24	MJ surplus

Table 2-11 Characterization score of damage categories

Damage category	Amount	Unit
Human health	0.004	DALY
Ecosystem quality	1,017.93	PDF*m2*yr
Climate change	15,789.18	kg CO2 eq
Resources	289,806.23	MJ primary

The characterization score of the emissions from the production of an m-Si PV module in all impact categories is shown in Table 2-10. Finally, the characterization scores obtained for the four damage categories are presented in Table 2-11.

Due to the complexity to understand the information provided in the tables above, the normalisation of results was performed. The reference values for both impact and damages categories are listed in Table 2-12. Table 2-13 shows the normalised values.

2.5.4 *Interpretation of results*

Figure 2-24 represents the normalised scores. Comparing among the impact categories, GW and NR are those with the highest values. This result indicates that on the one hand GW and NR have a major influence within the overall environmental assessment for a module of m-Si. On the other hand, half of the impact categories have a very small contribution.

GW and NR are mainly related to the energy requirements of the process. Looking at the process flow for manufacturing the m-Si PV module, a large amount of energy is consumed to achieve the temperatures required to get the degree of purity and uniformity needed by this type silicon module. Because of this, a question arises: what would happen if the module was manufactured in another country with a different energy mix?. The Ecoinvent database has different energy mix. Five scenarios will be tested. USA, China, Spain and France energy mix are chosen. The composition of the five

Table 2-12 IMPACT 2002+ reference values for normalisation (Margni et al., 2005)

Midpoint category	Reference value	Unit	Damage category	Reference value	Unit
Carcinogens	2,533.00	kg C_2H_3Cl eq/ pers/year[1]	Human health	0.0071	DALY/ pers/year
Non-carcinogens	2,533.00	kg C_2H_3Cl eq/ pers/year			
Respiratory inorganics	10.00	kg PM2.5 eq/ pers/year			
Ionizing radiation	33,772,000	Bq C-14 eq/ pers/year			
Ozone layer depletion	6.75	kg CFC-11 eq/ pers/year			
Respiratory organics	3,330.00	kg C_2H_4 eq/ pers/year			
Aquatic ecotoxicity	272,881,000	kg TEG water/ pers/year	Ecosystem quality	13,700	PDF * m^2 * yr/pers/year
Terrestrial ecotoxicity	1,732,000	kg TEG soil/ pers/year			
Terrestrial acid/nutri	13,100.00	kg SO_2 eq/ pers/year			
Land occupation	12,600.00	m^2org.arable/ pers/year			
Aquatic acidification	*Under development*				
Aquatic eutrophication	*Under development*				
Global warming	9,900.00	kg CO_2 eq/ pers/year	Climate change	9,900	Kg_{eq} CO_2/pers/yr
Non-renewable energy	151,975.00	MJ primary/ pers/year	Resources	152,000	MJ/ pers/yr
Mineral extraction	150,600.00	MJ surplus/ pers/year			

Table 2-13 Normalised scores for both impact and damage categories

Midpoint category	Reference value	Unit	Damage category	Reference value	Unit
Carcinogens	0.03057	pers/year	Human health	0.57482	pers/year
Non-carcinogens	0.02094	pers/year			
Respiratory inorganics	0.50899	pers/year			
Ionizing radiation	0.01327	pers/year			
Ozone layer depletion	0.00023	pers/year			
Respiratory organics	0.00082	pers/year			
Aquatic ecotoxicity	0.00183	pers/year	Ecosystem quality	0.07431	pers/year
Terrestrial ecotoxicity	0.05948	pers/year			
Terrestrial acid/nutri	0.00898	pers/year			
Land occupation	0.00402	pers/year			
Aquatic acidification	-----				
Aquatic eutrophication	-----				
Global warming	1.59471	pers/year	Climate change	1.59471	pers/yr
Non-renewable energy	1.90653	pers/year	Resources	1.90693	pers/yr
Mineral extraction	0.00040	pers/year			

[1] The reference value used by IMPACT 2002+ considered the European population in a year.

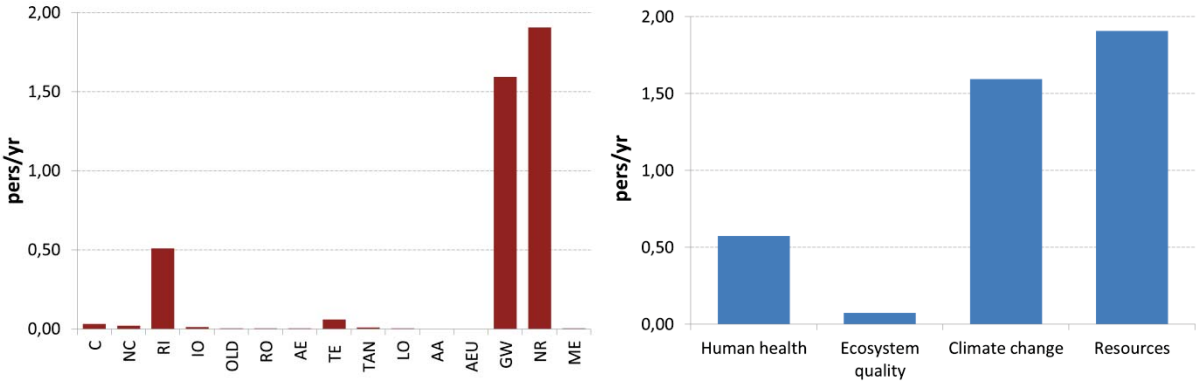

a) Midpoint categories b) Damage categories

Figure 2-24 Normalised scores for both midpoint and damages categories. IMPACT 2002+

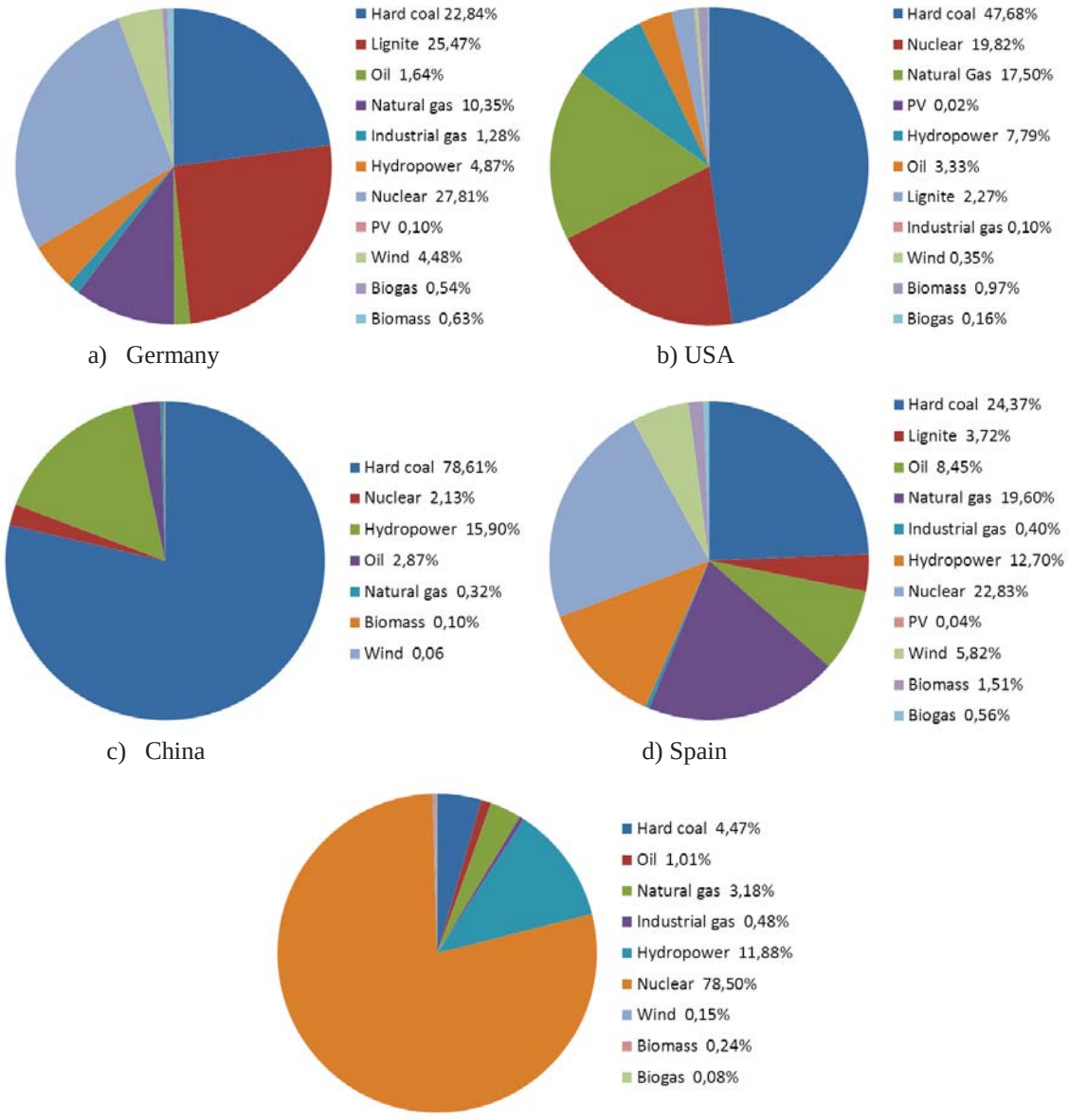

a) Germany b) USA

c) China d) Spain

f) France

Figure 2-25 Energy mix composition of Germany, USA, China, Spain and France

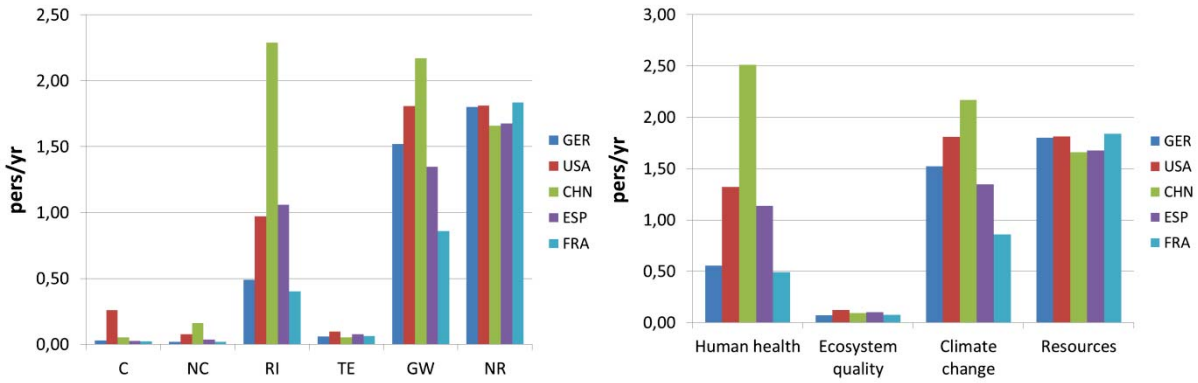

a) Main score at midpoint categories b) Damage categories

Figure 2-26 Normalized scores both midpoint and damages categories of five scenarios. IMPACT 2002+

energy mixes is displayed in Figure 2-25.

To make the comparison, it was necessary to change the energy source used for each of the unit process according to the energy mix scenario. Once again LCI was performed for each scenario as well as the classification and characterization of emissions. Normalisation of score was also performed to compare the results. In Figure 2-26, it can be seen that an m-Si PV module made in China generates the high environmental affectations among the five scenarios, especially into Human Health and Climate Change categories. The large dependence of hard coal, a fossil source, in Chinese mix causes these high values. The opposite case is found when the PV module is made entirely using the French mix. The low scores are due to the way that emissions from nuclear are classified and characterized.

2.6 LCA study for silicon-based PV modules

Another advantage of LCA technique is the possibility to carry out a comparative analysis between processes, products or services. In this second example, a comparison between three technologies of PV modules (m-Si, p-Si and ribbon-Si) is made. LCA is conducted following the data published by Alsema et al. (Alsema & Wild-scholten, 2006; de Wild-Scholten & Alsema, 2005) to manufacture PV modules based on silicon.

2.6.1 *Goal and scope definition*

More precisely, the aim of this study is to compare the environmental impact of some manufacturing processes of crystalline silicon-based PV module (m-Si. p-Si and ribbon-Si). The standard manufacturing processes for these PV modules were described Section 2.2.1. Figure 2-27 shows the system boundaries. Data on the assembly of all components were collected by choosing a functional unit 1 kW_p of installed power[2], which is more convenient as several technologies have to be compared. The manufacturing process for each of the three c-Si-based PV module technologies is divided into 4 main groups: SoG-Si, wafer, solar cell, and PV module (see Figure 2-27). In the case of m-Si and p-Si PV modules, the process of ingot growth and wafer sawing were grouped together.

[2] A kW_p specifies the output power achieved by a PV module under Standard Test Conditions (an incident sunlight of 1000 W/m², a cell temperature of 25°C and an Air Mass of 1.5)

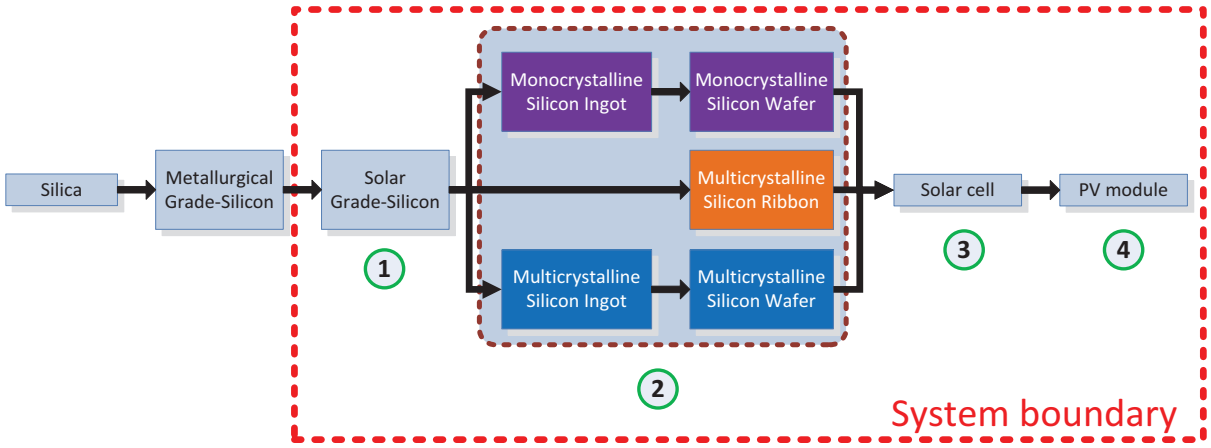

Figure 2-27 Scheme of system boundaries

2.6.2 *Technology assumptions, LCI and data collection*

The wafer dimensions that are considered are set at 125 x 125 mm as the standard size for all wafer technologies (including ribbon). Wafer thickness lies in the range of 270-300 µm for m-Si and p-Si wafers and 300-330 µm for ribbon wafers. Only one standard module type with 72 cells (1.25 m^2 module area) and with glass/EVA/Tedlar lamination is considered. Glass thickness is set at 3.6 mm.

LCI for the three technologies is established from data published by de Wild-Scholten and Alsema (de Wild-Scholten & Alsema, 2005). Complementary data were acquired from Ecoinvent database implemented in SimaPro LCA software tool for all manufacturing processes. As previously mentioned, a German electricity mix is chosen.

2.6.3 *LCIA results and interpretation*

IMPACT 2002+ (Jolliet et al., 2003) method is selected for LCIA. The same procedure used in Section 2.5.3 was followed to classify and characterize the emissions. As in the previous case, the score of both impact and damage categories are normalized using the same factors contained in Table 2-12. Figure 2-28 shows the normalised results of main midpoint categories and damages categories for the three types of PV modules in order to analyze the importance of the respective contribution of each category in the overall environmental impact. Not surprisingly, it is observed that m-Si technology has the highest score for all impact categories while the silicon ribbon modules have the lowest impact. When comparing the categories of damage (see Figure 2-28b), it can be seen that Resource depletion and Climate Change have the largest contributions in terms of global environmental impacts. Figure 2-28a indicates that the categories relating to Non-renewable energy and Global Warming lead to higher scores among the midpoint categories.

A more realistic comparison to evaluate different technologies for PV is to consider the number of panels required to meet a given amount of energy. Using the same considerations as above, the minimum number of panels required to meet a demand of 1 kWh (see Table 2-14) with an average daily irradiance of 1 kWh / m² is computed. The new FU is the demand of 1kWh. This functional unit corresponds now to the service t hat is produced corresponding to energy production which is more

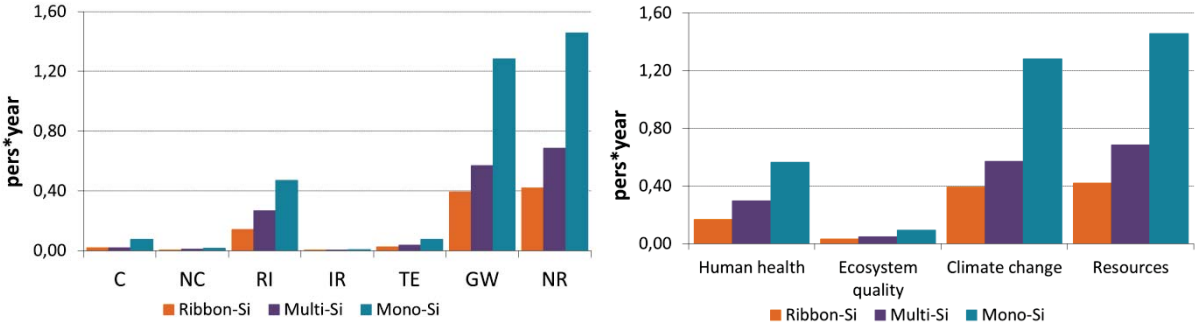

(a) Midpoint categories (b) Damage categories

Figure 2-28 Normalised results for the three PV module technologies. IMPACT 2002+

realistic. The conversion efficiency of the modules is based on the average efficiency of each technology proposed by de Wild-Scholten and Alsema (Alsema & Wild-scholten, 2006) (see Table 2-14). LCI was created from Ecoinvent database. IMPACT 2002+ was kept as the LCIA method. Figure 2-29 shows the results of the LCA. A similar trend relative to the impact of each technology assessed is observed.

A closer look can be made to identify the steps of the manufacturing process that generate the highest impact. Global warming midpoint category is selected for the analysis.

Figure 2-30 demonstrates that the largest contribution comes from the first two stages of module manufacturing (i.e. silicon wafer and solar cell) for the three technologies. It can be clearly pointed out that for the m-Si module, the wafer manufacturing process generates more than half of the total impact of the category, because of the high energy consumption involved during CZ crystal growth. The main causes are related to the emissions corresponding to the energy needs of the process as it can be highlighted through the analysis of the resources involved in the manufacturing process of m-Si wafers (see Figure 2-31).

Table 2-14 Efficiencies and number of PV modules required

	Ribbon-Si	**p-Si**	**m-Si**
Efficiency	11.5%	13.2%	14.0%
No. PV module	7	7	6

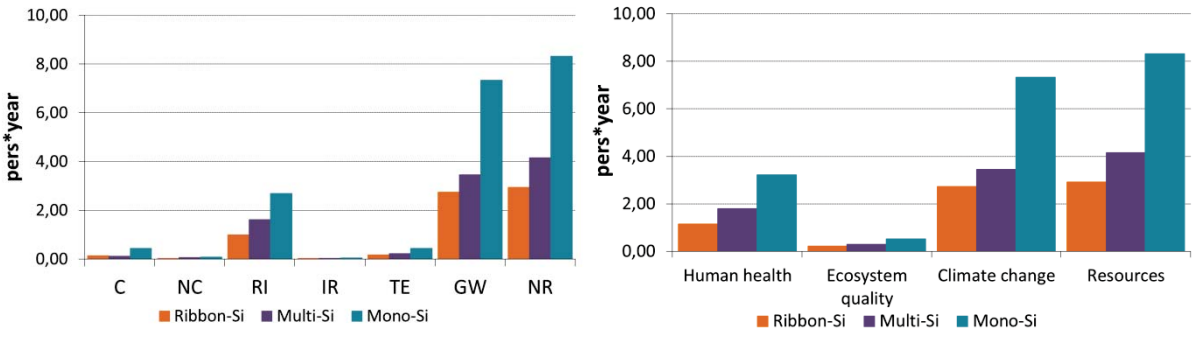

(a) Midpoint categories (b) Damage categories

Figure 2-29 Normalised results for the three PV module technologies. FU: 1 kWh demanded. IMPACT 2002+

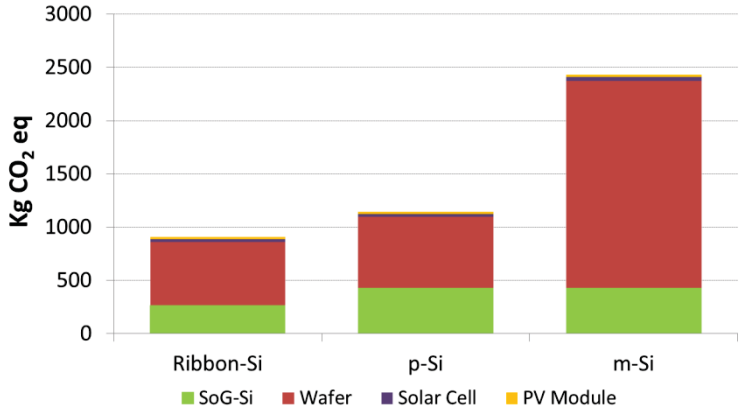

Figure 2-30 Result of main processes in Global Warming category for 3 PV module technologies

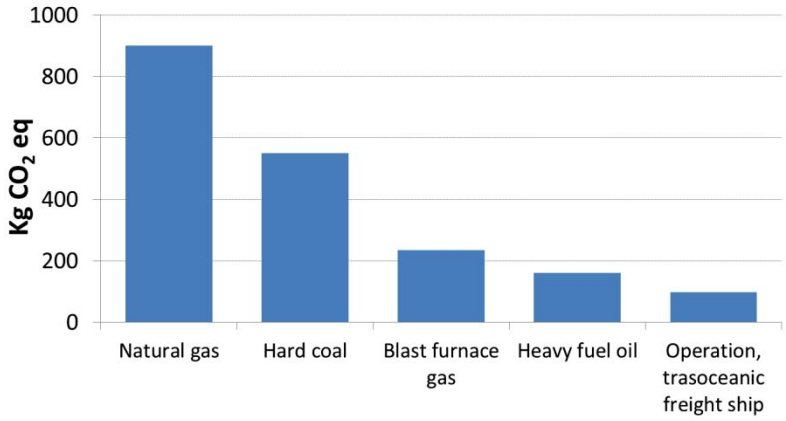

Figure 2-31 Score of the five main resources that contribute to GW characterization for m-Si PV module at wafer elaboration process.

2.7 LCA study for PVGCS

Another LCA is implemented to compare 5 different PV modules technologies in a large-scale PVGCS. The five PV module technologies are the most commercialized ones: m-Si, p-Si, a-Si, CdTe and CIS. In this example all the components of a PV system (PV modules, BOS components and the mounting system) are analysed. The procedure followed in this example as well as the resulting flow inventory will provide the basis for the integration and evaluation of the environmental aspect into the main model for the dimensioning of a large-scale PV system.

A guide published by International Energy Agency (V. Fthenakis et al., 2011) for LCA of PV system determines four main aspects that must be taken into consideration:

- **Technical characteristics related to PV systems.** The life expectancy of PV components and systems is not the same. e.g. 20-30 years for PV modules or 10 year for AC/DC inverter. Depending on the goal of the study, the irradiation collected by modules or their degradation can be important.
- **LCI/LCA modelling aspects.** The appropriate system model depends on the goal of the LCA. It can have a short-term prospective as for the choice of a PV electricity-supplier or comparisons between PV systems or electricity-generating technologies; or long-term

prospective as for comparison of future PV systems or of future electricity-generating technologies. The electricity mix must be considered carefully as well as the reference flow to enable comparisons. The reference flow can be expressed in *kWh electricity produced* (used for comparing PV technologies and modules), m² of module or *kWp rated power*.

- **Discuss and interpretation of results.** Beside the impact indicators used in LCIA it may be helpful use another indicator as energy payback time (EPBT)
- **Reporting and communication.** Some key parameters must be kept in mind : irradiance level and location; PV module efficiency; type of mounting system; components expected lifetime; system boundaries; technical and modelling assumptions; LCA tool and database used.

2.7.1 *Goal and scope definition*

This LCA study aims at comparing the environmental impact associated with electricity production with different PVGCS configurations using the 5 most commercial PV module technologies. As in previous LCA study, the functional unit is fixed as energy demand. It concerns here the demand of 5 MWh that must be supplied by the PV power plant each year during 20 years. System boundaries are represented in Figure 2-32. They include the manufacturing of core infrastructures (modules, mounting system, cabling, and AC/DC inverter), the plant installation (excavation and mounting system) and the energy generation for a 20 year period (including component replacement).

Recycling processes of the different components of PVGCS are not included in this study due to lack of reliable information for all PV modules technologies evaluated. The different recycling processes currently implemented for PV modules and their implementation in LCA will be discussed in Chapter 6.

2.7.2 *Technology assumptions, LCI and data collection*

A yearly irradiation 1200 kWh/m^2 on an inclined plane (30°) is considered. A fixed-mounting system with aluminium supports is used. A 10-years lifetime is considered for AC/DC inverter and 20-year life time is considered for the other components. The conversion efficiency of PV modules is constant over time and is based on the characteristic given by PV modules contained at Ecoinvet database.

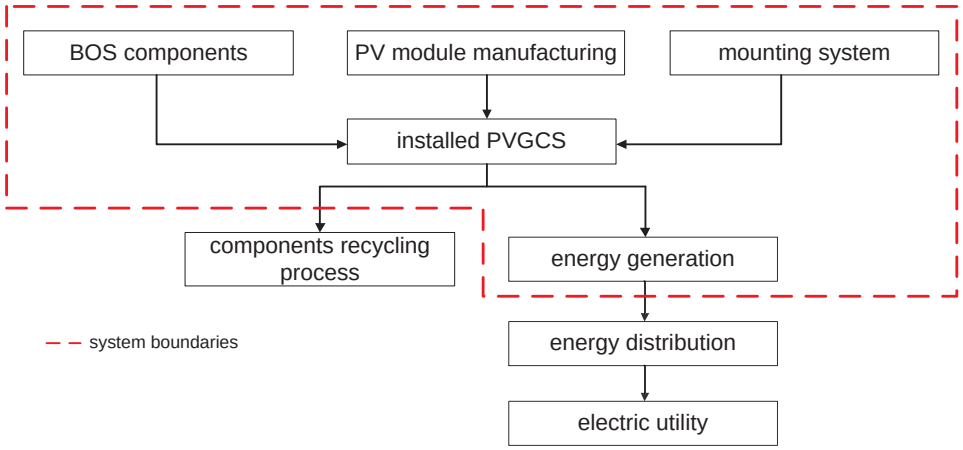

Figure 2-32 Boundaries of the system examined to compare different PV technologies

The five PV modules are found in Ecoinvent database. The datasheets contain the input and output flows in order to calculate the total emission flows. The reason why these PV modules were used was the lack of data for material and energy flow found in the literature for manufacturing process of thin-film modules. Ecoinvent database is constantly under improvement to become a more accurate tool for create the LCI of total emission for a given process or product.

The 2.5kW inverter is selected from Ecoinvent database for the five PV installations. The number of PV modules and DC / AC inverters needed to supply the energy demanded during the evaluation period as well as the main features are summarized in Table 2-15. The calculation was made taking into account the amount of irradiation received, the PV module efficiency as well as the electrical characteristics of the DC / AC inverter.

From the values shown in the Table 2-15 is noticed that the PV modules based on thin film technologies require a greater number of panels due to the low efficiency they have.

LCI of each technology under evaluation was performed from data displayed at the Table 2-15. The procedure followed was similar to the two last examples.

2.7.3 *LCIA results and interpretation*

IMPACT 2002+ method was applied for evaluating the environmental impacts. The characterization scores were obtained as in previous examples. The environmental assessment was carried out both in the main midpoint impact categories as in the four damage categories. The total score for each category was separate in order to compare the different elements that compose a PVGCS. Figure 2-33 shows the normalized results.

Looking at the total score for each of the five configurations in all categories shows that the highest environmental impacts in almost every category midpoint are obtained when a-Si PV modules are used. Only into the categories related with climate change and resources m-Si PV module configuration has the highest impacts.

A more detailed analysis, focusing into the components of a PVGCS, shows that the most influential process is PV module manufacturing for the total impact scores in all the categories. Among the five PV technologies under analysis, m-Si PV module leads in almost all the categories. CdTe PV modules had interesting results: it has the lowest total scores.

Table 2-15 Key features for LCA study

Module technology	**m-Si**	**p-Si**	**a-Si**	**CdTe**	**CIS**
Module efficiency η (%)	14.00	13.2	6.45	9.00	10.00
Module surface (m²)	1.46	1.46	1.10	0.72	0.72
Module life expectancy (years)	20	20	20	20	20
No. PV modules	22	24	58	62	69
No. AC/DC inverters	4	6	6	4	6

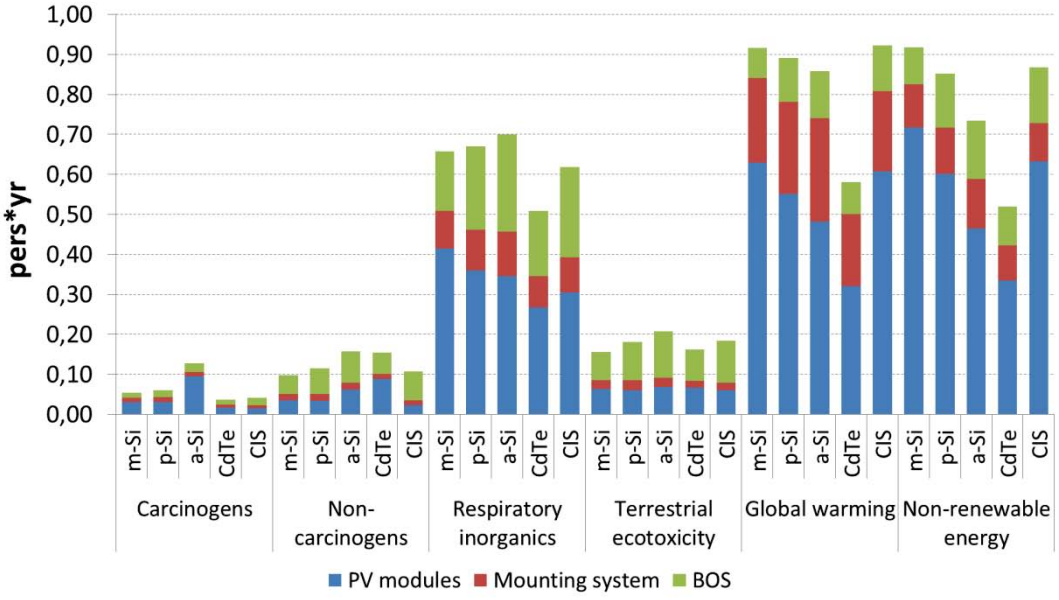

(a) Midpoint categories

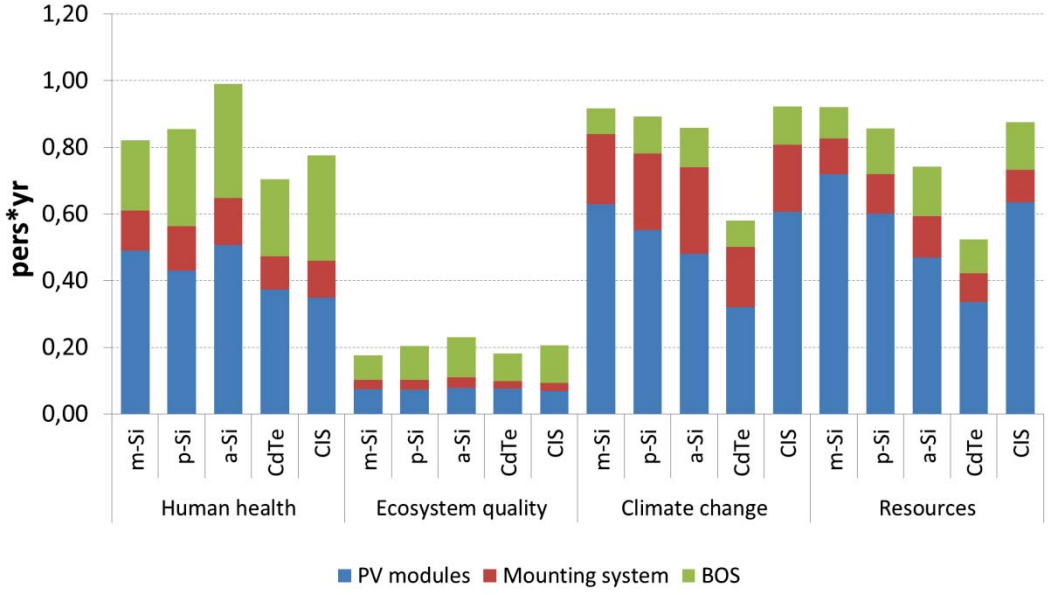

(b) Damage categories

Figure 2-33 Normalized results for the five PV installation considering 1200 kWh/m^2 yr of irradiation on an inclined plane (30°). IMPACT 2002+

The LCI as well as the procedure followed in this example will be used in the latter chapter when the evaluation of environmental impacts will be included and taken into consideration as criteria for the design of large-scale PV power plants.

2.8 Conclusion

The analysis of the manufacturing processes of the five main modules PV technology highlights that it is necessary to quantify the embodied primary energy required for their manufacture, especially with c-Si based technologies to guarantee the sustainable nature of a technology. An environmental assessment is required to confirm that, indeed, PV systems really help to reduce and / or prevent pollution. There are many techniques developed for environmental assessment and among them Life

Cycle Assessment (LCA) which is particularly interesting for energy production. Three cases have been tackled with LCA. The results show that the PV modules are the elements of a PVGCS that contribute most to the overall environmental impacts. Another aspect to mention is the influence of the composition of the electricity mix in the assessment of environmental impacts generated by a PV module.

This discussion reinforces the need for a multi-criteria study that allows establishing a methodology that conciliates both the technical-economic and environmental criteria. The procedure of LCA applied in a PVGCS will serve to integrate the environment criterion into the proposed study. To our knowledge, this kind of approach has not yet been implemented. The classical LCA tools (SimaPro and other LCA software) are generally not flexible and do not exchange with other programs. From a practical viewpoint, a specific environmental module was designed from extraction of the dedicated EcoInvent database that is used for PV systems.

It must be highlighted that this kind of study has been extended to other kinds of solar systems to compare two heliostat configurations (autonomous and classical heliostats) for heliothermodynamic power plants for concentrated solar power. This research was conducted within the OSSOLEMIO project in collaboration with the *Laboratoire Plasma et Conversion d'Energie* (LAPLACE) in the framework of Alaric Maintenon's PhD thesis (Montenon, 2013), under the supervision of Prof. Pascal Maussion.

The results indicate that even if variation between the two configurations is not so high at design stage, the electrical grid heliostat generates the most important impacts to the environment after 20 years of operation. The energy supplied for operating the grid-connected heliostat is the main element that affects the different categories analyzed in LCA. It also depends on the energy mix of the country in which the power station will be built. This work was presented at First International Conference on Renewable Energies and Vehicular Technology (REVET) (see Appendix A).

Chapter 3

A MODELLING AND SIMULATION FRAMEWORK FOR SIZING LARGE-SCALE PHOTOVOLTAIC POWER PLANTS

L'objectif de ce chapitre est de présenter l'approche de modélisation qui sera utilisée dans ce travail pour représenter les performances d'une installation photovoltaïque. Une analyse des logiciels disponibles qui peuvent être utilisés pour concevoir et évaluer la performance de PVGCS à grande échelle est tout d'abord présentée dans un but d'intégration dans une démarche d'écoconception. Les manques ou limitations des approches recensées ont conduit à développer un cadre spécifique pour la modélisation et la simulation du système PV système, basé par une méthodologie en trois étapes. La première étape consiste en l'estimation d'un rayonnement solaire reçu par le système en fonction de la localisation géographique. Un modèle mathématique pour le dimensionnement du PVGCS qui fournit l'énergie annuelle produite par les caractéristiques des composants et les limites de la conception des installation constitue la deuxième étape. La dernière étape correspond à l'évaluation des critères technico-économiques (retour économique et retour énergétique) et environnementaux (catégories intermédiaires de la méthode Impact 2002+). L'approche est ensuite validée par un exemple extrait de la littérature. Une comparaison de cinq technologies de modules photovoltaïques sert également d'illustration de la démarche. Les résultats obtenus confirment l'intérêt d'utiliser une approche d'optimisation pour rechercher la solution la plus intéressante en tenant compte simultanément des aspects technico-économiques et environnementaux.

Nomenclature

Acronyms

ADEME	Agence de l'Environnement et de la Maîtrise de l'Energie
AI	Artificial Intelligence
CdTe	Cadmium telluride
CIS	Copper indium diselenide
EPBT	Energy PayBack Time
LCA	Life Cycle Assessment
MBE	Mean Squared Error
NREL	National Renewable Energy Laboratory
PBT	PayBack Time
PV	Photovoltaic
PVGCS	Photovoltaic Grid-Connected System
RMSE	Root Mean Square Error
a-Si	Amorphous silicon
m-Si	Monocrystalline silicon
p-Si	Polycrystalline silicon
VBA	Visual Basic for Applications
WAP	Weinstock and Appelbaum approach

Symbols

α	Sun elevation angle, degree
β	PV collector inclination angle, degree
η	PV module efficiency, %
θ	Angle of incidence
θ_z	Zenith angle
ρ	Reflectivity ground index
D	Distance between PV sheds, m
D_{min}	Minimum distance between PV sheds, m
E_{max}	Maximum PV collector height above ground, m
G	Global irradiance, W/m²
G_b	Beam irradiance, W/m²
G_d	Diffuse irradiance, W/m²
G	Extraterrestrial irradiance, W/m^2
G_{sc}	Solar constant, 1367 W/m2
G_β	Global irradiance onto PV module tilted, W/m²
$G_{\beta,b}$	Beam irradiance onto PV module tilted, W/m²
$G_{\beta,d}$	Diffuse irradiance onto PV module tilted, W/m²
$G_{\beta,r}$	Reflected irradiance onto PV module tilted, W/m²
H	PV collector height, m
H_m	PV module height, m
H_{max}	Maximum PV collector height, m
K	Number of PV sheds
Kt	Clearness index
L	Solar field length, m

Symbols

L_C	PV collector length, m
L_m	PV module length, m
n	Day number; 1 to 365
N_c	Number of PV modules columns in the collector
N_r	Number of PV modules rows in the collector
Q_m	PV module's output energy, kWh
Q_{out}	Yearly output energy of the field, kWh
r_b	Beam ratio factor
t	Hour number, 1 to 24
T_m	PV module temperature, °C
W	Solar field width, m
Z^+	Positive natural number set

3.1 Introduction

System modelling forms a key part of the PV system design. It can provide answers to a number of important issues such as the overall array size, orientation and tilt, and the electrical configuration. The design criteria depend generally on the nature of the application. The applications of PVGCS vary from small building integrated systems to PV power plants. The performance of PVGCS depends upon solar resource at site, system configuration and load parameters. Modelling tools are available to provide solar radiation data, assess possible shading effects and produce the resulting electrical layout of the array.

The objective of this chapter is to present the modelling approach that will be used in this work to represent the performance of a PV power plant, taking into account its mains features.

This chapter is dived into seven sections. Section 2 first presents an overview of the available software tools that can be used to design and evaluate the performance of large-scale PVGCS. The list of software tools is not exhaustive but includes the most reported ones in the dedicated literature. The analysis of the reported contributions led to the development of a specific framework for PV modelling and simulation purpose that is proposed in section 3. The objective is then to couple it with an outer optimization module for generating optimal configuration alternatives. The system implies a three-step methodology:

(1). The estimated solar radiation received by the system according to the geographic location is the core of section 4.

(2). A mathematical model for PVGCS sizing is presented in section 5: it provides the annual energy generated from the characteristics of the system components and limitations on the design of the installation.

(3). The evaluation of techno-economic (PayBack Time and Energy PayBack) and environmental (IMPACT 2002+ midpoint categories) criteria is then presented in section 6.

The approach is then validated with a reference example from the literature (Weinstock and Appelbaum (Weinstock & Appelbaum, 2009)).

Finally, the integration of the proposed model in order to compute evaluation functions, based on techno-economic and environmental aspects, in an optimization loop is a natural extension of this work.

3.2 Literature review on PV System design tools and work objective

Following the guidelines presented in Chapter 1 (Figure 1-12) for PVGCS design, the first step is the estimation of the radiation received at the site as well as the amount of energy supplied to the utility grid.

Power generation through photovoltaic conversion is very difficult to make an accurate assessment when designing a PVGCS because it depends upon incident solar radiation and PV module performance which are affected by uncertain parameters such as daily weather conditions or ambient air temperature. These parameters change all the time and they are not the same every year. The hourly, daily, monthly or yearly mean value is considered for PVGCS design.

Numerous commercial and academic computer models using different algorithms for modeling, analyzing, simulating PV systems are available. These tools present different degrees of complexity and accuracy depending on the specific tasks that each tool has been developed for. It is usual to distinguish between sizing tools (which determine the component size and the corresponding configuration) and simulation/modelling tools, which analyse the system output and performance once its specifications are known. Examples of these sizing and simulation tools are given in Table 3-1. They involve generally the estimation of solar radiation (using meteorological databases or mathematical models) and/or the estimation of the energy generated by the system taking into account the characteristics and location on the field of PV components (e.g. modules, the balance of system), weather consideration and solar radiation.

The main problem that can be encountered when using one of the available tools as those presented in Table 3-1 is the lack of an approach that allows the optimization of the sizing of a PVGCS considering economic and environmental criteria. Sizing is made taking into account technical objectives. In addition, the coupling of all the components via an external program to optimize the PV plant taking into consideration the three main criteria is difficult due to the closed structure used in each tool.

To overcome the problem of interoperability, the design of a simulator for received solar radiation coupled with a sizing module constitutes the most suitable option. The simulator must be designed in an open manner so that it can be interfaced easily with an outer optimization loop. The estimation of solar radiation and the output energy of the system are the two most critical aspects of any PV System design and sizing tools.

Table 3-1 System sizing and simulation programs

Program	Source	Objective	Type of system	Main characteristics	Resultants	Advantages	Inconvenient
CalSol	Institut National de l'Energie Solaire (INES), France	Simulation and data analysis of PV system	Grid-connected, stand-alone and DC-grid system	- Economic analysis tool.	- CO_2 balance. - Report of yield production and monthly irradiation. - Economic report.	- Easy to handle. - Pre-sizing. - Available online.	- Only French meteorological database - No PV components database. - Insufficient energy loss calculation and economic analysis. -No interconnection with another program is allowed.
NSol	Orion Energy Corporation, USA	PV system sizing	Grid-connected and PV-generator hybrid power	- Insolation and PV components databases.	- Quick screening analyses. - System performance.	- Easy to handle. - Optimize the array size to the inverter capacity.	-No interconnection with another program is allowed. - No shading loss calculation.
PVGIS	Institute for Energy and Transport – European Commission	Estimation of solar radiation and simulation of a PV system	Grid-connected	- Meteorological database. - Interactive maps.	- Report of yield production. - Monthly or daily radiation.	- Easy to handle. - Import meteorological data. - Available online.	- Exclusive to Europe and Africa. - No PV components database. - No energy loss calculation and economic analysis. -No interconnection with another program is allowed.
PVSOL	Solar Design Company, UK	Design, simulation and data analysis of PV system	Grid-connected and stand-alone	- Extensive meteorological and PV components database. - Calculate shading losses. - 3D design tool. - Economic analysis tool.	- Report of yield production, efficiency of system and losses. - Economic report.	- Easy to handle. - 3D animation. - Import meteorological data. - Possibility of parameter settings. - Good quality results.	- No interconnection with another program is allowed.

Table 3-1 (*continued*)

Program	Source	Objective	Type of system	Main characteristics	Resultants	Advantages	Inconvenient
PVsyst	University of Geneva, Switzerland	Size, design, simulate and data analysis of PV system	Grid-connected, stand-alone and DC-grid system	- Extensive meteorological and PV components database. - Calculation of shading losses. - 3D design tool. - Economic analysis tool.	- Report of yield production, irradiation, efficiency of system and losses. - Economic report.	- Import meteorological data. - 3D animation. - Possibility of parameter settings. - Good quality results.	- Unfriendly use. - Sizing restricted to collector configuration. - No interconnection with another program is allowed.
SolarPro	Laplace System Co., Japan	Design and simulate PV system	Grid-connected	- Meteorological and PV components database. - 3D design tool. - Calculation of shading losses.	- Report of yield production.	- Easy to handle.	- No energy loss, calculation and economic analysis. - No interconnection with another program is allowed.
System Applications and Design Consideration	Sandia National Laboratories, USA	Simulate PV system	Grid-connected	- Creation of a specific PV module and inverter. - Five models for diffuse irradiance calculation	- Report of yield production and losses. - Economic report.	- Import meteorological data. - Collaborative work. - Web site with documents and general instruction.	- No meteorological and PV components database. Programming background needed. - Restrictive interconnection with another program.

3.3 Development of the simulation tool

Most of the reported studied (Gong & Kulkarni, 2005; Aris Kornelakis & Marinakis, 2010; Mondol, Yohanis, & Norton, 2006; Notton, Lazarov, & Stoyanov, 2010; Weinstock & Appelbaum, 2007, 2009) involve PVGCS optimization considering only one criterion. Other investigations (Dones & Frischknecht, 1998; Ito, Kato, Komoto, Kichimi, & Kurokawa, 2008; Kannan, Leong, Osman, Ho, & Tso, 2006; Pacca, Sivaraman, & Keoleian, 2006) address only the issue of the environmental impact assessment of the components of a PV system with emphasis on PV module technology. The main purpose consists in generating alternatives of optimal PVGCS configurations taking into account technical and economic aspects as well as their environmental impact.

The closed structure of the tools listed in Table 3-1 makes complicated to couple them with an environmental module and with an outer optimization loop to solve the resulting optimization problem. This explains why a dedicated simulation tool was developed in order to develop the proposed methodology.

Figure 3-1 illustrates the system flow diagram for modeling solar radiation and estimating the output energy of a PVGCS. The proposed modeling framework will then coupled with an optimization module for generating optimal configuration alternatives. The system is based on the following models:

(a). The estimated solar radiation received by the system according to the geographic location.

(b). The PVGCS sizing based on a mathematical model that provides the annual energy generated from the characteristics of the system components and limitations on the design of the installation.

(c). The evaluation of economic, technical and environmental criteria.

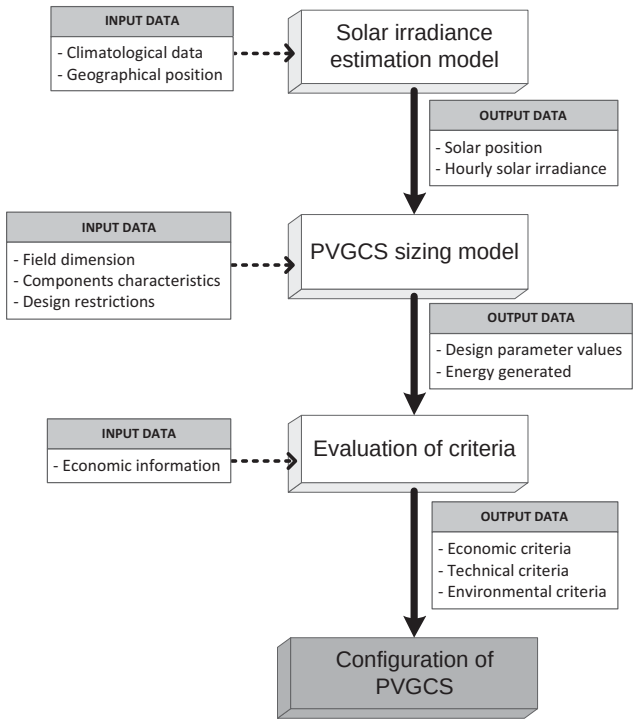

Figure 3-1 Functional flow diagram of the proposed methodology

3.4 Solar radiation model

3.4.1 *Solar radiation*

Solar radiation on tilted planes is very important to design flat plate PV collectors for power plants. When radiation passes through Earth's atmosphere, it suffers changes in its trajectory by the elements present in the atmosphere. Elements such as ozone, oxygen, carbon dioxide and water vapor absorb the radiation; some are reflected by the clouds. The dust and water droplets also cause disturbances. To eliminate the effects of local features, solar radiation is measured on horizontal surfaces free of obstacles. The result is the decomposition of the incident solar radiation into a receiver placed on the surface in different components (Lorenzo, 2003). Consequently, solar radiation data are most often given in the form of global radiation on a horizontal surface. Since PV modules are usually positioned at an angle to the horizontal plane, the radiation input to the system must be calculated from this data.

Global radiation on a tilted plane consists of three components (Figure 3-2):

- *Beam radiation.* The radiation received from the sun without having been scattered or reflected that reaches the surface. It is also known as direct radiation.
- *Diffuse radiation*. The radiation received from the sun after its direction has been changed by scattering by the atmosphere.
- *Reflected radiation*. The radiation received from the sun that is reflected by the ground. Albedo radiation is another name.

Global radiation. The total radiation falling on a surface is the sum of beam, diffuse and reflected radiation.

The calculation of irradiance arriving on a tilted surface, using as input global horizontal data, raises two main problems related on the one hand to the separation of the global horizontal radiation into its direct and diffuse components and, from them, on the other hand to the estimation of the irradiance components falling on an inclined surface.

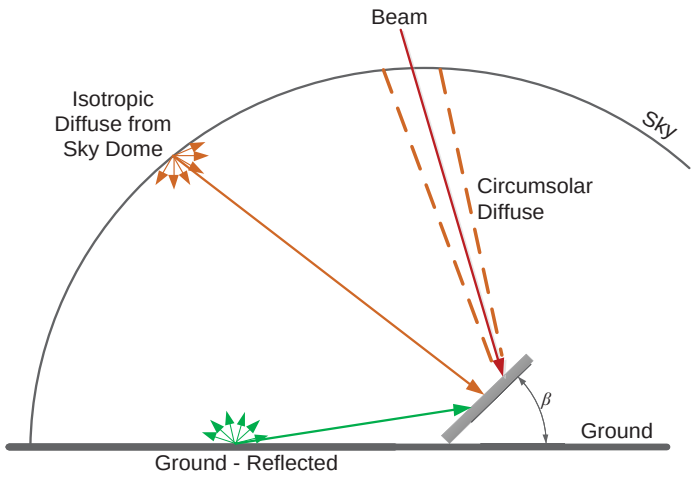

Figure 3-2 Different components of solar radiation in a tilted surface

Over the years, different models have been developed to estimate solar radiation over tilted planes (Demain, Journée, & Bertrand, 2013; Duffie & Beckman, 2006; Noorian, Moradi, & Kamali, 2008). The models can be classified as isotropic or anisotropic models. Yet, almost all models use the same method of calculating beam and ground-reflected radiation, the main difference is the treatment of diffuse radiation.

Isotropic models assume that the intensity of sky diffuse radiation is uniform over the sky dome. Hence, the diffuse radiation incident on a tilted surface depends on the fraction of the sky dome seen by it. The most widely used model belonging to this category is the one developed by Liu and Jordan (Noorian et al., 2008). Because of its simplicity, this model has achieved great popularity, despite the fact that it underestimates diffuse irradiance on surfaces tilted to the equator.

The second group of models assumes both the anisotropy of the sky diffuse radiation in the circumsolar region (sky near the solar disc) and an isotropically distributed diffuse component from the rest of the sky dome. Better results are obtained with this type of model.

3.4.2 *Model Description*

The solar radiation model computes the radiation received in the site where the future plant will be built. Figure 3-3 shows the input data necessary for the operation of the model, sub-models and the outputs.

Visual Basic for Applications (VBA) in Excel was used for simulation purpose. The main advantages include the automation of repetitive tasks and calculations, the easy creation of macros in a friendly programming language, the possibility to use existing Excel functions and formulas, ability to import and export data and the classification and management of results.

It is relevant to make a difference between power and energy when considering PV systems. The radiation term is used as a general one for referring both aspects. The following concepts are used to distinguish between:

- *Irradiance.* The density of power falling on a surface per unit area of surface at a specific time. The SI units is watt per square meter (W/m^2); others units are $MJ/m^2/day$ or $kWh/m^2/day$.

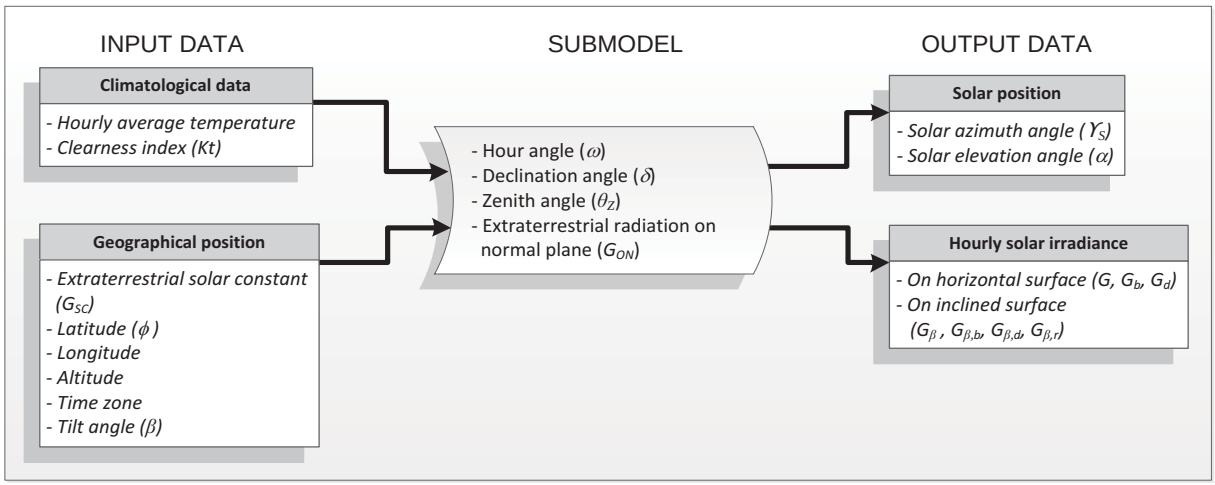

Figure 3-3 Data flow diagram of solar irradiance estimation model

- *Irradiation.* The density of energy that falls on the surface over a period of time. It is measured in Wh/m^2 or J/m^2. It is the result of the integration of the irradiance over a specific time, usually an hour or a day.

Irradiation over an hour (in Wh/m^2) is numerically equal to the mean irradiance during this hour (in W/m^2); irradiance values can be assimilated to hourly irradiation values (Duffie & Beckman, 2006). The developed model calculates the irradiance received by the PV collector surface every hour for a standard calendar year.

The inputs for this module are classified into two groups. The former group is composed of climatological data of the studied site. The average hourly temperature is obtained from collected information that is available in various databases. Another important element to establish the relationship between solar radiation on the surface of the Earth and the extraterrestrial radiation is the index of transparency of the atmosphere or clearness index (*Kt*). This index is the radio between the horizontal radiation of a particular hour and the extraterrestrial radiation for that hour, as expressed by:

$$K_t = \frac{G}{G_o} \tag{3.1}$$

Kt is imported from climatological databases.

The latter group is composed of all the data inherent to the geographic location of the site where the facility will be placed. This information allows us to estimate the position of the sun and the solar radiation that the facility will handle every hour.

Before making any estimation of the amount of energy generated by a PV system, it is necessary to understand how the energy radiated by the sun reaches the earth and the effect of the atmosphere in its way to impact the surface of the panel solar.

The Sun is a sphere composed of extremely hot gas with a diameter of 1.39×10^9 m. It acts as a perfect emitter of radiation (black body) at a temperature close to 5800° K. The sun is indeed a continuous fusion reactor, and these reactions are the cause of the energy radiated by this celestial body.

Figure 3-4 shows the relationship between the Sun and Earth. Radiation emitted by the sun and its relation to the Earth gives an almost constant solar radiation outside the Earth's atmosphere.

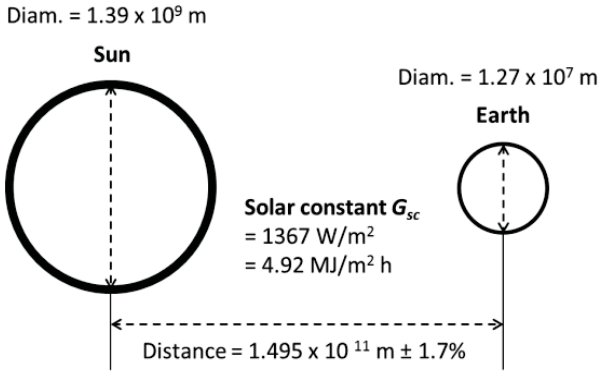

Figure 3-4 Sun-Earth relationship

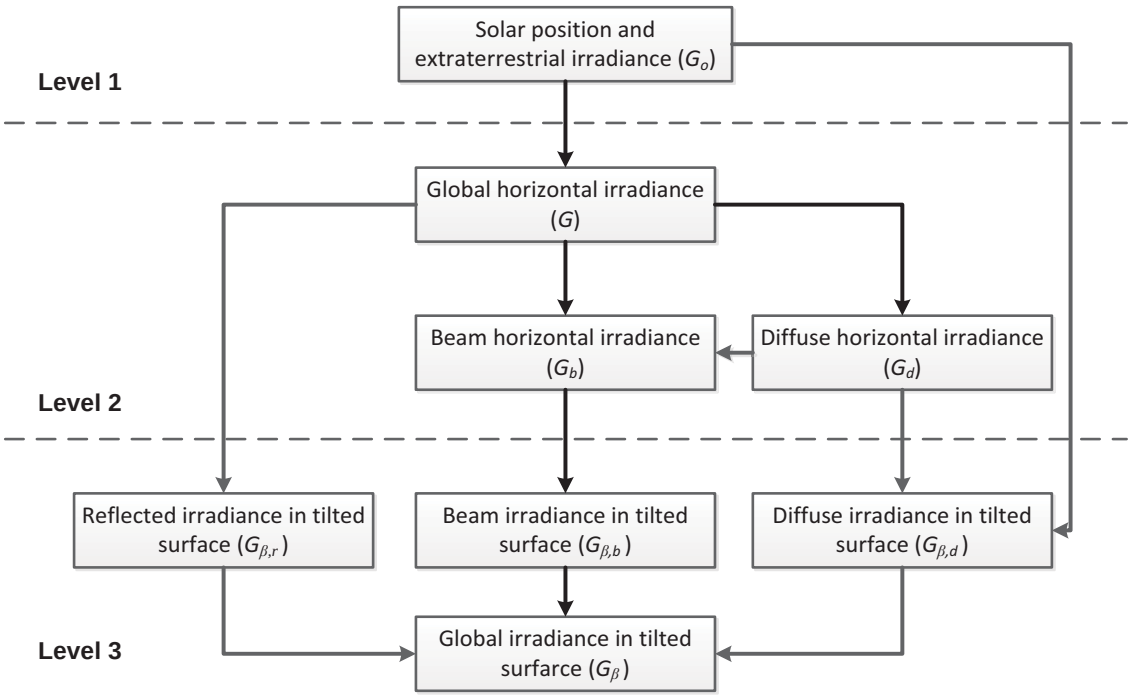

Figure 3-5 Sequence for determination of hourly global tilted irradiance

The solar constant (G_{sc}) is defined as the amount of incoming solar energy per unit area incident on a plane perpendicular to the direction of propagation of radiation, to the distance of an astronomical unit (1,495 x 10^{11} m) and before passing through the atmosphere. According to the World Radiation Center (*WRC*) (Perpiñan Lamigueiro, 2012), a value of 1,367 W/m^2 has been adopted, with an uncertainty of about 1%. The radiation falling on the ground before crossing the atmosphere known as extraterrestrial radiation (G_o) consists almost exclusively of the radiation passing through the space in a straight line from the sun.

When radiation passes through Earth's atmosphere, it suffers changes in its trajectory by the elements present in the atmosphere. The overall amount of global irradiation that reaches a receiver placed on the surface of the earth is extremely variable. On one hand extraterrestrial radiation experiences a daily variation due to the apparent motion of Sun. On the other hand, there is random variation caused by weather: clouds, rain, sandstorm, etc. Figure 3-5 shows the relations among the different levels of solar irradiance.

To estimate each of the components of the global irradiance is important to understand the relationship between a plane at any orientation at any given time and the incoming solar radiation due to the position of Sun with respect to the plane (see Appendix B). The equations employed to calculate the sun's position and their encoding were taken from the research work of Montenon (Montenon, 2013) as part of the collaboration between the two laboratories.

3.4.2.1 Components of hourly irradiance on horizontal surface

Solar irradiance received onto a horizontal surface is split into its beam and diffuse components. These components provide the basis for estimating solar radiation on tilted surfaces. Hourly irradiance received on the horizontal surfaces may be expressed by:

$$G=G_b+G_d \tag{3.2}$$

The estimation of diffuse irradiance is very complex because it depends on the composition, shape and position of the elements that cause the scattering of radiation and this may vary with time. Diffuse irradiance is essentially anisotropic. The amount of reflected radiation is affected by the nature of the ground and by a wide range of features (snow, vegetation, water, etc.).

Miguel et al. (Noorian et al., 2008) establish a correlation between the *diffuse fraction* of hourly global horizontal irradiance and the *clearness index*. This correlation is given by the following expressions:

$$\frac{G_d}{G}=\begin{cases}0.995-0.081Kt & if \quad Kt<0.21\\ 0.724+2.738Kt-8.32Kt^2+4.967Kt^3 & if \quad 0.21\le Kt\le 0.76\\ 0.180 & if \quad Kt>0.76\end{cases} \tag{3.3}$$

Then, the beam irradiance can be calculated reformulating Equation (3.2) as follows:

$$G_b=G-G_d \tag{3.4}$$

3.4.2.2 Components of hourly irradiance on tilted surface

The global irradiance on an inclined surface, G_β, is integrated by beam, diffuse and albedo irradiance (Equation (3.5)). The most adequate procedure to calculate the global irradiance on a tilted surface is to obtain separately the components.

$$G_\beta = G_{\beta,b}+G_{\beta,d}-G_{\beta,r} \tag{3.5}$$

3.4.2.2.1 Beam irradiance

The amount of beam irradiance on a tilted surface can be calculated by multiplying the beam horizontal irradiance by the *beam ratio factor* (r_b).

$$G_{\beta,b} = G_b\, r_b \tag{3.6}$$

$$r_b=\frac{cos\,\theta}{cos\,\theta_Z} \tag{3.7}$$

One consideration must be taken into account in calculating this component, when the sun shines on the back of the surface ($\cos\theta < 0$) the irradiance on the PV modules is normally not utilized, $G_{\beta,b} = 0$. A factor max (0, $\cos\theta$) is introduced in Equation (3.7).

$$r_b=\frac{\max(0,cos\,\theta)}{cos\,\theta_Z} \tag{3.8}$$

3.4.2.2.2 Reflected irradiance

The reflectivity of most types of ground is rather low (Lorenzo, 2003) except snow and ice. Consequently, the contribution of this type of irradiance falling on a receiver is low. Equation (3.9) computes ground-reflected irradiance.

$$G_{\beta,r} = \rho G\frac{1-cos\,\beta}{2} \tag{3.9}$$

where ρ is the reflectivity of the ground and depends on the composition of the ground. A value of 0.2 is commonly adopted.

3.4.2.2.3 Diffuse irradiance

The methods used to estimate the diffuse irradiance on a titled surface are classified as either *isotropic* or *anisotropic* models. The isotropic models assume that the intensity of diffuse sky radiation is uniform over the sky dome. Hence, the diffuse irradiance incident depends on the fraction of the sky dome where the surface is located. A well-known *isotropic* model was proposed by Liu and Jordan (1963).

$$G_{\beta,d} = G_d \frac{1 + \cos\beta}{2} \tag{3.10}$$

Better results are obtained with the so-called *anisotropic* models. This type of models includes a circumsolar brightening, which assumes that the highest intensity is found at the periphery of the solar disk and falls off with increasing angular distance from the periphery.

Hay and Davies (Noorian et al., 2008) propose a model based on the assumption that all of the diffuse can be represented by a circumsolar component coming directly from the sun and an isotropic component coming from the entire celestial hemisphere. The diffuse irradiance on a tilted surface is then:

$$G_{\beta,d} = G_d r_d \tag{3.11}$$

$$r_d = \frac{G_b}{G_o} r_b + \left(1 - \frac{G_b}{G_o}\right)\left(\frac{1 + \cos\beta}{2}\right) \tag{3.12}$$

Reindl et al. (Noorian et al., 2008) propose another model (Equation (3.13)).. This model extends the Hay and Davies model by adding the *horizon brightening*. The horizon brightening is assumed to be a linear source at the horizon and to be independent of azimuth. In fact, for clear skies, the horizon brightening is highest at the horizon and decreases in intensity away from the horizon. For overcast skies, the horizon brightening has a negative value.

$$r_d = \frac{G_b}{G_o} r_b + \left(1 - \frac{G_b}{G_o}\right)\left(\frac{1 + \cos\beta}{2}\right)\left[1 + \sqrt{\frac{G_b}{G_o}}\sin^3\left(\frac{\beta}{2}\right)\right] \tag{3.13}$$

3.4.2.3 Validation

The simulator was used to estimate the annual radiation received in 4 different positions: Toulouse, France (43.4° N, 1.2°E,altitude 152 m), Sydney, Australia (33.5°S, 151.1°E, altitude 42 m), Mexico City, Mexico (19.2° N, 99.1°W, altitude 2277 m) and Singapore, Singapore (1.1° N, 104.1°E, altitude 5 m). The results were compared with those estimated for the same cities by MIDC SOLPOS Calculator 2.0 (National Renewable Energy Laboratory, 2000) for extraterrestrial irradiance and PVsyst software (University of Geneva, n.d.) for horizontal and tilted irradiance. MIDC SOLPOS Calculator 2.0 was developed by the National Renewable Energy Laboratory (NREL), a research laboratory for the U.S. Department of Energy. This software tool contains a Solar Position Algorithm (SPA) (Reda & Andreas, 2008) for solar radiation applications developed by the NREL. The algorithm can calculate the sun zenith and azimuth angle with uncertainties equal to ± 0.0003°. MIDC SOLPOS Calculator calculates the position of the sun in the sky and its intensity for any given location, day and

time. It is valid from the year 1950 to 2050 and has an uncertainty of ±0.01° (National Renewable Energy Laboratory, n.d.).

As mentioned in Table 3-1, PVsyst is a PV simulation tool developed at the University of Geneva, Switzerland to be used by architects, engineers and researchers. In 2011, PVsyst got excellent results in the PHOTON Magazine evaluation (Mermoud, 2011). The evaluation considered about 20 different PV simulation software available on the market for the study of PV systems yield and tried to assess the accuracy of irradiance data in the horizontal plane and ambient temperature, as well as horizon shading.

Two statistical tests based on root mean square (RMSE) and mean bias error (MBE), were used to compare the results of the model developed in this work and the aforementioned software tools (Diez-Mediavilla, de Miguel, & Bilbao, 2005; Noorian et al., 2008).

$$RMSE = \sqrt{\frac{C_i - M_i}{n}^2} \tag{3.14}$$

$$MBE = \frac{C_i - M_i}{n} \tag{3.15}$$

where C_i is the i^{th} calculated value, M_i is the i^{th} measured value of the radiation, and n is the total number of observations for a specified period of time. The lower the RMSE, the more accurate the model is. A positive MBE indicates an overestimation of the calculated values while a negative MBE indicates an underestimation.

Dimensionless measures of RMSE and MBE, relative RMSE (% RMSE) and relative MBE (% MBE), were also used. They are defined as follows.

$$\%RMSE = 100\frac{RMSE}{M} \tag{3.16}$$

$$\%MBE = 100\frac{MBE}{M} \tag{3.17}$$

where M is the mean of the measured values. The results can be observed in Table 3-2 and Table 3-3. Units of RMSE and MBE are kW/m².

The difference found was minimal especially when the model uses the formulation of Hay et al. (Noorian et al., 2008) for the calculation of diffuse irradiance. Table 3-3 shows the mean of results exposed in Appendix C for estimate G_β following Lu et al., Hay et al. and, Reindl et al. equation for calculate $G_{\beta,d}$. This explains why the model of Hay et al. model was adopted in this work.

Table 3-2 Root mean square (RMSE) and mean bias errors (MBE) of proposed simulator

	Horizontal Global Irradiance				Diffusse Horizontal Irradiance				Beam Global Irradiance			
	RMSE	MBE	% RMSE	% MBE	RMSE	MBE	% RMSE	% MBE	RMSE	MBE	% RMSE	% MBE
Mexico City	39.523	-1.529	18.786	-0.727	23.401	1.706	24.345	1.774	25.065	-3.234	21.935	-2.830
Singapore	39.523	-1.529	18.786	-0.727	24.780	0.345	23.749	0.331	21.503	-2.026	26.493	-2.497
Sydney	34.634	-0.978	18.870	-0.533	23.683	4.028	28.928	4.920	25.450	-5.006	25.033	-4.924
Toulouse	27.486	-1.283	17.943	-0.837	20.181	1.909	25.464	2.409	19.480	-3.192	26.348	-4.317

Table 3-3 Comparison of G_β estimated

	Titl (°)	Lu et al.	Reindl et al.	Hay et al.
Mexico City	**RMSE**	43.688	39.231	40.704
	MBE	8.618	-1.343	0.913
	% RMSE	23.577	20.861	21.838
	% MBE	2.597	-0.636	0.898
Singapore	**RMSE**	31.051	27.197	28.190
	MBE	2.414	-0.669	1.302
	% RMSE	22.933	19.286	20.225
	% MBE	2.534	-0.391	1.576
Sydney	**RMSE**	46.319	35.474	47.361
	MBE	-5.318	-1.488	0.394
	% RMSE	26.714	19.979	27.407
	% MBE	-3.032	-0.839	0.347
Toulouse	**RMSE**	36.105	34.267	34.523
	MBE	-5.462	-1.099	0.522
	% RMSE	24.285	23.019	23.222
	% MBE	-3.636	-0.704	0.512

3.5 PVGCS sizing model

The second model of the system aims at calculating annual energy generated by the system from the radiation computed by the first model and the characteristics of the electrical components. This model considers the following aspects:

a) The field dimension where the PVGCS will be installed;
b) Technical aspects of the different elements of the PVGCS.
c) Design restrictions due to maintenance and safety purposes. These restrictions concern not only the maximum weight that the structure where the PV modules will be placed support but also the standards and best practices to ensure appropriate maintenance in case of problems during operation of PVGCS.

Figure 3-6 describes the main elements of this model. VBA in Excel was used to encode this model.

3.5.1 *Output energy estimation*

The design of PVGCS must take into account the dimensions of the field, solar radiation data and the so-called balance of system components (BOS). The BOS encompasses all the components of a photovoltaic system other than the photovoltaic panels. In addition, shading and the effect of mask (i.e. corresponding to shades on a solar panel caused by obstacles such as buildings, vegetation or relief for example) affect the collector deployment by decreasing the incident energy on collector plane of the field.

In a solar field, collectors, an array of PV modules, are deployed in different sheds with spacing allowing tilting and being useful for maintenance purpose. In this arrangement, a collector may cast a shadow on the adjacent row during the day, thus decreasing the amount of collected energy. This shading effect depends on the spacing between the collector rows, the collector height, and the tilt

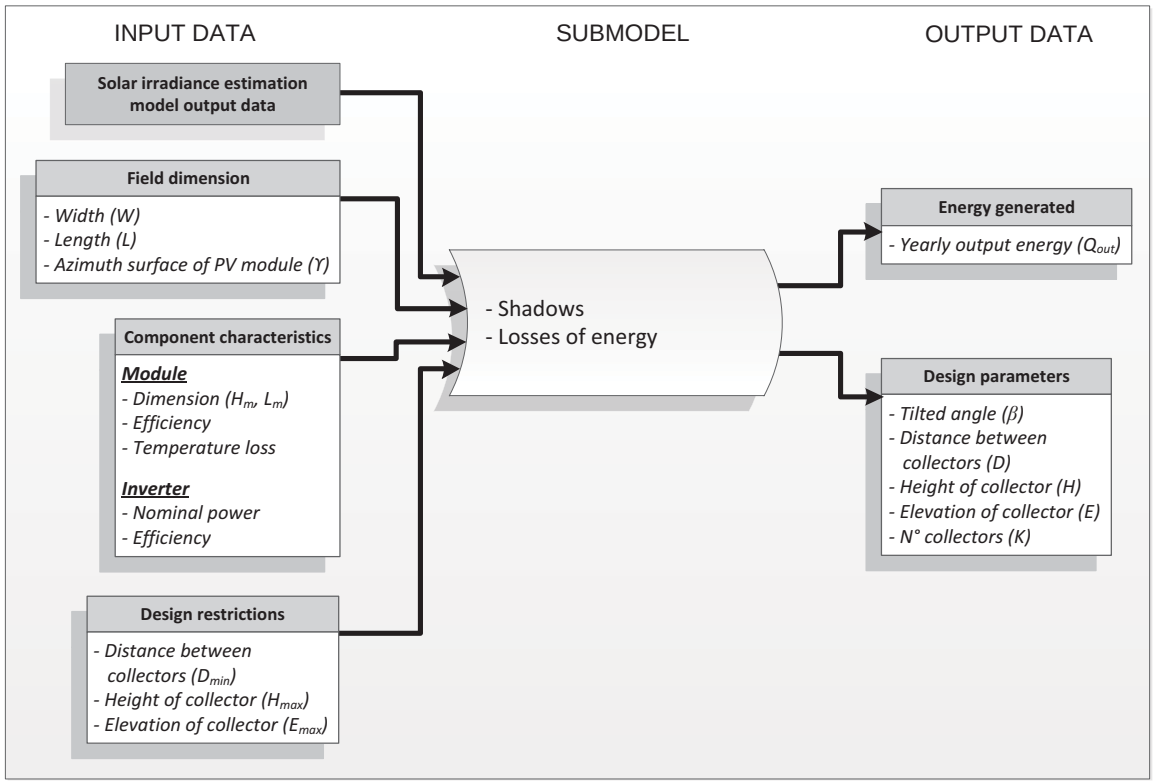

Figure 3-6 Data flow diagram of PVGCS model

angle and also on the row length and on the latitude of the solar field. The use of many rows of collectors densely deployed increases the surface that is available to transform solar irradiation but also increases the shading.

The spacing and, consequently, shading have also and influence on local environmental not allowing grass or culture to grow between and enter the PV panels. This environmental consequence was not evaluated in this work.

The balance of system (BOS) also influences the estimate of annual energy generated by the facility because of the efficiency of electrical components.

3.5.2 *Techniques for sizing PV systems*

In any PVGCS, sizing represents an important part of the design that must satisfy techno-economic requirements. Undoubtedly, at the current stage of development of PV technology, the major impediment to a wider market penetration is the high investment costs of the PV systems (EPIA, 2012).

The solar field design problem may be described by a mathematical formulation, usually multivariable and nonlinear in both the objective and constraint functions.

In the literature, the configuration of PV is made following only one objective such as the minimum field area required for producing a given amount of energy, the maximum energy generated from a given field or minimum cost of investment.

3.5.3 *Mathematical sizing model*

Weinstock and Appelbaum (Weinstock & Appelbaum, 2007) formulated the PVGCS sizing problem as a mathematical problem. The optimal design parameters of the solar field were determined to obtain the maximum annual incident energy on the collector planes from a given field size.

The improvements that were implemented relative to the model presented in (Weinstock & Appelbaum, 2007) concern the computation of the output power of the system, mainly in the following aspects:

- The equation used for calculating the diffuse irradiance received by the collector is replaced by the anisotropic model of Hay et al. (Noorian et al., 2008).
- The reflected irradiance is included in the calculation of the radiation received by the installation.
- The method used to calculate energy loss caused by the shadow generated by adjacent collectors is changed. An array indicating the number of panels covered in a collector is created following the method proposed by Ziar et al. (Ziar, Mansourpour, Salimi, & Afjei, 2011)

The model considers a horizontal field without elevations with a fixed length L and a fixed width W. It comprises K rows of solar collectors with a horizontal distance D between the rows; each collector has a length L_C, a height H, and a tilted with an angle β with respect to the horizontal Figure 3-7. Each collector is an array of PV modules arranged in N_r rows and N_c columns. The length of collector row L_C and its height H_C are given by:

$$L_c = N_c\, L_m \tag{3.18}$$

$$H = N_r\, H_m \tag{3.19}$$

The variables considered in this model are β, D, K, H where K is a discrete variable. The following constraints are also involved:

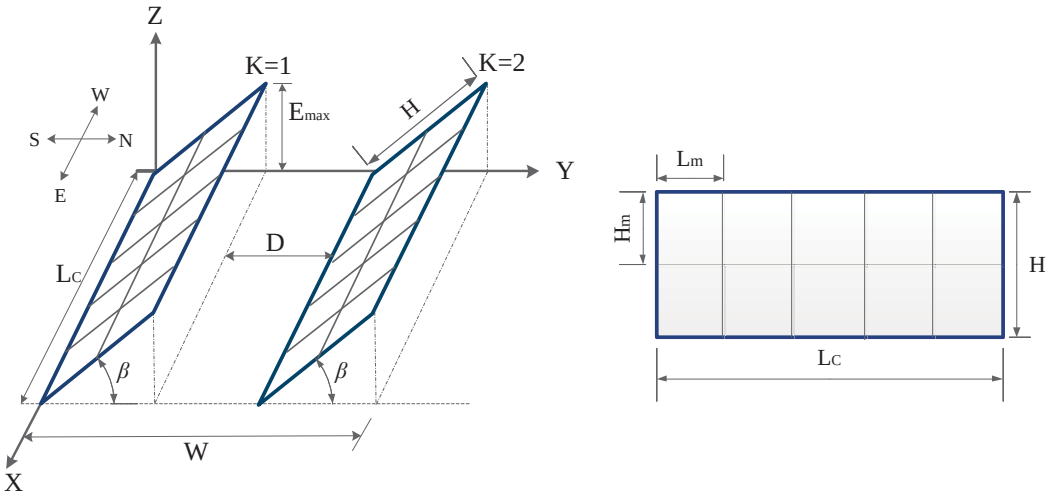

a) Position of two tilted sheds b) Solar collector configuration

Figure 3-7 Solar collector field reproduced from (Weinstock & Appelbaum, 2009)

- The variation of the collector parameter values and distances are considered by the field width, i.e.:

$$K\,H\cos\beta\ + (K-1)D \leq W \tag{3.20}$$

- The space between collector rows D is at least equal to a distance D_{min}, i.e.:

$$D \geq D_{min} \tag{3.21}$$

- Maintenance and installation constraints are required to limit the height of collector above the ground E_{max}, i.e.:

$$H\sin\beta\ \leq E_{max} \tag{3.22}$$

- The collector height H itself can be limited by the solar field construction, maintenance and by PV module manufacturer, i.e.:

$$H \leq H_{max} \tag{3.23}$$

- The collector tilt angle may vary in the range of 0° to 90°:

$$0° \leq \beta \leq 90° \tag{3.24}$$

- The number of PV shed of the final array is a least equal to 2 and takes a discrete value:

$$2 \leq K\ \in\ Z^{+} \tag{3.25}$$

3.5.3.1 Direct shading

They can be due to trees, posts, nearby buildings, etc. placed between the sun and the panels during the day, or if there are several sheds of panels arranged in the same horizontal plane. Losses can be important, because of that, the location must be carefully chosen to avoid shading as much as possible. In the case of large-scale solar plants, collectors are set in several sheds and shading by neighbors may become inevitable. The shadow that is projected from a shed to another one varies throughout the day and can be determined geometrically (Weinstock & Appelbaum, 2004a) (Appendix D).

The amount of shading depends on the distance between the collector rows D, their height H, the row length L_c, the tilt angle β and the latitude ϕ (see Figure 3-8).

A status matrix is defined, $M(j, k, t, n)$, as follows in order to determine the shaded modules of the collector in a specific hour t and in a specific day n (Weinstock & Appelbaum, 2009).

$$M(j,\,k,\,t,\,n) = \begin{cases} 1 & \text{if module in column } j \text{ and row } k \text{ is unshaded at hour } t \text{ in day } n \\ 0 & \text{if module in column } j \text{ and row } k \text{ is shaded at hour } t \text{ in day } n \end{cases} \tag{3.26}$$

This matrix makes it possible to determine if a module receives solar irradiation during the whole day or only at given hours of the day. In addition, the status matrix assumes that any partially shaded module at a given time is considered as a fully shaded module. The modelling of a partially shaded module represents a complex situation. A solution found in the literature is to consider that a module is "shaded" once a shadow is cast on it even on a smallest part of its area. This is of course the extreme case because some power may be delivered by the module when partially shaded. This hypothesis is supported by the fact that a matrix of shaded/unshaded modules simplifies the algorithmic aspect and reduces the computational time while the results are not so different to those obtained by using PVsyst.

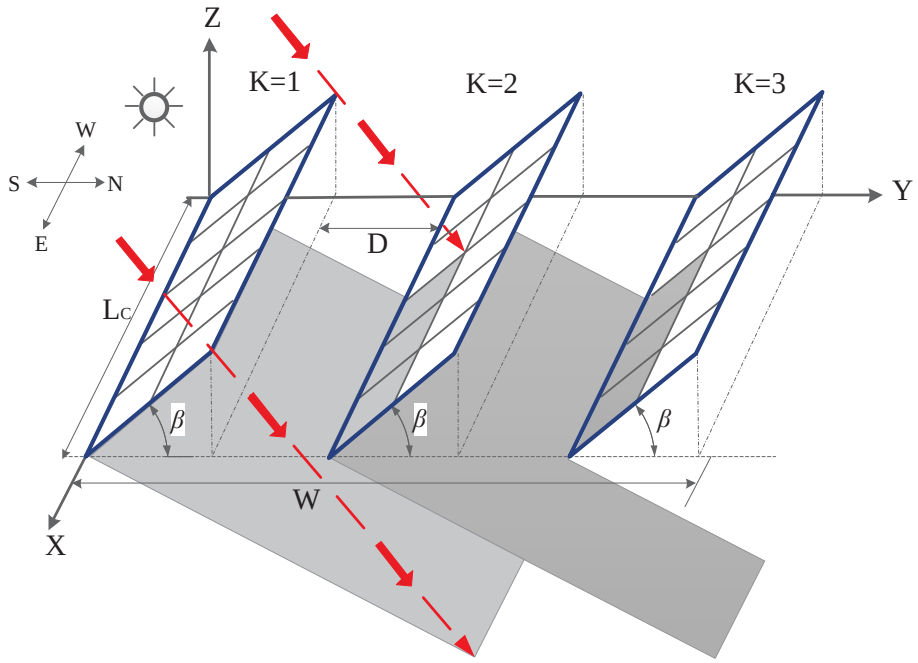

Figure 3-8 Shading by collectors in a stationary solar field reproduced from (Weinstock & Appelbaum, 2009)

3.5.3.2 Output energy of solar field

The output power of the modules in a row connected in series depends on three main factors: module efficiency (η), module temperature (T_m), and the number of shaded modules at a given time. The meteorological data at the specific site together with the geographical coordinates of the site allow calculating the power delivered by a module as a function of time.

$$Q_m(t) = \eta A G_\beta(t) \tag{3.27}$$

The module temperature was calculated according to Van Overstraeten et al. (Weinstock & Appelbaum, 2004b), Equation (3.28)), and the loss of power due to temperature rise above 25°C is taken into account in Equation (3.29)) for the power delivered by a module in time *t* at day *n*:

$$T_m(t) = 20 + 0.35 G_\beta(t) \tag{3.28}$$

$$Q_m(t,n) = \eta A G_\beta\ t,n\ [T_m(t,n) - 25] \tag{3.29}$$

The integration of Equation (3.29) over a year predicts the annual energy produced of a module. The yearly incident solar energy of the PV collectors placed in the field is given by:

$$Q_{out} = N_r N_c \sum_{n=1}^{365} \sum_{t=1}^{24} Q_m\ t,n\ + K-1 \sum_{n=1}^{365} \sum_{t=1}^{24} \sum_{k=1}^{N_r} \sum_{j=1}^{N_c} M\ j,k,t,n\ Q_m\ t,n \tag{3.30}$$

The first part of the Equation (3.30) represents the energy produced by the unshaded first shed and the second part comprises the energy produced by the *K-1* shaded sheds. This value represents the maximum amount of energy that is sent to the DC / AC inverter.

3.5.3.3 Energy losses

The losses inherent in any energy conversion process are numerous. These losses have different origins. In this chapter, we have already mentioned some of them. Table 3-4 summarizes the main

Table 3-4 Summary of the main energy losses (Brigand, 2011; Hayoun & Arrigoni, 2012)

Origin of loss	Loss (%)	Observations
Shading loss	Variable	Loss related to the geographic location of PVGCS in addition to the inclination, spacing and dimensions of the shed. (Section 3.5.3.2).
PV conversion	Variable	Loss due to the type of technology of PV module (*module* efficiency). Value indicated in the technical data sheet of the PV module.
Thermal loss	Approx. 0,5 %/°C	Loss caused by the temperature rise of the PV module. Value indicated in the technical data sheet of the PV module.
Modules array mismatch loss	≤ 3%	Loss caused by the interconnection of PV module.
Ohmic wiring loss	≤ 3%	Loss linked to the characteristics of the wiring that connects all electrical devices.
Loss due to DC/AC inverter	3-10%	Loss caused by the internal characteristics of the components of the DC / AC inverter. Value indicated in the specifications of the DC / AC inverter.

energetic losses to consider sizing a PVGCS, starting from available global horizontal irradiance until to obtain the total energy injected into the grid.

3.6 Evaluation model

The third model of the integrated system is dedicated to the evolution of the three criteria. For each criterion, a performance index was selected. These indexes will allow the evaluation and comparison of the resulting options. Figure 3-9 summarizes the different elements required by this model.

In order to determine the requirement of construction material and electric components necessary for the design of the PV power plant and, the cost incurred as well the associated environmental impacts, the scheme proposed by Kornelakis and Koutroulis (A. Kornelakis & Koutroulis, 2009) is used. A fixed mounting structure is selected because of the simplicity. A centralized inverter zone is proposed as it is indicated by the guidelines published by the Agence de l'Environnement et de la Maîtrise de

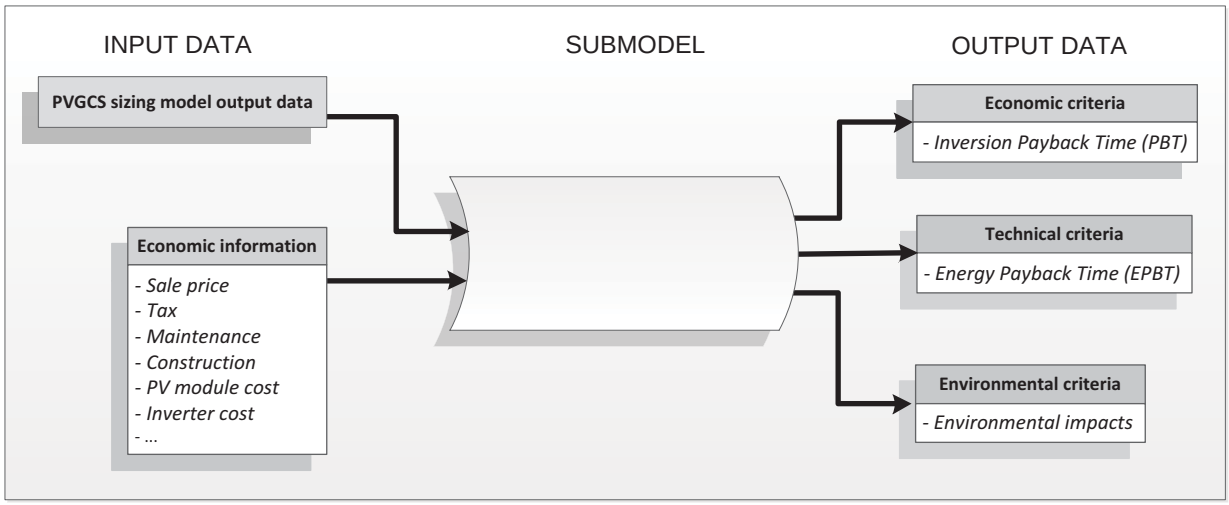

Figure 3-9 Evaluation of criteria model

l'Energie (ADEME) (Boulanger, 2003). Appendix D shows in detail the techniques used for designing the mounting structure and electrical components.

3.6.1 *Techno-economic criteria*

The techno-economic criteria chosen in this study concern the *payback time of investment* and *energy payback time,* respectively. These are classical criteria when energy production is involved. Their choice is summarized in what follows.

In project evaluation and capital budgeting, the *payback time* (PBT) is an estimation of the time that will be necessary for an investor to recover the initial investment. It is used to compare investments that might have different initial capital requirements. It is calculated by the following expression:

$$PBT = \frac{\text{Cost of project}}{\text{Annual Cash Inflows}} \tag{3.31}$$

The cost of project considers the considering all the components that make up the installation purchasing (PV modules, cables, mounting system ...), the construction and the edification cost as well as the cost of connection to grid. Annual cash flow represents the incomes by selling all energy production.

Table 3-5 summarizes the main elements of economic evaluation considered in the model. The price of electrical components (PV modules and DC / AC inverters mainly) is set by the manufacturer and the price often depends on the volume purchased. Solarbuzz (Solarbuzz, 2012a, 2012b) together with PV magazine (Schachinger, 2012) make regularly a study of PV modules technologies and DC/AC inverters market price. They proposed a price by W_p and W_{AC} respectively. The others costs were taken from (Hayoun & Arrigoni, 2012), (Di Dio, Miceli, Rando, & Zizzo, 2010) and, (A. Kornelakis & Koutroulis, 2009) works. The average sell price for the electricity generated by the PVGCS was obtained from the reports of the European Renewable Energies Federation (Fouquet, 2009, 2012).

Energy payback time (EPBT) is the time in which the input energy during the PV system life-cycle

Table 3-5 Main elements of economic evaluation

Description	**Value**
PV module	
- m-Si	0.85 €/W_p
- p-Si	0.82 €/W_p
- a-Si	0.74 €/W_p
- CdTe	0.77 €/W_p
- CIS	0.86 €/W_p
DC/AC inverter	0.40 €/W_{AC}
Fixed support structure	33.00 €/m
Cables	0.50 €/m
Concrete basements	230.00 €/m^3
Network connecting	0.05 €/W_p
Construction fee	0.39 €/W_p
Price of energy sold	0.276 €/kWh

(which includes the energy requirement for manufacturing, installation, energy use during operation, and energy needed for decommissioning) is compensated by electricity generated by the PV system.

$$EPBT = \frac{\text{Primary energy required for manufacturing}}{\text{Annual primary energy produced}} \quad (3.32)$$

Primary energy required for manufacturing is obtained as a result of the Life Cycle Assessment, identified here in the *Non-renewable energy* category. A conversion factor of 2.58 is used to transform 1 kWh electricity into primary energy (ADEME, n.d.).

3.6.2 *Environmental criteria*

As it was mentioned in Chapter 2, the environmental assessment is performed following the methodology of Life Cycle Assessment (LCA). Following the guidelines indicated in the LCA study described in Section 2.7, the system boundaries are kept without considering recycling processes (see Chapter 5). PV modules and BOS component characteristics will be modified in accordance with the data and characteristics of each situation under evaluation.

IMPACT 2002+ (Jolliet et al., 2003), included in SimaPro 7.3, was selected as a method for evaluating the environmental impacts. Only the midpoint categories are considered.

3.7 Validation of the model

3.7.1 *Comparison with Weinstock and Appelbaum's model performances*

The example given by Weinstock and Appelbaum (Weinstock & Appelbaum, 2009) (referred as WAP in the following) is used to validate the proposed model.

It must be kept in mind at this level that the objective is to verify the validity of the proposed modelling and simulation approach without considering optimization, that will be the core of the subsequent chapter. The maximization of the annual energy generation by the facility is used the reference objective. In order to check the relevance of the model, the same scenarios as those used in the WAP approach were used. WAP offers the best configuration of a PV power plant for the maximum energy generation under three different scenarios:

- in the first scenario, PV power plant is sized when maximizing the incident energy on to the total surface of PV modules without any type of energy losses;
- the second one maximizes the output energy when only considering the module efficiency and shading;
- the third one maximizes the output energy of the PVGCS with accounting of all possible energy losses (shading, temperature and interconnections losses).

The PV power plant is located in Tel Aviv, Israel (32.0°N, 34.8°E, altitude 4 m, GMT +2). The PV module has a length L_m = 1.293 m and a height H_m = 0.33 m. The technology of the PV module used by WAP is not mentioned explicitly but the computation is performed with the assumption of an efficiency of 12.42%.

The field and PV collector parameters are the following ones: W = 150 m, L = 12.93 m, and N_r = 6, N_c = 10.

The simulation of each configuration calculated by WAP for each of the three proposed scenarios was performed with the model proposed in this work. The goal is to compare the amount of energy generated between both approaches. The site data, the dimension of the field and PV module characteristics were used in the simulation runs. It must be yet emphasized that because each configuration in WAP example was obtained by optimizing a mathematical model, the value of K, β and D are not the same in each run. Table 3-6 contains the values of these parameters for each scenario.

Table 3-7 shows the comparison between the results obtained by our approach and the WAP example. The results estimated by the proposed simulator tool have a difference of about 20% with respect to the estimation of WAP. As mentioned in Section 3.5.3, this difference can be attributed to the modifications made in the model for predicting the annual amount of the energy generated.

3.7.2 *Comparison with PVsyst*

To verify this assumption, a second set of simulation runs is performed with PVsyst software (mentioned in Table 3-1) taking into account the technology type. For the simulations, the location of PV plant, the field dimensions and the parameter values for the three WAP cases (see Table 3-6) are used again.

The objective is to study the five main PV modules technologies available in the market: monocrystalline silicon (m-Si), polycrystalline silicon (p-Si), amorphous silicon (a-Si), cadmium telluride (CdTe) and copper indium diselenide (CIS). Table 3-8 shows the main characteristics for each of the 5 PV modules technologies used in the simulations.

Table 3-6 Parameter values for each scenario of WAP example

Objective function	***K***	***β (°)***	***D (m)***
Maximum incident energy on to the total surface of PV modules	58	24.62	0.80
Maximum output energy with shading losses	58	24.62	0.80
Maximum output energy of PV array (shading, temperature and interconnections losses)	57	21.23	0.80

Table 3-7 Comparison of output energy from the example of WAP and the proposed tool

Objective function	Q_{out} (kW h)		
	Weinstock et al.	This approach	Diff
Maximum incident energy on to the total surface of PV modules	2 641 034	3 187 715	+ 20,70%
Maximum output energy with shading losses	328 048	395 914	+ 20,69%
Maximum output energy of PV array (shading, temperature and interconnections losses)	268 000	326 692	+ 21,90%

Table 3-8 Typical features of various commercial PV modules technologies

Technology	H_m (m)	W_m (m)	η (%)	Nominal power (Wp)
m-Si	1.56	1.05	20.10	327.00
p-Si	1.64	0.94	15.50	240.00
a-Si	1.31	1.11	7.20	105.00
CdTe	1.20	0.60	11.50	82.50
CIS	1.26	0.98	12.20	150.00

Table 3-9 Values of *Nc* and *Nr* for simulation

Technology	N_r	N_c
m-Si	1	12
p-Si	1	13
a-Si	1	11
CdTe	1	21
CIS	1	13

The values of N_c and N_r for each of the technologies are shown in Table 3-9. In the simulations, only one technology is assumed per field which means that no mixed technologies are allowed. In order to compare the results, each of the 5 configurations is modelled with PVsyst software.

It must be highlighted that PVsyst is a software tool developed by the University of Geneva, Switzerland. This architect- and engineer-oriented tool is suitable for working in the field of renewable energy but is also for education. This program has three modules:

- *a preliminary design,* which allows making a quick evaluation of a grid-connected installation, a stand-alone installation or a pumping system;
- *a project design,* it allows sizing an installation connected to the DC network using detailed hourly simulations;
- a *tool module,* in which it possible to adjust certain parameters of the software.

PVsyst includes a database of around 330 sites in the world and it possible to import weather data from many popular meteorological sources. The component database holds over 1,750 PV modules from all common commercial technologies, 650 inverters and dozens of batteries or regulator models.

The *Preliminary design* module permits the definition of the plane orientation, PV components and location. It offers detailed parameters allowing fine effects analysis, including thermal behaviour, wiring and mismatch losses, and module quality loss. A detailed economic evaluation could be performed. A final report summarises all system parameters and the most significant result plots and tables for one given simulation.

PVsyst includes a 3-D CAD tool to draw the geometry of the system. It computes a shading factor for beam component as a function of the sun's position. Animation over a whole chosen day could be made for clarify the shading impact of a given situation.

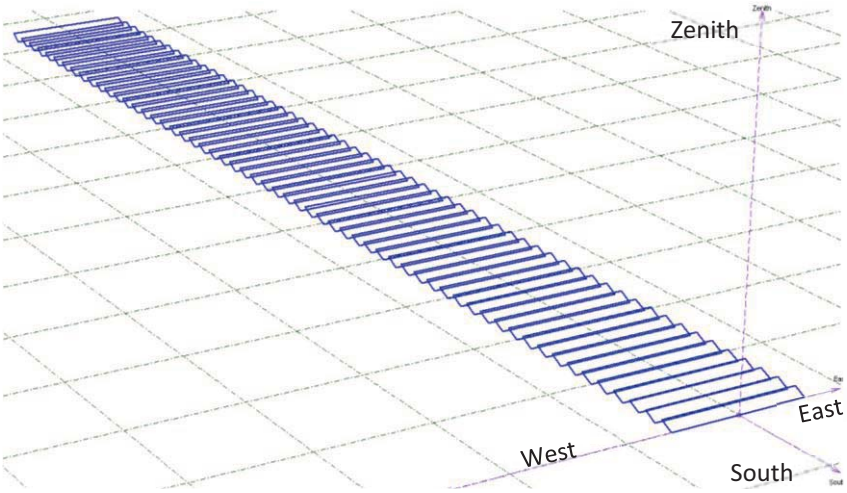

Figure 3-10 Field layout of PV power plant made in PVsyst

Figure 3-10 shows the layout generated in PVsyst showing the position of the PV sheds for calculation of the energy generated for each of the three scenarios under evaluation. The blue rectangles represent PV shed with south orientation. Each square in the floor represents 100 m². Table ***3-10*** contains the results obtained from the modelling of the three scenarios with the different types of PV modules technology both PVsyst and the simulation tool proposed in this chapter.

It must be highlighted that a good agreement is obtained between the prediction of the proposed tool and those of PVsyst. The deviation that is observed may be due to the precision adopted in PVsyst for

Table 3-10 Comparison of output energy from PVsyst and the proposed tool

		Q_{out} (kW h)		
Objective function	**Techno**	PVSyst	Simulator	Deviation
Maximum incident energy onto total surface of PV modules	m-Si	2 497 636	2 558 693	+2,44%
	p-Si	2 723 105	2 631 590	-3,36%
	a-Si	2 036 096	2 084 487	+2,38%
	CdTe	1 936 192	1 977 019	+2,11%
	CIS	2 043 586	2 084 206	+1,99%
Mean				+1,11%
Maximum output energy with shading losses	m-Si	483 935	486 919	+0,62%
	p-Si	383 003	361 782	-5,54%
	a-Si	145 525	145 813	+0,20%
	CdTe	216 193	221 715	+2,55%
	CIS	242 834	247 511	+1,93%
Mean				-0,05%
Maximum output energy of PV array (shading, temperature and interconnections losses)	m-Si	420 604	430 279	+2,30%
	p-Si	319 830	314 063	-1,80%
	a-Si	149 561	155 386	+3,89%
	CdTe	188 687	198 482	+5,19%
	CIS	210 516	218 421	+3,76%
Mean				+2,67%

some parameters required for the estimation of the output energy of the system such as PV collector inclination and position of the sun throughout the evaluation period work only: integer numbers are used in PVSyst while the proposed simulation tool uses decimal numbers. This situation concerns in particular the amount of irradiance that PV power plant can receive and the energy loss due to the shadows cast by the PV shed.

The main disadvantage of using PVsyst, as presented in Table 3-1, is its closed structure, not allowing it to be embedded in an outer optimization loop. It is then difficult to achieve the main objective of this work, which consists in the development of an ecodesign tool for PV panels.

Another disadvantage of this software tool is that, although involving a 3-D CAD tool, the use of this tool requires the configuration and arrangement of all the elements of the system to be evaluated. A change in the dimensions of the PV collector or in the number of PV sheds placed in the field cannot be performed automatically by the program. A trial and error procedure must thus be implemented.

Additional information can also be obtained with the proposed simulation tool. The result of the evaluation of PBT and EPBT for each configuration is shown in Table 3-11.

The results are presented through radar charts normalised to unity. Figure 3-11 presents the radar chart of the results of the environmental impact assessment (15 midpoint categories). To facilitate the comparison, normalisation was performed by assigning the value 1 to the maximum value of each category. The computed relative impacts represent the ratio between the environmental impact and this maximum value.

From Table 3-11, it can be seen that the choice of the PV power plant that uses PV modules of m-Si has a lower PBT as the revenue generated by the large amount of annual energy that can be injected into the grid is the highest one and compensates for the highest unit cost of all the technologies considered. Considering EPBT, the use of PV modules based on CdTe has the shortest time. This is due to the low amount of primary energy needed for manufacturing (see Chapter 2).

The graphics show that the configuration that uses technology based on m-Si has the highest impact in 13 of 15 categories, while in the other categories (Carcinogens and Mineral Extraction) the highest impacts are observed when using PV modules based on a-Si.

Another analysis is then performed taking into account the energy generated by each configuration.

This new analysis consists in assessing the environmental impact per kWh produced, as follows:

Table 3-11 PBT and EPBT for each configuration

PV module	PBT (yr)	EPBT (yr)
m-Si	6,35	1,18
p-Si	8,19	1,33
a-Si	12,28	1,37
CdTe	10,08	0,99
CIS	8,71	1,24

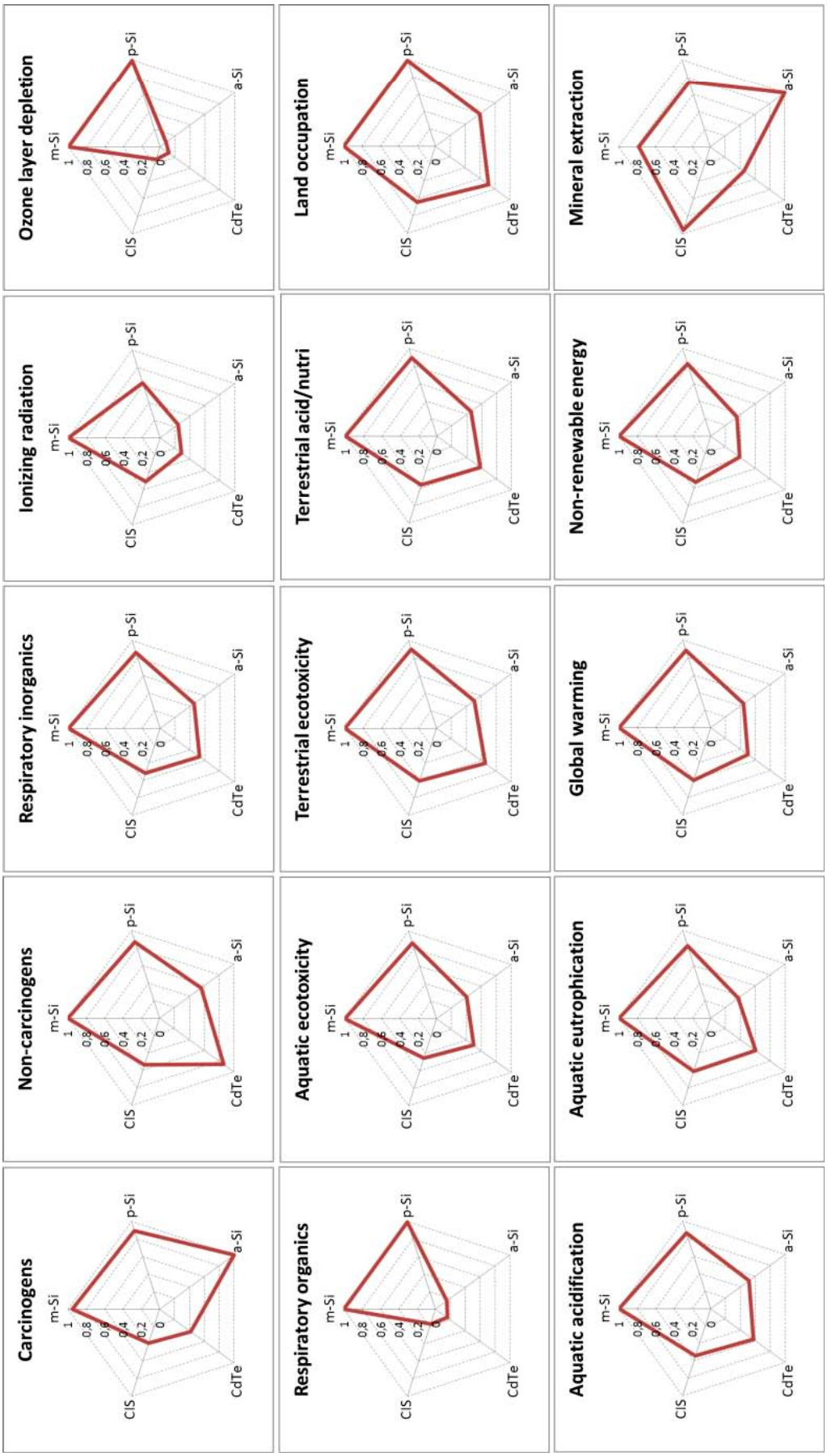

Figure 3-11 Results of the environmental impacts normalized to unity

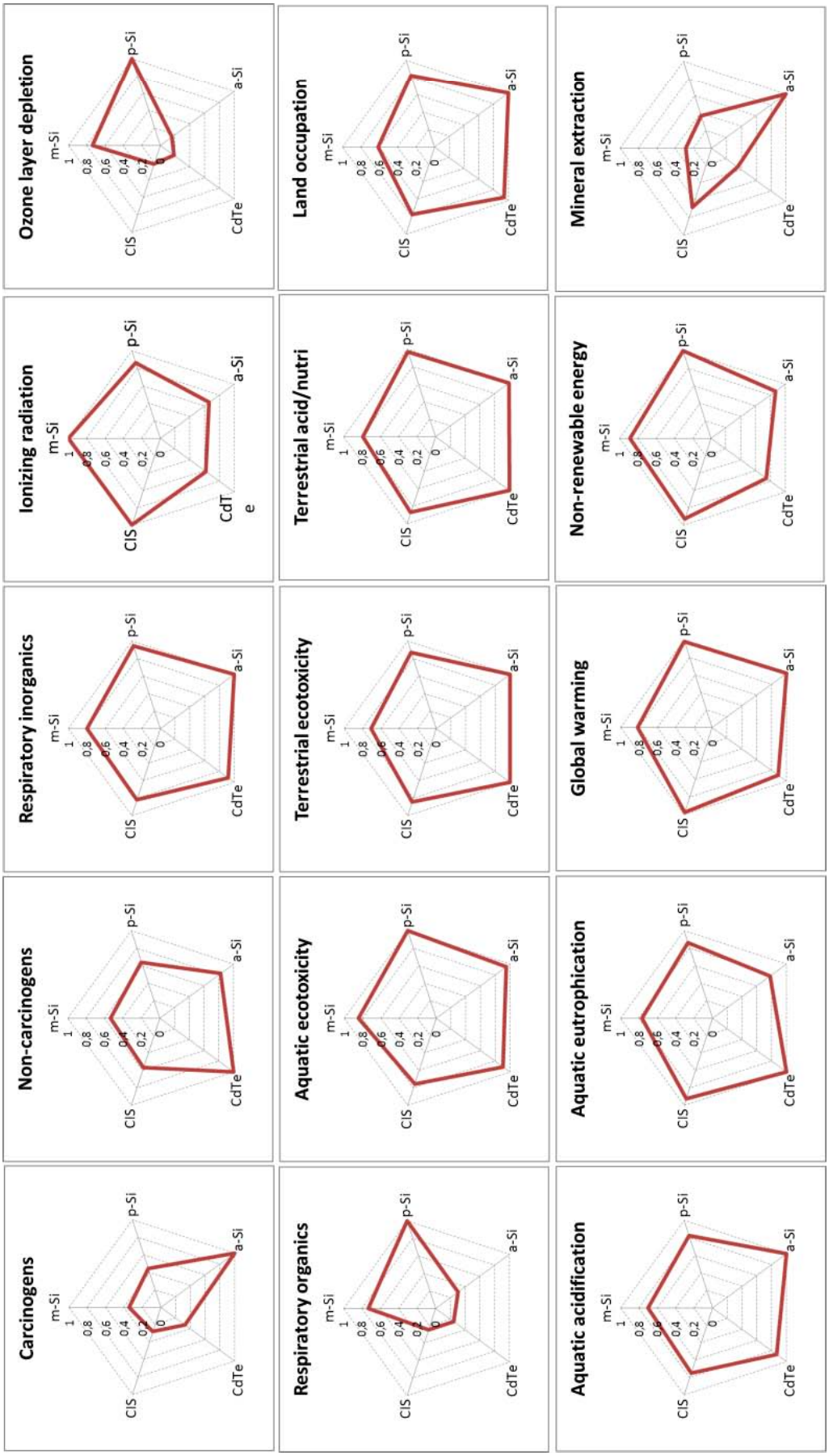

Figure 3-12 Results of the environmental impacts per annual energy generated ratio normalized to unity

$$Index = \frac{midpoint\ environmental\ impact}{yearly\ output\ energy\ of\ the\ field} \tag{3.33}$$

The results are presented through radar charts normalized to unity (Figure 3-12). It emphasizes the substantial reduction of categories led by m-Si technology from 13 to just one. The opposite case is the technology based on a-Si that increases of 2 to 6 category. These changes highlight the influence of the energy generated in a PVGCS to assess the environmental impacts generated.

Another fact to note from the graphics presented is the similarity in behaviour between some of the categories of environmental assessment. In the next chapter, a methodology will be proposed to identify the correlated impacts and the antagonist behaviour of the criteria in order to reduce their number in the optimization step.

3.8 Conclusion

The chapter was dedicated to the model developed in this work to represent the performance of a PV power plant. The model involves a three-step framework:

(1). The estimated solar radiation received by the system according to the geographic location

(2). The model provides the annual energy generated from the characteristics of the system components and limitations on the design of the installation. The design of PVGCS must take into account the dimensions of the field, solar radiation data (see first item) and the so-called balance of system components (BOS). Let us recall that BOS encompasses all the components of a photovoltaic system other than the photovoltaic panels. WAP does not consider BOS.

(3). The model is then coupled with two modules for evaluation of techno-economic (PayBack Time and Energy PayBack) and environmental (IMPACT 2002+ midpoint categories) criteria.

From the technical viewpoint, the model performance was validated for a reference example taken from the literature (Weinstock & Appelbaum, 2009) with a standard simulation tool and exhibited a good agreement.

A preliminary assessment of the economic and environmental performance of some typical technologies that can be used for PV modules shows that the proposed approach can predict with a good accuracy monocrystalline silicon (m-Si), polycrystalline silicon (p-Si), amorphous silicon (a-Si), cadmium telluride (CdTe) and copper indium diselenide (CIS).

This analysis then confirms the interest to use an optimization approach to search for the most interesting solution taking into account simultaneously techno-economic aspects and environmental concern.

The integration of the proposed model in an outer optimization loop is therefore a natural extension of this work and is the core of the following chapter.

Chapter 4

METHODS AND TOOLS FOR ECODESIGN: COMBINING MULTI-OBJECTIVE OPTIMIZATION (MOO), PRINCIPAL COMPONENT ANALYSIS (PCA) AND MULTIPLE CRITERIA DECISION MAKING (MCDM)

Les problèmes d'écoconception nécessitent en général la considération d'un grand nombre d'objectifs, induit par le jeu de catégories d'impact, de l'ordre d'une dizaine, lors de l'application de l'analyse du cycle de vie. Les méthodes d'optimisation multi-objectif, quant à elles, impliquent d'un point de vue de leur mise en œuvre pratique, des problèmes ayant un nombre plus réduit de fonctions objectifs: la résolution d'un problème bicritère ou tricritère peut se révéler complexe selon la nature des contraintes et des critères mis en jeu. Les principaux obstacles au traitement d'un grand nombre d'objectifs sont divers : stagnation possible du processus de recherche, augmentation de la dimension du front de Pareto, temps de calcul élevé, et enfin difficulté à visualiser et analyser les résultats. Par ailleurs, l'analyse des résultats de l'analyse du cycle de vie pour un produit, processus ou service montre que certains critères peuvent être redondants : les groupes de critères liés dépendent du problème à traiter. Il est donc important de bien formuler le problème pour identifier le choix de critères indépendants et mener le processus d'optimisation de façon rationnelle.

Ce chapitre, consacré aux outils et méthodes utilisés dans le cadre de ce travail, est divisé en trois parties principales. La première partie est consacrée à l'optimisation multi-objectif et le choix d'une variante de la méthode dite NSGA-II est justifié. La partie 2 présente une approche fondée sur une analyse en composantes principales (ACP) couplée avec la variante de NSGA-II sélectionnée. L'idée est d'identifier les objectifs redondants des solutions obtenues par NSGA-II et de les éliminer dans le processus d'optimisation proprement dit. La partie 3 concerne les outils d'aide à la décision multicritère mis en œuvre afin de sélectionner le meilleur compromis parmi les critères antagonistes à partir des solutions du front de Pareto.

Nomenclature

Acronyms

ACO	Ant Colonies Optimization
AI	Artificial Intelligence
CUT	CUT value for PCA
DE	Differential Evolution
EPBT	Energy Payback Time
GA	Genetic Algorithm
LCA	Life Cycle Assessment
MCDM	Multiple-Criteria Decision Making
MGA	Multi-objective Genetic Algorithms
MILP	multi-objective Mixed-Integer Linear Program
MOGA	Multi-Objective Genetic Algorithm
MOO	Multi-Objective Optimization
M-TOPSIS	Modified Technique for Order Preference by Similarity to the Ideal Solution
NSGA	Non-dominated Sorting Genetic Algorithm
NN	Neural Networks
NPGA	Niched Pareto Genetic Algorithm
PBT	Payback Time
PCA	Principal Component Analysis
PSO	Particle Swarm Optimization
PV	Photovoltaic
PVGCS	Photovoltaic Grid-Connected System
SPEA	Strength Pareto Evolutionary Algorithm
TOPSIS	Technique for Order Preference by Similarity to the Ideal Solution
VBA	Visual Basic for Applications
VEGA	Vector Evaluated Genetic Algorithm
WTG	Wind Turbine Generators

Symbols

λ_e	e^{th} eigenvalue remained in PCA method
A^+, A^-	Ideal and non-ideal solution in M-TOPSIS method
a_{ij}	Normalized result of alternative i into the criterion j
D_i^+, D_i^-	Euclidean distance for ideal and non-ideal solution for alternative i
G_j	Cumulative explained variance
R_i	M-TOPSIS ratio value for alternative i
Q_{out}	Yearly output energy of the field, kWh
v_{ij}	Weighted normalized result of alternative i into the criterion j
w_j	Weight of the individual criterion j
x^+	Most positive element of principal component
x^-	Most negative element of principal component
X_{ij}	Value of alternative i into the criterion j

4.1 Introduction

Ecodesign problems involve a large number of objectives, generally more than ten when carrying out Life Cycle Assessment. Multi-objective optimization methods are yet applied only to problems having a lower number of objectives. Among these methods, existing evolutionary multi-objective optimization methods, which turned out to be very attractive due to their ability to lead to a well-representative set of Pareto-optimal solutions in a single simulation run, are generally applied only to problems having about 5 objectives or so. The major impediments in handling a large number of objectives relate to stagnation of search process, increased dimensionality of Pareto-optimal front, large computational cost, and difficulty in visualization of the objective space. Furthermore, several objectives are redundant so that a multi-objective strategy is not, strictly speaking, necessary.

The methods and tools that are proposed in this chapter can be viewed as generic approaches for ecodesign problems. They are applied more particularly here to the PVGCS problem which is the subject of this PhD work. The PVGCS strategy and the results obtained will not be presented in this chapter. They will be deeply analysed in the following chapter.

This chapter is divided into three main sections. Section 1 is dedicated to multi-objective optimization and the choice of a variant of the so-called NSGA-II method is justified. Section 2 addresses a principal component based approach coupled with the variant of NSGA-II that is selected. The idea is to identify redundant objectives from the solutions obtained by NSGA-II and to eliminate them from further consideration. Section 3 concerns Multiple Criteria Decision Making, in order to select from the optimal Pareto front the best compromises among the antagonist criteria.

4.2 Multi-objective optimization for sizing PV systems

In any PVGCS, sizing represents an important part of the design that must satisfy techno-economic requirements. Undoubtedly, at the present stage of development of the PV technology, the major impediment to a wider market penetration is the high investment costs of the PV systems (EPIA, 2012).

The solar field design problem may be described by a mathematical formulation. The configuration of PV is based on criteria such as the minimum field area required for producing a given amount of energy, the maximum energy generated from a given field or minimum cost of investment.

Several methods for solving optimization problems have been developed. These methods can be grouped into two main groups (Figure 4-1). The former group follows a linear formulation for the constraints (either of equality or inequality type) and objective functions. In the latter group, the non-linear formulation involves a set of non-linear constraints and/or objective functions.

There are recent methods developed for sizing the parameters for PVGCS based on Artificial intelligence (AI) and Genetic algorithm (GA) techniques (Gong & Kulkarni, 2005; A. Mellit, Kalogirou, Hontoria, & Shaari, 2009; Adel Mellit & Benghanem, 2007; Mondol et al., 2006; Mondol, Yohanis, & Norton, 2009).

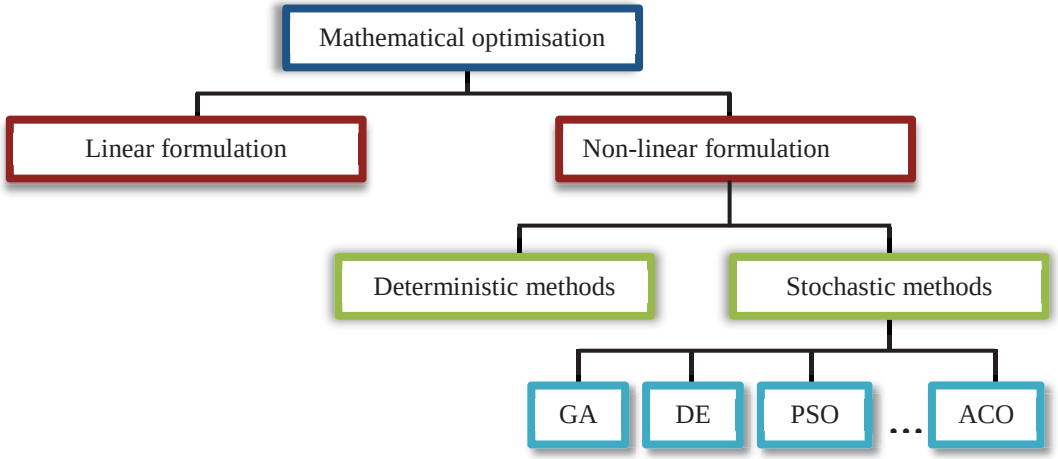

Figure 4-1 Classification of optimization methods (Garcia, Avila, Carpes, & Avila, 2005)

The literature review reveals that evolutionary or stochastic methods e.g. Genetic Algorithms (GAs), Ant Colonies Optimization (ACO), Neural Networks (NN), Particle Swarm Optimization (PSO) and Differential Evolution (DE) (Mondol et al., 2006; Notton et al., 2010) are particularly attractive for non-linear problems. These methods are suitable for "black box" problems where the mathematical properties (continuity, convexity, derivability …) of the problem are difficult to establish. The evaluation of the criteria and constraints of a set of values of independent variables is only required. These methods do evolve in one or more series of initial solutions supported by a set of probabilistic rules often imitating a process of nature.

The solar field design problem can be described by a mathematical formulation as it was explained in Chapter 3 and can be viewed as an optimization problem. Several works deal with the configuration of PVGCS based on criteria to optimize such as the field area required for producing a given amount of energy (minimization case), the energy generated from a given field (maximization case), or cost of investment (minimization case) (García-Valverde, Miguel, Martínez-Béjar, & Urbina, 2009; Kaushika & Rai, 2006; A. Kornelakis & Koutroulis, 2009; Mondol et al., 2009; Senjyu, Hayashi, Yona, Urasaki, & Funabashi, 2007; Weinstock & Appelbaum, 2004b, 2007).

From the mathematical formulation performed to describe the problem of sizing a PVGCS presented in Chapter 3, it is possible to identify that:

- the set of equations does not respect the principle of linearity;
- the relevant meteorological data, especially solar radiation, are estimated from a mathematical model.

From the abovementioned reasons, it can be deduced that the use of solution methods from linear formulation (first group) may be difficult and that an optimization method for the design of PV systems representing a comprehensive set of variables from the solar radiation estimation to PV system configuration is required.

In order to deal with this situation, several studies are reported in the dedicated literature in which PV systems are optimized based on stochastic algorithms (Gómez-Lorente, Triguero, Gil, Estrella, &

Espín Estrella, 2012; Adel Mellit & Benghanem, 2007). Stochastic algorithms have proved to be particularly efficient for solving complex problems with either linear or non-linear functions (Gómez-Lorente et al., 2012).

This study is carried out in the framework of a multi-objective problem where multiple antagonist objectives must be optimized simultaneously: an economic objective (PBT), a technical goal (EPBT) and several environmental objectives. The selected method is based on Multi-objective Genetic Algorithms (MGA). A brief overview of the main features of a GA and how it works is presented below in order to understand the operation of MGA.

4.2.1 *Genetic algorithms*

Genetic algorithms (GA) are inspired by how the organisms are adapted to the harsh realities of life in a hostile world, i.e., by evolution and inheritance. The algorithm imitates in the process the evolution of population by selecting only fit individuals for reproduction.

GAs were proposed by Holland in the 1970s as an algorithmic concept based on a Darwinian-type survival-of-the-fittest strategy with sexual reproduction, where stronger individuals in the population have a higher chance of creating an off-spring. A genetic algorithm is implemented as a computerized search and optimization procedure that uses principles of natural genetics and natural selection. The basic approach is to model the possible solutions to the search problem as binary strings. Various portions of these bit-strings represent parameters in the search problem. If a problem-solving mechanism can be represented in a reasonably compact form, then GA techniques can be applied using procedures to maintain a population of knowledge structure that represent candidate solutions, and then let that population evolve over time through competition (survival of the fittest and controlled variation). A GA will generally include the three fundamental genetic operations of selection, crossover and mutation (see Figure 4-2). These operations are used to modify the chosen solutions and select the most appropriate off-spring to pass on to succeeding generations. GAs consider many points in the search space simultaneously and have been found to provide a rapid convergence to a near optimum solution in many types of problems: in other words, they usually exhibit a reduced chance of converging to local minima.

The first step in any GA is to generate an initial population with a group of individuals randomly created. The individuals in the population are then evaluated and assigned a fitness value. The evaluation function is provided by the operator and gives the individuals a score based on how well they perform at the given task. The fitness value is always defined with respect to other members of the current population. Fitness can be assigned based on an individuals' rank in the population and forms the relation between the evaluation score and the average evaluation of all the individuals in the population. Two individuals are then selected based on their fitness, the higher the fitness, the higher the chance of being selected.

After selection has been carried out, crossover is applied to randomly paired individuals. The recombined individuals create one or more off-spring. This can be viewed as creating the new

population. The randomly mutation of the offspring is then applied. In terms of GAs, mutation means a random change of the value or a gene in the population as shown in Figure 4-2.

After the process of selection, recombination and mutation, the next population can be evaluated. The process continues until a suitable solution has been found or when a given number of generations has been reached. Figure 4-3 represents the flow chart of the process described above.

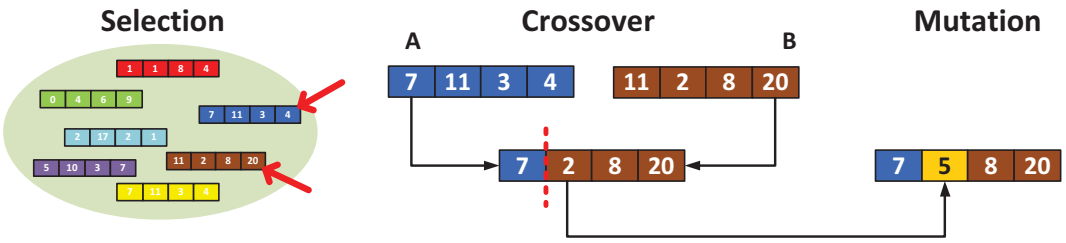

Figure 4-2 Genetic Algorithm operators

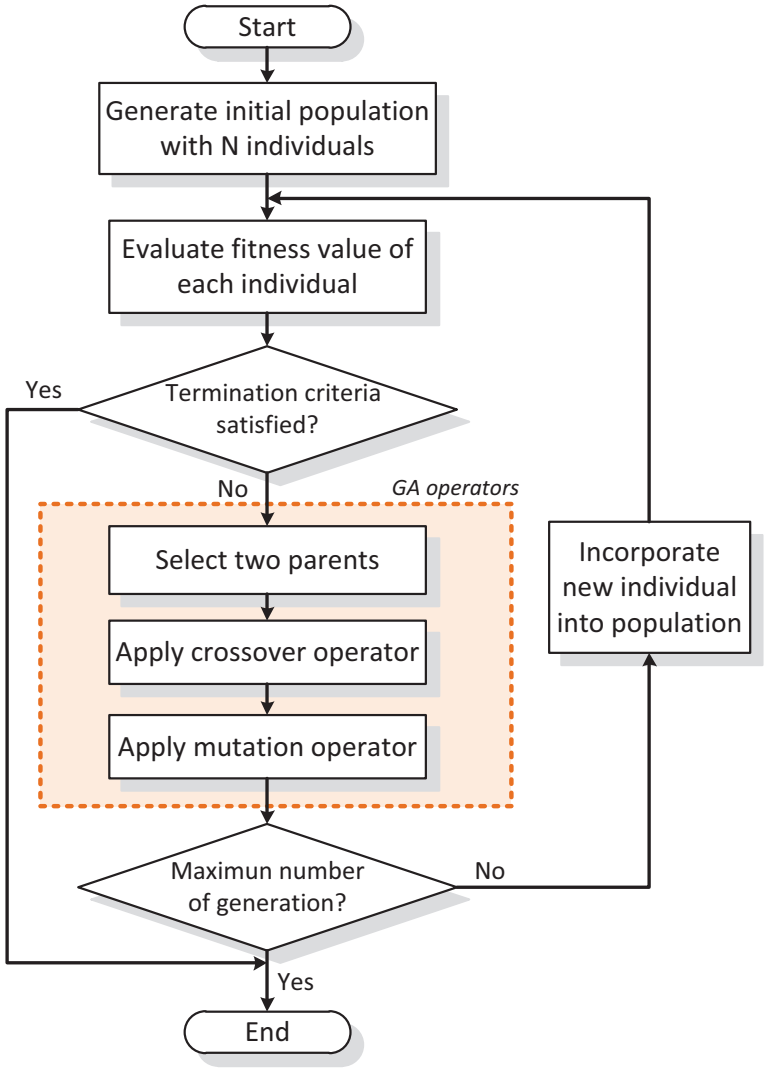

Figure 4-3 Genetic Algorithm flow chart

4.2.2 *Multi-objective Genetic Algorithm*

GAs are well suited to solve multi-objective optimization problems. The ability of GA to simultaneously search different regions of a solution space makes it possible to find a diverse set of solutions for difficult problems.

A multi-objective decision problem tries to find a vector *x** that minimizes a given set of *K* objective functions $z(x^*) = \{z_1(x^*), \dots, z_K(x^*)\}$ given a *n*-dimensional decision variable vector $x = \{x_1, \dots, x_n\}$. A set of constraints restricts the solution space (Konak, Coit, & Smith, 2006).

In many real-life problems, objectives under consideration conflict with each other. Therefore, optimizing with respect to a single objective often results in unacceptable results with respect to the other objectives. It is almost impossible to find the vector *x** that simultaneously optimizes each objective function. A reasonable solution is to investigate a set of solutions which satisfies the objectives at an acceptable level without being dominated by any other solution.

A feasible solution *x* is said to dominate another feasible solution *y*, if and only if, $z_i(x) \leq z_i(y)$ for *i* = 1,…, *K* and $z_j(x) < z_j(y)$ for least one objective function *j*. Multi-objective optimization provides a set of non-dominated solutions in the solution space called Pareto optimal set. While moving from one Pareto solution to another, there is always a certain amount of sacrifice in one objective to achieve a certain amount of gain in the other. For a given Pareto optimal set, the corresponding objective function values in the objective space are called the Pareto front. The ultimate goal of a multi-objective optimization algorithm is to identify solutions in the Pareto optimal set. The size of Pareto optimal set is related with the number of objectives.

The crossover operator of GA allows creating new non-dominated solutions in unexplored parts of the Pareto front. Another important characteristic is that most multi-objective GA do not require the user to prioritize, scale, or weigh objectives, which constitutes a major asset for MOO methods.

Several survey papers (Coello & Becerra, 2009; Coello Coello, 2005) have been published on evolutionary multi-objective optimization. A list of more than 2000 references was published by Coello Coello in his website (Coello Coello, 2010). Generally, MGAs differ according to their fitness assignment procedure, elitism, or diversification approaches. Table 4-1 highlights the advantages and disadvantages of some well-known MGA techniques found by Konak et al. (Konak et al., 2006).

4.2.3 *PVGCS optimization approach*

GA applications are appearing as alternatives to conventional deterministic approaches and in some cases are useful where other techniques have been completely unsuccessful. GAs are also used with intelligent technologies such as neural networks, expert systems, and case-based reasoning. GAs constitute a quite popular method used in engineering field.

It must be emphasized that GAs are not yet widely used for PV system sizing. A summary of applications of GAs in this field is proposed in Table 4-2. It must be highlighted that they concern mainly hybrid technologies involving either stand-alone or grid connected panels.

Table 4-1 List of well-known MGA (based on (Konak et al., 2006))

Algorithm	Fitness assignment	Elitism	Advantages	Disadvantages
MOGA (Fonseca & Fleming, 1993)	Pareto ranking	No	Simple extension of single objective GA	Usually slow convergence Problems related to niche size parameter
NSGA (Srinivas & Deb, 1994)	Ranking based on non-domination sorting	Yes	Fast convergence	Problems related to niche size parameter
NSGA-II (K. Deb, Pratap, Agarwal, & Meyarivan, 2002)	Ranking based on non-domination sorting	Yes	Single parameter (N) Well tested Efficient	Crowding distance works in objective space only
NPGA (Horn, Nafpliotis, & Goldberg, 1994)	No fitness assignment, tournament selection	No	Very simple selection process with tournament selection	Problems related to niche size parameter Extra parameter for tournament selection
SPEA (Zitzler & Thiele, 1999)	Ranking based on the external archive of non-dominated solutions	Yes	Well tested No parameter for clustering	Complex clustering algorithm
VEGA (Schaffer, 1985)	Each subpopulation is evaluated with respect to a different objective	No	Straightforward implementation	Tend to converge at the extreme of each objective

Table 4-2 Summary of applications of GAs for sizing PV systems

Authors	Year	Subject
(Dufo-López, Bernal-Agustín, & Contreras, 2007)	2007	Optimization of control strategies for stand-alone renewable energy systems with hydrogen storage
(Senjyu et al., 2007)	2007	Optimal configuration of power generating systems in isolated island with renewable energy
(Koutroulis, Kolokotsa, Potirakis, & Kalaitzakis, 2006)	2006	Methodology for optimal sizing of stand-alone photovoltaic/wind-generator systems
(El-Hefnawi, 1998)	1998	Photovoltaic diesel-generator hybrid power system sizing
(Yokoyama, Yuasa, & Ito, 1994)	1992	Multiobjective Optimal Unit Sizing of Hybrid Power Generation Systems Utilizing Photovoltaic and Wind Energy
(Seeling-hochmuth, 1998)	1998	Optimisation of hybrid energy systems sizing and operation control
(Xu, Kang, & Cao, 2006)	2006	Graph-Based Ant System for Optimal Sizing of stand-alone Hybrid Wind/PV Power Systems
(Xu, Kang, Chang, & Cao, 2005)	2005	Optimal sizing of stand-alone hybrid wind/PV power systems using genetic algorithms

For instance, proper design of standalone renewable energy power systems (Xu et al., 2005) is a challenging task, as the coordination among renewable energy resources, generators, energy storages and loads is very complicated. The types and sizes of wind turbine generators (WTGs), the tilt angles and sizes of photovoltaic (PV) panels and the capacity of batteries must be optimized when sizing a standalone hybrid wind/PV power system, which may be defined as a mixed multiple-criteria integer programming problem. A GA with elitist strategy is investigated for optimally sizing a standalone hybrid wind/PV power system. The objective is selected as minimizing the total capital cost, subject to the constraint of the loss of power supply probability. The literature review reveals that PV planners are not quite familiar with GA optimization techniques for PV design.

As explained in the previous chapter, several programs and mathematical models have been developed to calculate solar irradiance received at a given point of the planet and size a PVGCS separately. Most of the studies reviewed (Gong & Kulkarni, 2005; Aris Kornelakis & Marinakis, 2010; Mondol et al., 2006; Notton et al., 2010; Weinstock & Appelbaum, 2007, 2009) consider exclusively PVGCS optimization with only one criterion. Other authors (Dones & Frischknecht, 1998; Ito et al., 2008; Kannan et al., 2006; Pacca et al., 2006) address only the issue of the environmental impact assessment of the elements of a PV system with emphasis on PV module technology. Our main purpose consists in generating alternatives of optimal PVGCS configurations taking into account technical and economic aspects as well as their environmental impact.

The main problem found in the programs described in Table 3-1 is the lack of an integrated approach that allows the optimization of the sizing of a PVGCS. The coupling of all elements via an external program to optimize the model using a genetic algorithm is difficult due to the closed structure used.

To overcome the problem of interoperability, the design of a simulator for received solar radiation coupled with a sizing module constitutes the most suitable option. The simulator must be designed in an open manner so that it can be interfaced easily with an outer optimization loop.

The MULTIGEN environment previously developed in our research group (Gomez et al., 2010) was selected as the genetic algorithm platform. A variant of NSGA-II developed for mixed problems and implemented in the MULTIGEN environment is selected. The stopping criterion proposed in MULTIGEN (in addition to the maximum number of generations) consists in comparing the Pareto fronts associated with non-dominated solutions for populations n and $n + p$, where the period $p \in [10, 20, 30, 40, 50]$ for example. If the union of the two fronts provides a single non dominated front, the procedure stops; else the iterations continue.

It can treat either mono- and multi-objective problems. The potential of GAs to solve multi-objective problems serves as an incentive to use such an optimization strategy. This constitutes a natural way to extend this work. As it was initially developed in Visual Basic for Applications (VBA) in Excel, the same language is used for simulation purpose. The main advantages of VBA include the automation of repetitive tasks and calculations, the easy creation of macros in a friendly programming language.

NSGA-II was selected, as it is explained in (Gomez, 2008), because of the way to manage the diversity of populations. Algorithms based on the concept of niche as NPGA and MOGA do not ensure a proper convergence of the Pareto front. Algorithms such as SPEA or NSGA-II are based on the principle that single non-dominated individuals are better than individuals in dense areas. In SPEA, the probability of selection is based on the isolation of the individual, which implies a quantification of that probability, and therefore the implementation of more complex algorithms. NSGA-II opts for a simple elimination of individuals at dense areas after a sorting according to their density. In addition, NSGA-II needs low computational requirements.

The step-by-step procedure is illustrated in Figure 4-4 to Figure 4-6. Initially, a random parent population P_0 of size N is created. The population is sorted based on the non-domination principle.

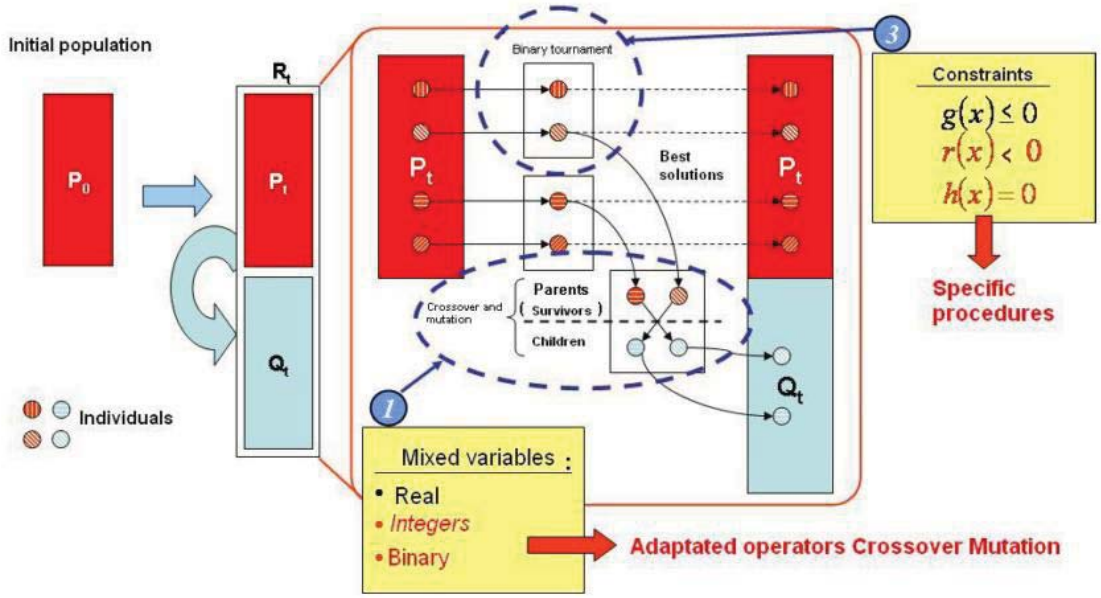

Figure 4-4 Operating principle of NSGA-II (Part 1) (Gomez, 2008)

Each individual is assigned a fitness (or rank) equal to its non-domination level (1 is the best level, 2 is the next-best level, and so on). Thus, the maximization of fitness can be performed. At first, the usual binary tournament selection, recombination and mutation operators are used to create an off-spring population Q_t of size N (Figure 4-4). Since elitism is introduced by comparing the current population with the previously best found non-dominated solutions, the procedure is different after the initial generation.

First, a combined population $R_t = P_t \cup Q_t$ is formed (Figure 4-5). The population R_t is of size $2N$. Then, the population is sorted according to non-domination. If the size of F_1 (set of individuals of rank 1) is lower then N, all the members of the set F_1 for the new population $P_t +1$ are definitely chosen. The remaining members of the population $P_t +1$ are chosen from subsequent non dominated fronts in the order of their ranking. Thus, solutions from the set F_2 are chosen next, followed by solutions from the set F_3, and so on. This procedure continues until no more set can be accommodated. Let us consider that the set F_1 is the last non-dominated set beyond which no other set can be accommodated. In general, the number of solutions in all sets from F_1 to F_l is higher than the population size.

In order to choose exactly the population members, the solutions of the last front using the crowded-comparison operator are sorted in descending order and the best solutions needed to fill all population slots are selected. The new population $P_t +1$ of size N is now used for selection, crossover and mutation to create a new population $Q_t +1$ of size N. It must be highlighted that a binary tournament selection operator is used but the selection criterion is now based on the crowded-comparison operator. Since this operator requires both the rank and crowded distance of each solution in the population, these quantities are calculated while forming the population $P_t +1$, as shown in Figure 4-6. The MULTIGEN library and NSGA-II are described in detail in (Gomez, 2008).

4.3 Reduction of environmental objectives by Principal Component Analysis (PCA) method.

LCA requires a large amount of data in its different phases and when the comparative analysis of products or processes is performed, the amount of data obtained as a result of the environmental impact assessment may be large and hard to interpret thus complicating the subsequent decision-making processes. One of the limitations of MGA when it is applied to environmental problems is that its computational burden grows rapidly in size with the number of environmental objectives.

The dimensionality of a data set can often be reduced easily without disturbing the main features of the whole data set by using multivariate reduction techniques such as Principal Component Analysis (PCA).

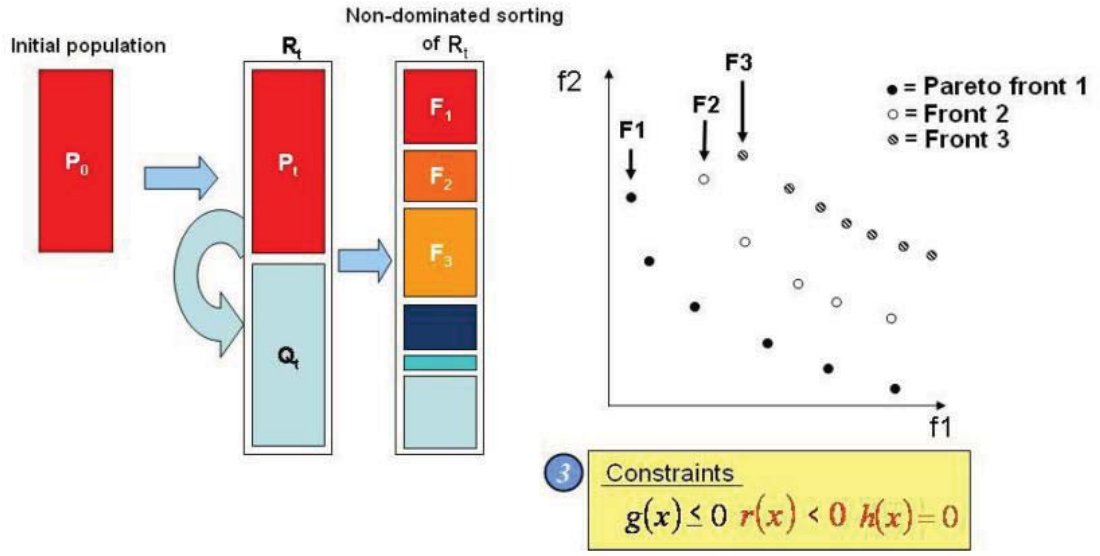

Figure 4-5 Operating principle of NSGA-II (Part 2) (Gomez, 2008)

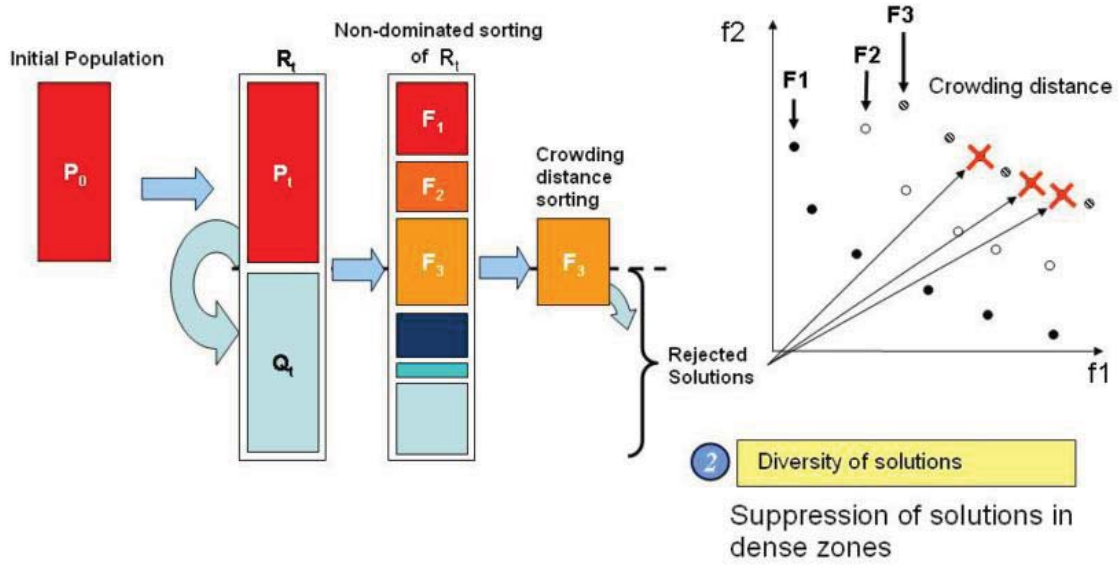

Figure 4-6 Operating principle of NSGA-II (Part 3) (Gomez, 2008)

PCA is a statistical tool for multivariate analysis. Its objective is to reduce the dimensionality of a data set with a large number of interrelated variables, retaining as much variation of the data set, as possible. This reduction in dimension is achieved by transformation of the original variables to a new smallest set of variables, called *principal components*. Each principal component is a linear combination of a subset of the original variables that have some similar characteristics. These components are uncorrelated and ordered: all principal components are ranked according to their ability in explaining the variance in the original data set. It is indeed useful to reduce the number of variables, thus avoiding extra variables, which complicate the data but do not give any extra information. The computational time will be reduced and the results analysis will be then more consistent.

PCA is computed using either the correlation matrix or the covariance matrix. The use of the correlation matrix is advantageous when measurements are in different units. The computation of principal components is usually posed as an eigenvalue-eigenvector problem. This eigenvalue used to indicate the proportion of the total variance explained from the original data by the corresponding principal component.

This technique has been applied successfully in several researches (Guillén-Gosálbez, 2011; Gutiérrez, Lozano, Moreira, & Feijoo, 2010; Sabio, Kostin, Guillén-Gosálbez, & Jiménez, 2012) for the reduction of environmental impact categories. The methodology proposed by Sabio et al. for reducing environmental impact categories in the configuration of the supply chain of hydrogen distribution in Spain was applied to the case presented in this work. This methodology follows the guidelines edited by Deb and Saxena (Kalyanmoy Deb & Saxena, 2005).

The purpose is to apply PCA once the Pareto optimal set of the optimization for sizing the PVGCS considering both technical and economic criteria as well as environmental criterion is found in order to reduce the environmental categories.

The steps to apply PCA method are:

Step 1: **Get the data**. First, it is necessary to generate a Pareto optimal set of the original problem by using the selected multi-objective algorithm (NSGA-II in this work).

Step 2: **Subtract the mean.** The data set is standardized to make its centroid equal to zero. This is done by subtracting the mean of each column from each data point in the matrix for PCA to work properly.

Step 3: Calculate the correlation matrix. For reducing the environmental categories, the correlation matrix is the best option because of the different units which each category uses.

Step 4: Calculate the eigenvectors and eigenvalues of the correlation matrix. The eigenvector corresponding to the largest eigenvalue is referred as the first principal component; one corresponding to the second largest eigenvalue is called the second principal component and so on.

Step 5: Choosing components. Applying the Kaiser-Guttman rule (Sabio et al., 2012), the eigenvalues that are less or equal to 1 are excluded from the analysis. The cumulative explained variance (G_j) of remaining eigenvalues in descendant order is determined by the equation:

$$G_j = \sum_{e=1}^{j} \frac{\lambda_e}{\sum_{e=1}^{|\lambda|} \lambda_e} \tag{4.1}$$

where λ_e represents e^{th} eigenvalue remained. A second reduction is made from G_j values. A threshold cut value (CUT) must be established in order to keep for the PCA the eigenvalues with cumulative explained variance below this value ($G_j \leq CUT$). Deb and Saxena (Kalyanmoy Deb & Saxena, 2005) suggest a CUT value of 0.95 (95%).

Step 6: Selecting environmental impact categories. This is done by analyzing the eigenvectors to identify conflicts among the categories. The heuristic procedure suggested by Deb and Saxena is followed to identify conflicts and redundancies among all the environmental categories. Technical details about this strategy are summarized in Figure 4-7. In this figure, x^+ denotes the most positive element of principal component and x^- represent the most negative element of principal component.

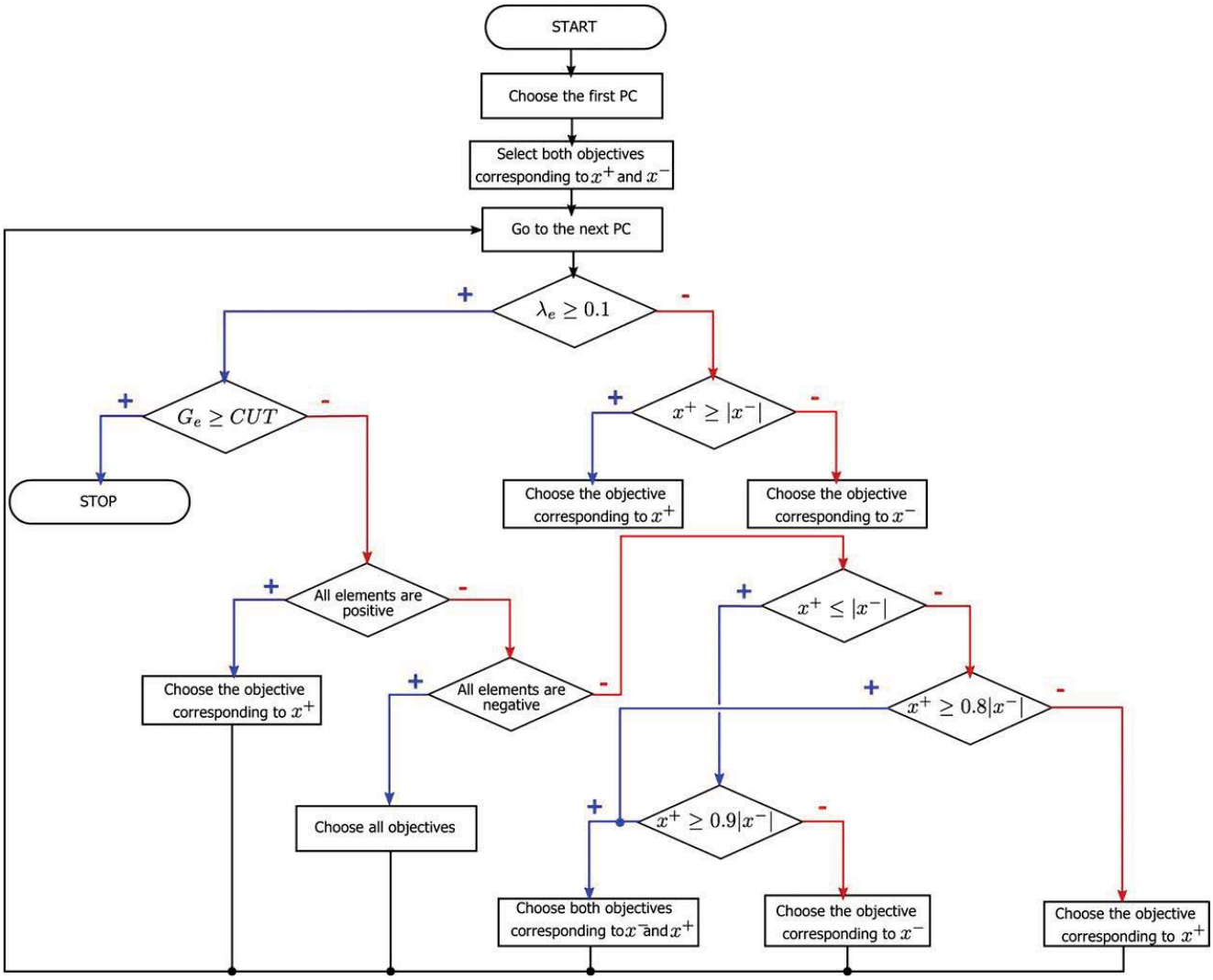

Figure 4-7 Scheme of the PCA procedure for selecting environmental impact categories (Sabio et al., 2012)

The main advantage of applying PCA for environmental objectives is the elimination of redundant environmental categories, which reduces the objectives to consider in the multi-objective optimization, decreases the resolution time of the AG and makes easier the interpretation of results.

4.3.1 *PCA for environmental categories*

An example will illustrate the usefulness of PCA method for the reduction of environmental categories. The case reported by Sabio et al. (Sabio et al., 2012) will be used to explain the method.

The goal of the problem addressed by Sabio et al. is to determine the optimal configuration of a three-echelon hydrogen supply chain for vehicle use (production-storage-market) in terms of cost and damage to the environment. A multi-objective mixed-integer linear program (MILP) formulation is employed to solve the problem. The environmental performance of the hydrogen supply chain is assessed by following 8 environmental LCA indicators: damage to human health caused by carcinogenic substances (CS), damage to human health caused by respiratory effects (RE), damage to human health caused by climate change (CC), damage to human health caused by ozone layer depletion (OLD), damage to ecosystem quality caused by ecotoxic substances (ES), damage to ecosystem quality caused by acidification and eutrophication (AE), damage to minerals (DM), and damage to fossil fuels (DFF).

The methodology described above was applied for reducing the environmental categories. After obtaining the Pareto set of solutions for the configuration of the hydrogen supply chain and standardizing the results (Steps 1 and 2), the correlation matrix is generated (See Table 4-3). It can be seen that CS, OLD and ES are highly correlated with DM, whereas AE is highly correlated with CC.

From the correlation matrix given above, the eigenvectors and eigenvalues matrix are calculated. The eigenvectors and eigenvalues of the correlation matrix are presented in Table 4-4, where the principal components are arranged in a descending order.

A graphical screen test was performed to decide the number of principal component to be kept for further analysis applying the Kaiser-Guttman rule. As observed in Figure 4-8, the fourth and subsequent components do not satisfy the Kaiser-Guttman rule. The three remain principal components represent almost the 100% of cumulative variability.

Table 4-3 Correlation matrix for Sabio et al. case

	CS	**RE**	**CC**	**OLD**	**ES**	**AE**	**DM**	**DFF**
CS	1	0.4400	0.4007	0.9995	1.0000	0.6729	0.9988	-0.0375
RE		1	0.0735	0.4517	0.4435	0.3886	0.4792	-0.8966
CC			1	0.4235	0.4027	0.9237	0.377	0.2743
OLD				1	0.9996	0.6938	0.9984	-0.0453
ES					1	0.6753	0.9989	-0.0408
AE						1	0.6621	0.0165
DM							1	-0.0847
DFF								1

Table 4-4 PCA results for Sabio et al. case. Eigenvalues and eigenvectors

	PC_1	PC_2	PC_3	PC_4	PC_5	PC_6	PC_7	PC_8
Eigenvalue (λ_e)	5.073	1.889	1.039	0.000	0.000	0.000	0.000	0.000
Variability (%)	63.407	23.609	12.983	0.002	0.000	0.000	0.000	0.000
Cumulative % (G_j)	63.407	87.016	99.998	100.000	100.000	100.000	100.000	100.000
CS	-0.4290	0.0188	0.2517	0.3581	-0.3265	0.5347	-0.0827	-0.4739
RE	-0.2436	**-0.5752**	-0.2668	0.3797	0.4647	-0.1424	-0.3915	-0.0696
CC	-0.2529	0.3791	**-0.6238**	0.1948	-0.2479	-0.4454	0.1347	-0.2955
OLD	**-0.4322**	0.0189	0.2230	-0.6102	-0.1216	-0.3151	-0.5086	-0.1337
ES	-0.4295	0.0171	0.2478	0.3595	-0.2663	-0.2309	0.0645	0.7044
AE	-0.3659	0.1852	-0.4966	-0.2990	0.1950	0.5695	-0.0363	0.3634
DM	-0.4293	-0.0165	0.2498	-0.1412	0.4973	-0.1322	0.6567	-0.1925
DFF	**0.0571**	**0.6999**	0.2370	0.2805	0.4949	-0.0298	-0.3553	0.0012

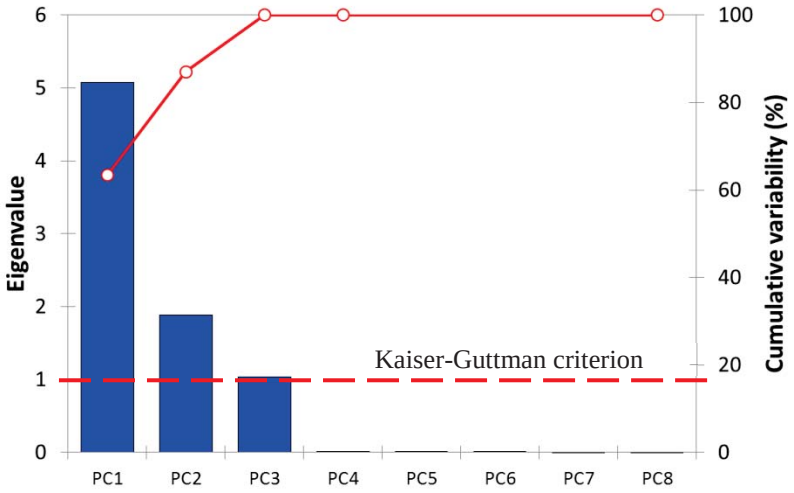

Figure 4-8 Screen plot for Sabio et al. case

The next steps consists in select the environmental impact categories. Based on the heuristic procedure of Figure 4-7 and with a CUT of 100% selected by Sabio et al., the environmental impact categories retained are highlighted in bold font in Table 4-4. Four categories were eliminated (CS, ES, AE, DM). Figure 4-9 shows the bi-dimensional and tri-dimensional plots representing the loads of the environmental objectives projected onto the sub-spaces of the first three principal components. The redundant categories are grouped based on the correlation matrix. Only RE, CC, OLD and DFF must be used in further analysis.

4.4 Multiple-criteria decision making (MCDM)

MCDM approaches are major parts of decision theory and analysis. MCDM are analytic methods to evaluate the advantages and disadvantages of multicriteria alternatives.

The objective is to help decision-makers to learn about the problems they face, and to identify a preferred course of action for a given problem. Huang et al. (Huang, Poh, & B.W., 1995) mentioned that decision analysis (DA) was first applied to study problems in oil and gas exploration in the 1960s

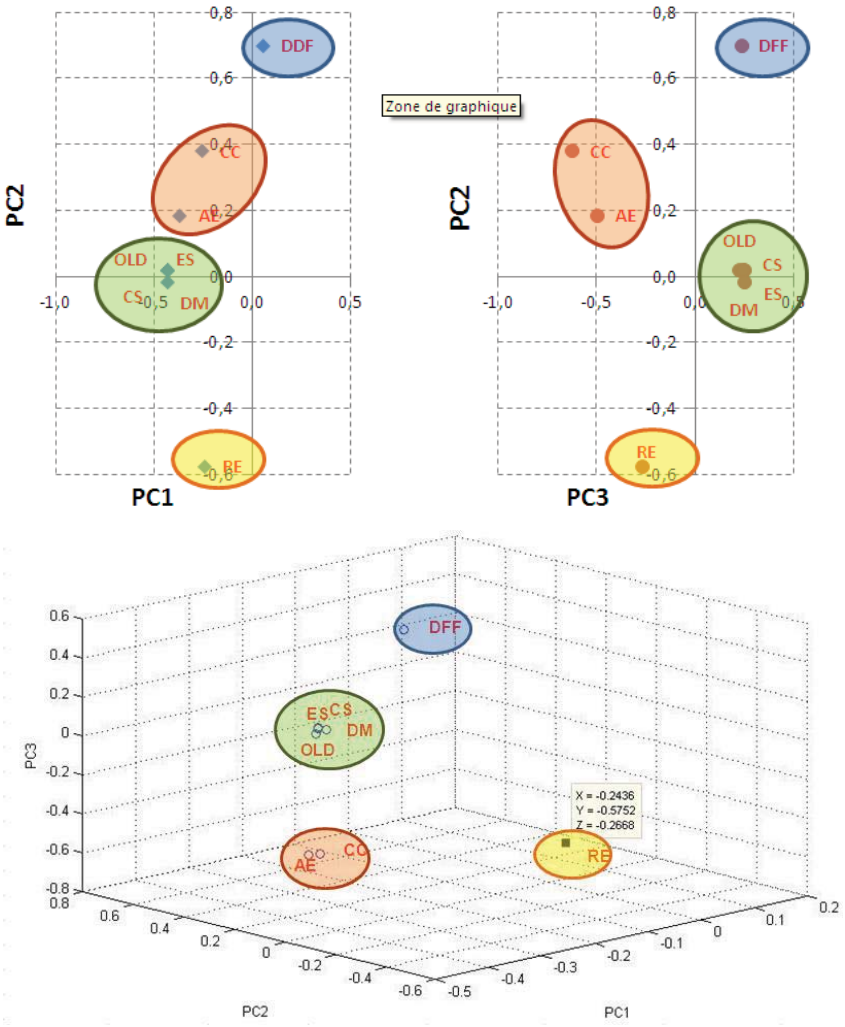

Figure 4-9 PCA results in the bi- and tri-dimensional spaces for Sabio et al. case

and its application was subsequently extended from industry to the public sector. Till now, MCDM methods have been widely used in many research fields. Different approaches have been proposed by many researchers, including single objective decision-making (SODM) methods, MCDM methods, and decision support systems (DSS). Literature shows that among MCDM methods, DA strategies are the most commonly used (Zhou, Ang, & Poh, 2006).

One of the most popular MCDM methods is TOPSIS for identifying solutions from a finite set of alternatives based upon simultaneous minimization of distance from an ideal point and maximization of distance from the nadir point. The acronym TOPSIS stands for Technique for Order Preference by Similarity to the Ideal Solution. The first developments of TOPSIS were carried out by Hwang and Yoon (Hwang & Yoon, 1981) and later by Lai et al. (Lai, Lui, & Hwang, 1994). Among the MCDM methods, TOPSIS is attractive since it requires limited subjective inputs from decision makers. The only subjective inputs needed are weights assigned to objectives. This may explain why TOPSIS (Lifeng Ren, Zhang, Wang, & Sun, 2007) is very popular in chemical engineering applications.

MCDM methods, especially TOPSIS, have often been used in multi-criteria optimization problem. Boix (Boix, 2011) used the TOPSIS method for selecting the best water network configuration

involving three criteria: amount of fresh and treated water entering the network and the number of connections.

Ouattara (Ouattara, 2011) shows how the results obtained by a MGA (NSGA-II) can be connected to a MCDM method (TOPSIS) to solve an ecodesign process problem. The objective is to take into account simultaneously the ecological and economic considerations at the preliminary design phase of chemical processes.

A variant of TOPSIS (M-TOPSIS) has been adopted in this work, integrating the guidelines proposed in (Ouattara, 2011)

4.4.1 *M-TOPSIS method*

M-TOPSIS method (Lifeng Ren et al., 2007) is an evaluation method that is often used to solve MCDM problems (Pinter & Pšunder, 2013). It is based on the concept of original TOPSIS (Hwang & Yoon, 1981). The basic idea of TOPSIS method is to choose a solution that is closest to the ideal solution (better on all criteria) and away the worst (which degrades all criteria) (Markovic, 2010; Opricovic & Tzeng, 2004; L. Ren, Zhang, Wang, & Sun, 2007) The modification introduced by Ren et al. in M-TOPSIS method could avoid rank reversals and solve the problem on evaluation failure when alternatives are symmetrical that often occurs in original TOPSIS.

A specific module with M-TOPSIS has been implemented as a tool for multi-criteria decision, thus facilitating its use after obtaining Pareto fronts. Particular attention was paid to the simultaneous treatment of problems involving minimization and maximization criteria. The stages of the M-TOPSIS procedure are listed below. The normalisation of the matrix is performed according to the original work of Hwang and Yoon (Hwang & Yoon, 1981).

Step 1: Build the decision matrix. Establish a matrix which shows *m* alternatives evaluated by *n* criteria (see Figure 4-10).

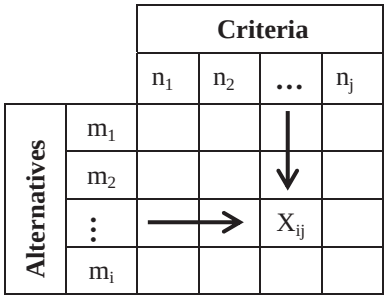

Figure 4-10 Decision matrix

All the original criteria receive tendency treatment. Usually the cost criteria are transformed into benefit criteria by the reciprocal ratio method as it shown in Equation (4.2). (García-cascales & Lamata, 2012; L. Ren et al., 2007)

$$X'_{ij} = \frac{1}{X_{ij}} \tag{4.2}$$

Step 2: Calculate the normalized decision matrix *A*. Since different criteria have different dimensions, the values in the decision matrix *X* are first transformed into normalized, non-dimensional values in order to convert the original attribute values within the interval [0, 1] under the following Equation:

$$A = [a_{ij}]_{m\,x\,n}, a_{ij} = \frac{X'_{ij}}{\sqrt{\sum_{i=1}^{n}(X'_{ij})^2}} \tag{4.3}$$

where a_{ij} stands for the normalized value; $i = 1, 2, \ldots, m$; $j = 1, 2, \ldots, n$

Step 3: Coefficient vector of importance of the criteria. This step allows decision makers to assign weights of importance to a criterion relative to others. The weighted normalized matrix *V* is calculated by multiplying each value within the individual criterion in the normalized matrix *A* by the weight of this criterion:

$$v_{ij} = w_j \cdot a_{ij} \tag{4.4}$$

where w_j stands for the weight of the individual criterion *j*; $i = 1, 2, \ldots, m$; $j = 1, 2, \ldots, n$.

Step 4: Determine the positive ideal and negative ideal solution from the matrix A. The ideal solution (A^+) is the group of weighted normalized criteria values, which indicates the ideal criteria values (maximum value for benefit criteria and minimum value for cost criteria), and the non-ideal solution (A^-) is a group of weighted normalized criteria values, which indicates the negative ideal criteria values (minimum value for benefit criteria and maximum value for cost criteria):

$$A^+ = \{v_1^+, v_2^+, \ldots, v_n^+\}, v_j^+ = \{max_i(v_{ij}), j \in J^+; min_i(v_{ij}), j \in J^-\} \tag{4.5}$$

$$A^- = \{v_1^-, v_2^-, \ldots, v_n^-\}, v_j^- = \{min_i(v_{ij}), j \in J^+; max_i(v_{ij}), j \in J^-\} \tag{4.6}$$

Where $J^+ = \{i = 1, 2, \ldots, m\}$ when *i* is associated with benefit criteria ; $J^- = \{i = 1, 2, \ldots, m\}$ when *i* is associated with cost criteria. $j = 1, 2, \ldots, n$.

Step 5: Calculate Euclidean distance. Calculate the separation measures, using the *n*-dimensional Euclidean distance. (García-cascales & Lamata, 2012; Pinter & Pšunder, 2013)

$$D_i^+ = \sqrt{\sum_{j=1}^{n}(v_j^+ - v_{ij})^2} \tag{4.7}$$

$$D_i^- = \sqrt{\sum_{j=1}^{n}(v_j^- - v_{ij})^2} \tag{4.8}$$

For $i = 1, 2, \ldots, m$.

Step 6: Calculate the relative closeness to the ideal solution. In M-TOPSIS, unlike TOPSIS, the positive ideal solution (D_i^+) and negative ideal solution (D_i^-) in finite planes are found at first; and then, the D^+ D^--plane is constructed and set the *optimized ideal reference point*. Finally, the relative distance from each evaluated alternative to the ideal reference point is calculated with (Lifeng Ren et al., 2007). Set the point A in Figure 4-11 [min (D_i^+), max (D_i^-)] as the *optimized ideal reference point* because the aim is to have the lowest distance

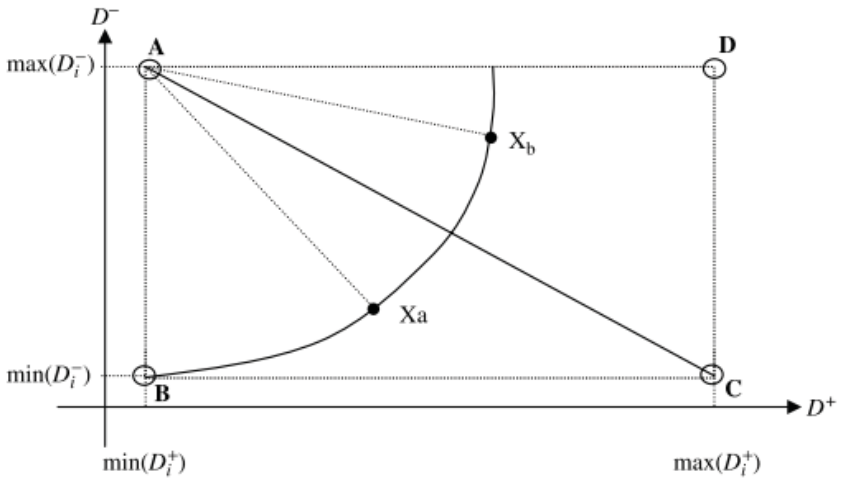

Figure 4-11 Example D^+ D^- – plane of M-TOPSIS method (Lifeng Ren et al., 2007)

between the ideal criteria set values (A^+) and get away as much as possible of non-ideal criteria set values (A^-). The ratio value of R_i is calculated as follows:

$$R_i = \sqrt{\left(D_i^+ - min\left(D_i^+\right)\right)^2 + \left(D_i^- - max\left(D_i^-\right)\right)^2} \tag{4.9}$$

Where $i = 1, 2, \ldots, m$.

Step 7: Rank order. Rank alternatives in increasing order according to the ratio value of R_i. The best alternative is the one that having the M-TOPSIS coefficient R_i nearest to 0.

4.4.2 *Example of application of M-TOPSIS method*

The M-TOPSIS procedure described above is applied here on 15 points from a Pareto front obtained after a bi-objective optimization, each point representing a potential solution. The criteria involve the maximization Q_{out} (kWh) and the minimization of EPBT (year). The different stages of the M-TOPSIS algorithm for this example are applied as follows:

From original data, the decision matrix is built (see Table 4-5). Because the *EPBT* criterion represents a cost criterion (minimization), it is transformed into benefit criterion (maximization) by Equation (4.2). The transformed values are displayed in Table 4-6.

Table 4-5 Decision data matrix

		Criteria	
		Q_{out} *max*	EPBT min
Alternatives	1	2,286,757.98	1.753
	2	1,072,808.71	1.699
	3	2,005,066.69	1.730
	4	1,710,340.98	1.711
	5	1,933,294.35	1.727
	6	2,183,467.41	1.747
	7	2,253,731.29	1.749
	8	716,068.22	1.692
Alternatives	9	1,424,028.60	1.701
	10	2,088,618.68	1.735
	11	716,057.32	1.692
	12	2,040,111.49	1.731
	13	358,578.79	1.691
	14	2,076,489.16	1.732
	15	1,760,111.18	1.718

Table 4-6 Transformed values matrix

		Criteria	
		Q_{out} *max*	EPBT max
Alternatives	1	2,286,757.98	0.5705
	2	1,072,808.71	0.5886
	3	2,005,066.69	0.5780
	4	1,710,340.98	0.5845
	5	1,933,294.35	0.5790
	6	2,183,467.41	0.5724
	7	2,253,731.29	0.5718
	8	716,068.22	0.5910
	9	1,710,340.98	0.5879
	10	2,088,618.68	0.5764
	11	716,057.32	0.5910
	12	2,040,111.49	0.5777
	13	358,578.79	0.5914
	14	2,076,489.16	0.5774
	15	1,760,111.18	0.5821

Table 4-7 Normalized decision matrix

		Criteria	
		Q_{out} *max*	EPBT max
Alternatives	1	0.3338	0.2534
	2	0.1566	0.2614
	3	0.2927	0.2567
	4	0.2497	0.2596
	5	0.2822	0.2572
	6	0.3188	0.2542
	7	0.3290	0.2539
	8	0.1045	0.2625
	9	0.2497	0.2611
	10	0.3049	0.2560
	11	0.1045	0.2625
	12	0.2978	0.2566
	13	0.0523	0.2627
	14	0.3031	0.2564
	15	0.2569	0.2585

Table 4-8 Weighted normalized matrix

		Criteria	
		Q_{out} *max*	EPBT max
Alternatives	1	0.3338	0.2534
	2	0.1566	0.2614
	3	0.2927	0.2567
	4	0.2497	0.2596
	5	0.2822	0.2572
	6	0.3188	0.2542
	7	0.3290	0.2539
	8	0.1045	0.2625
	9	0.2497	0.2611
	10	0.3049	0.2560
	11	0.1045	0.2625
	12	0.2978	0.2566
	13	0.0523	0.2627
	14	0.3031	0.2564
	15	0.2569	0.2585

The normalized decision matrix *A* is obtained using Equation (4.3) (see Table 4-7). None of the criteria is preferred over the other, so the coefficient vector of importance W is equal to [1, 1]. The normalized weighted matrix is then represented in Table 4-8. The positive ideal (respectively negative ideal, i.e. non-ideal) solution is determined from the matrix *A* as well as the Euclidean distance matrix (Equations (4.5) to (4.8)). The obtained results are shown in Table 4-9 and Table 4-10. Considering

the point A [min (D_i^+), max (D_i^-)] as the *optimized ideal reference point*, the Figure 4-12 displays the position of all the alternatives in D^+ D^-–plane.

M-TOPSIS coefficient R_i is calculated for each alternative by Equation (4.9) and the ranking is presented in Table 4-11. The Pareto front *EPBT*-Q_{out} in Figure 4-13 indicates the position of the three best alternatives after applying the M-TOPSIS method. The best alternative selected by M-TOPSIS method is alternative 1.

Table 4-9 A^+ and A^- values

	Criteria	
	Q_{out}	EPBT
A^+	0.3338	0.2627
A^-	0.0523	0.2534

Table 4-10 Euclidean distance matrix (D_i^+ and D_i^-)

Alternatives	D_i^+	D_i^-
1	0.0093	0.2815
2	0.1772	0.1046
3	0.0415	0.2404
4	0.0842	0.1974
5	0.0519	0.2299
6	0.0173	0.2664
7	0.0100	0.2767
8	0.2293	0.0530

Alternatives	D_i^+	D_i^-
9	0.0842	0.1975
10	0.0297	0.2526
11	0.2293	0.0530
12	0.0365	0.2455
13	0.2815	0.0093
14	0.0313	0.2508
15	0.0770	0.2047

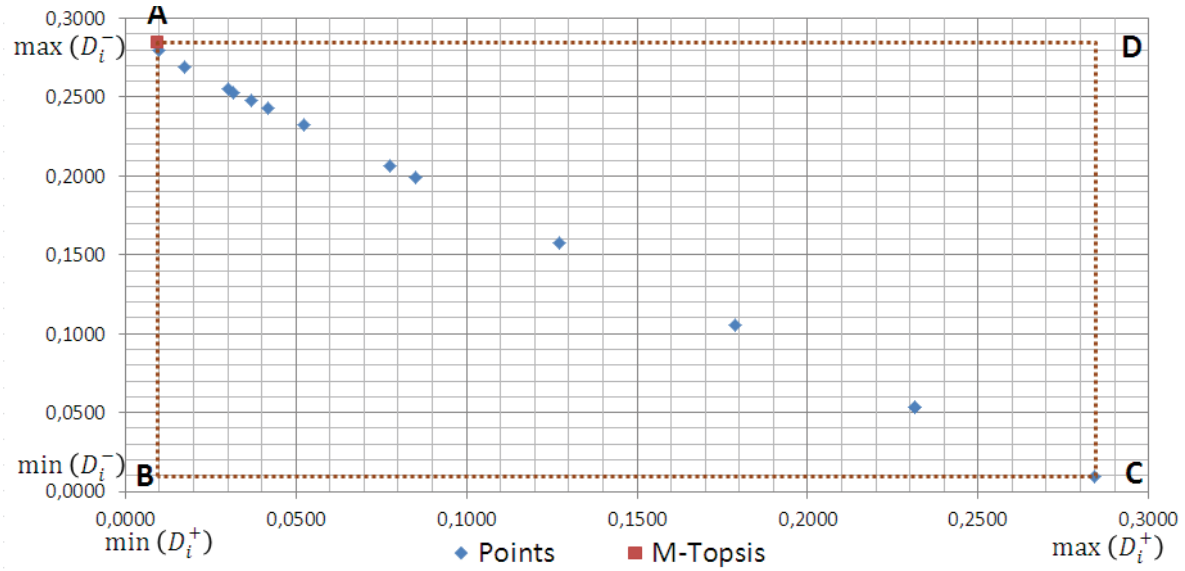

Figure 4-12 D^+ D^-plane for M-TOPSIS example

Table 4-11 Rank alternatives by M-TOPSIS coefficient R_i

Alternatives	R_i	Rank
1	***0.0000***	***1***
2	0.2439	12
3	0.0522	7
4	0.1126	11
5	0.0669	8
6	*0.0171*	*3*
7	*0.0049*	*2*
8	0.3172	13
9	0.1125	10
10	0.0354	4
11	0.3172	14
12	0.0451	6
13	0.3849	15
14	0.0378	5
15	0.1024	9

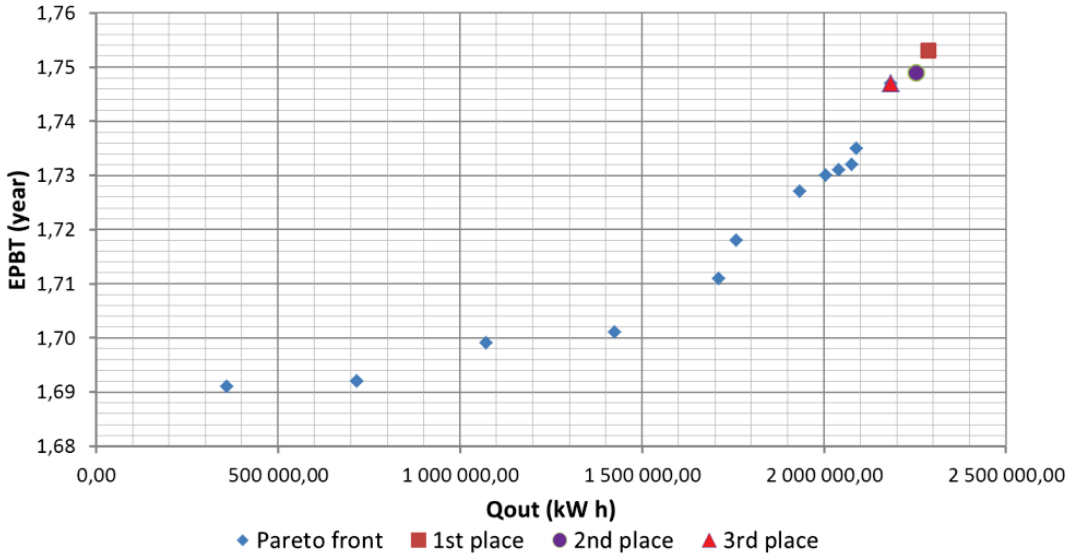

Figure 4-13 Pareto front EPBT-Q_{out} with top 3 ranked alternatives

As it can be seen in Figure 4-13, the best alternatives are located at the upper corner of the curve representing the Pareto front. If these three alternatives are compared with some of the alternatives that are in the knee of the curve, e.g. alternative 4 as shown in Figure 4-14, although EPBT is reduced, the energy produced is also strongly reduced. EPBT reduction is approximately 0.05 year while annual energy produced suffers a reduction of about 30%. The result provided by M-TOPSIS indicates that the best compromise that can be found at equal weight to both objectives in this example is to produce the maximum amount of energy because the difference between the growth in EPBT value is minimal as compared to the gain of Q_{out}.

4.5 Conclusion

In this chapter, three methods to be applied for sizing PVGCS were presented. The number of objectives and the characteristics of the model developed in Chapter 3 make attractive the use of a GA to obtain the best alternatives embodied through a Pareto front. A variant of NSGA-II, embedded in MULTIGEN library, is selected. It must be emphasized that most of the works reported for PVGCS sizing through AG only consider economic or technical aspects. The main contribution of this work will be to integrate the environmental aspect from earlier design stage and not at end-of-pipe stage as

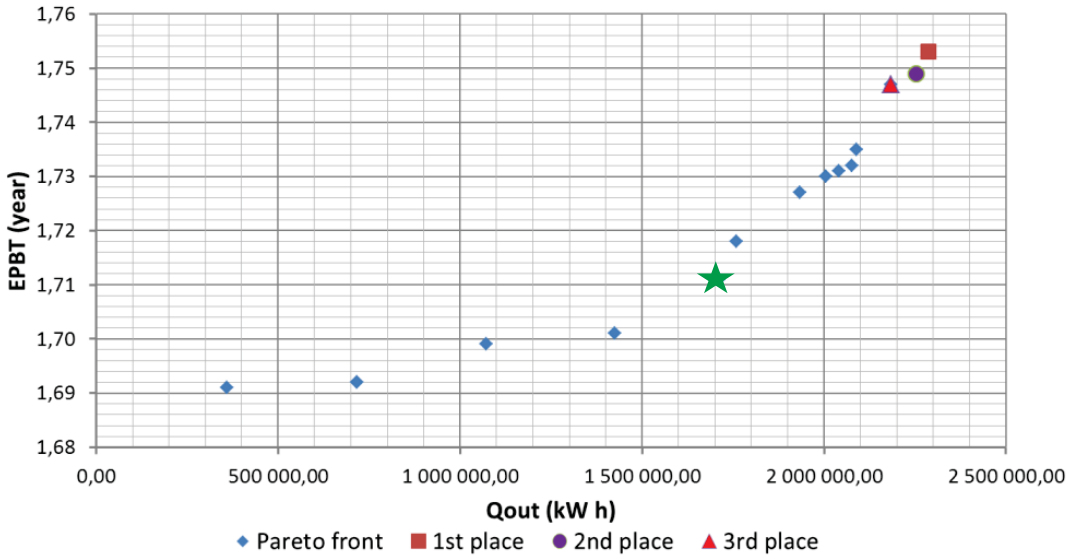

Figure 4-14 Pareto front EPBT-Q_{out} with top 3 ranked alternatives and alternative 4

currently carried out.

The use of PCA is particularly attractive to reduce the number of environmental categories that are generally involved in LCA impact methods as described in Chapter 2. The reduction of intermediate impact categories to be evaluated will save AG computational time and provide a better interpretation of the results. Finally, a post-optimization analysis by use of a MCDM method based on m-TOPSIS is implemented to search for the best configuration among the alternatives represented in the Pareto front.

Figure 4-15 summarizes how the three methods will be integrated and applied for PVGCS, which constitutes the core of the following chapter.

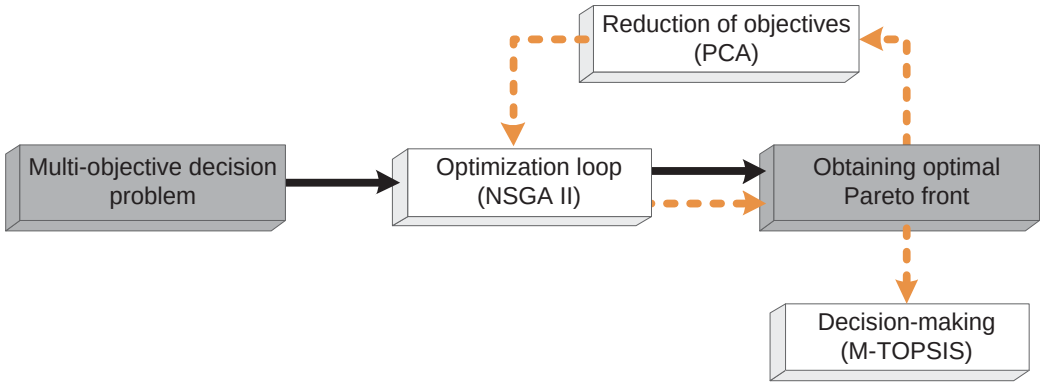

Figure 4-15 Integration of NSGA-II, PCA method and M-TOPSIS method

Lire
la seconde partie
de la thèse